



# THESIS

For the degree of doctor of philosophy in INTERNATIONAL JOINT DOCTORATE

(PhD) AGREEMENT between

École doctorale n° 432 : Sciences des Métiers de l'Ingénieur

**I'École Nationale Supérieure d'Arts et Métiers**

Spécialité “Mécanique - Matériaux”

and

**Universidad de los Andes**

*Presented and defended by*

**Angela María GARCÍA MORA**

15<sup>th</sup> January, 2015

**Kinetic modeling of oxygen absorption by unsaturated esters and linseed oil to be used as oxygen scavengers**

Thesis advisors  
**Jacques VERDU**  
**Jorge MEDINA**  
**Bruno FAYOLLE**

**Jury**

**Mme. Maria del Pilar NORIEGA**, Senior Research, ICIPC  
**Mme Florence JESTIN**, Associated Professor HDR à l'ENSCCF  
**M. Felipe SALCEDO**, Professeur Affilié, Universidad de los Andes  
**M. Jacques VERDU**, Professeur, PIMM, Arts et métiers ParisTech-Centre de Paris  
**M. Bruno FAYOLLE**, Professeur, PIMM, Arts et métiers ParisTech-Centre de Paris  
**M. Jorge MEDINA**, Associated Professor, CIPP-CIPEM, Universidad de los Andes

Président  
Rapporteur  
Rapporteur  
Examinateur  
Examinateur  
Examinateur

T  
H  
È  
S  
E



Gracias Díos por mi familia, por los amigos y los mentores que me acompañaron a recorrer este camino.

Merci à Dieu, à ma famille, à mes amis et à mes mentors qui m'ont tous accompagné dans le chemin.



*This doctorate has received funding by the Colombian « Departamento Administrativo de ciencia, Tecnología e Innovación- Colciencias Conv. 528/2011 »*

*This de los **uniandes** doctorate has received funding by the «Universidad Andes - Crédito educativo condonable para*

*estudiantes doctorales»*

# CONTENT

---

<b>CONTENT</b>	<b>5</b>
<b>SUMMARY (IN SPANISH LANGUAGE)</b>	<b>10</b>
<b>INTRODUCTION (IN FRENCH LANGUAGE)</b>	<b>12</b>
<b>INTRODUCTION</b>	<b>14</b>
<hr/>	
<b>REFERENCES</b>	<b>18</b>
<hr/>	
<b>CHAPTER I: BIBLIOGRAPHIC REVIEW AND STRATEGY</b>	<b>21</b>
<b>INDEX OF FIGURES</b>	<b>22</b>
<b>INDEX OF TABLES</b>	<b>22</b>
<b>RESUME DU CHAPITRE I</b>	<b>23</b>
<hr/>	
INTRODUCTION	26
1.1 ACTIVE PACKAGING	26
1.2 OXYGEN SCAVENGERS (OS)	26
1.3 OXIDATION OF LINSEED OIL	29
1.4 OXIDATION OF UNSATURATED FATTY ACIDS AND ESTERS	30
1.5 MODELS TO PREDICT OXYGEN IN THE HEADSPACE	31
1.6 INCORPORATION OF OS IN POLYMER MATRICES	38
1.7 SUMMARY OF BIBLIOGRAPHIC INFORMATION	40
1.8 OBJECTIVES	41
1.9 STRATEGY	41
1.9.1 <i>To evaluate the effect of processing variables over the scavenger efficiency of linseed oil encapsulated.</i>	41
1.9.2 <i>Calculate a theoretical oxygen uptake capacity (OC) of Linseed oil based in its chemical compositions.</i>	41
1.9.3 <i>Validate TGA as a method to follow scavenging capability of OS.</i>	42
1.9.4 <i>Comparison of theoretical and experimental oxygen uptake of Linseed oil, under different experimental methods.</i>	42
1.9.5 <i>Kinetic modelling of thermo-oxidation of Linseed oil.</i>	42

---

---

**CHAPTER II:MATERIALS AND METHODS 47**

**INDEX OF FIGURES 48**

**RESUME DU CHAPITRE II 49**

---

INTRODUCTION	50
2.1 MATERIALS	50
2.2 SOL-GEL ENCAPSULATION	50
2.3 MANUFACTURING OF ACTIVE FILMS	53
2.4 OXYGEN CONCENTRATION IN HEADSPACE	53
2.5 CHEMICAL CHARACTERIZATION	54
2.5.1 <i>Gas chromatography (GC)</i>	54
2.5.2 <i>Fourier Transform Infrared spectroscopy (FTIR)</i>	54
2.6 TGA AS TECHNIQUE TO EVALUATE OXYGEN UPTAKE CAPABILITY	54
2.7 DETERMINATION OF THE PEROXIDE VALUE BY IODOMETRIC TITRATION METHOD	55
2.7.1 <i>Principle</i>	55
2.7.2 <i>Calculation of Peroxide value (PV)</i>	55
2.7.3 <i>Reagents</i>	56
2.7.4 <i>Procedure</i>	56
2.8 KINETIC MODEL	56
REFERENCES	57

---

**CHAPTER III:EXPERIMENTAL RESULTS OF LINSEED OIL 59**

**INDEX OF FIGURES 60**

**INDEX OF TABLES 61**

**RESUME DU CHAPITRE III 62**

---

INTRODUCTION	63
3.1 SOL-GEL ENCAPSULATION FOR INCLUSION OF OS IN POLYMER-BASED ACTIVE PACKAGING	63
3.1.1 <i>FTIR characterization</i>	63
3.1.2 <i>Electron Microscopy (SEM)</i>	65
3.1.3 <i>Linseed oil encapsulation</i>	65
3.1.4 <i>Linseed oil encapsulated + Polypropylene (PP)</i>	68

3.2 LINSEED OIL CHEMICAL CHARACTERIZATION	68
3.2.1 <i>Gas-Liquid Chromatography (GLC)</i>	68
3.2.2 <i>Fourier Transform Infrared Spectroscopy</i>	70
3.3 TGA TO EVALUATE OXYGEN UPTAKE CAPABILITY	74
3.3.1 <i>TGA in non-oxidative atmosphere</i>	74
3.3.2 <i>TGA in oxidative atmospheres</i>	75
3.4 MEASUREMENTS OF OXYGEN IN HEADSPACE.	76
3.5 COMPARISON BETWEEN TGA AND HEADSPACE RESULTS	78
3.6 RELATIONSHIP BETWEEN PEROXIDE VALUE AND TGA.	80
REFERENCES	82

---

**CHAPTER IV:EXPERIMENTAL RESULTS OF UFE 85**

**INDEX OF FIGURES 86**

**RESUME DU CHAPITRE IV 87**

---

INTRODUCTION	88
4.1 TGA IN NON-OXIDATIVE ATMOSPHERE OF UNSATURATED ESTERS	89
4.2 TGA IN OXIDATIVE ATMOSPHERE	90
4.3 DISCUSSION OF RESULTS FOR TGA OF UNSATURATED ESTERS	93
4.3.1 <i>TGA in non-oxidative atmosphere</i>	93
4.3.2 <i>TGA in oxidative atmosphere</i>	94
4.3.3 <i>Calculating oxygen scavenging capacity based on TGA</i>	95
REFERENCES	100

---

**CHAPTER V: SIMULATION APPROACH 102**

**INDEX OF FIGURES 103**

**INDEX OF TABLES 104**

**RESUME DU CHAPITRE V 105**

---

INTRODUCTION	106
5.1 KINETIC MODELING	106
5.2 MODEL PARAMETERS ASSESSMENT	108
5.2.1 <i>Parameters known</i>	108
5.2.2 <i>Strategy to assess kinetic constants <math>k_{lb}</math>, <math>k_6</math>, <math>k_4</math> and <math>k_5</math></i>	109

5.3	INITIAL CONCENTRATIONS OF GROUPS $[PH]_0$ AND $[POOH]_0$	110
5.4	PSEUDOCODE	111
5.5	OXIDATION SIMULATIONS OF PURE OILS	113
5.5.1	<i>Simulation of linolenate mass changes in oxygen excess</i>	113
5.5.2	<i>Simulation of linolenate mass changes in air</i>	113
5.5.3	<i>Simulation of linseed oil mass changes in air</i>	114
5.5.4	<i>Values of <math>k_b</math>, <math>k_4</math>, <math>k_5</math> and <math>k_6</math></i>	115
5.5.5	<i>Simulations of oxygen absorbed for linseed oil at 40°C</i>	116
5.6	OXIDATION SIMULATIONS OF ACTIVE PACKAGING	117
5.6.1	<i>Modeling approach</i>	117
5.6.2	<i>Oxygen diffusion parameter</i>	118
5.6.3	<i>Simulations</i>	118
REFERENCES		125

---

**CONCLUSIONS AND FUTURE WORK                  127**

---

CONCLUSIONS	128
CONTRIBUTION	129
FUTURE WORK	129

---

**ANNEX 1: PUBLICATIONS AND PRESENTATIONS DONE DURING THE THESIS    131**

---



# MODELO CINÉTICO DEL CONSUMO DE OXÍGENO POR PARTE DE ÉSTERES INSATURADOS Y ACEITE DE LINAZA, PARA SER UTILIZADOS EN EMPAQUES ACTIVOS

## Resumen

Extender la vida útil de productos perecederos sin afectar su calidad nutricional y propiedades organolépticas es uno de los grandes retos en la industria alimentaria. Los empaques activos, propuestos en las últimas décadas, son un campo de acción prometedor para cumplir con el reto. Este tipo de empaques incluyen intencionalmente composiciones que son capaces de afectar el ambiente que rodea al producto empacado. Los absorbentes de oxígeno, son una de las tecnologías con más desarrollo técnico y comercial ya que la oxidación y la proliferación de microrganismos aeróbicos son unas de las primeras causas de degradación, presencia de olores y sabores desagradables y pardeamiento, entre otros. Sin embargo, en países en desarrollo, como Colombia, con una gran industria agrícola, la investigación en empaques activos es aún incipiente.

Esta tesis hace una contribución en el estudio de la cinética de oxidación del aceite de linaza, propuesto como ingrediente activo para absorbentes de oxígeno. Se realiza un seguimiento a la oxidación térmica del aceite de linaza y de ésteres insaturados (utilizados como sustancias modelo) bajo diferentes condiciones de oxidación (calentamiento entre 40°C y 110°C y presiones parciales de oxígeno entre 0 y 1 bar). Dentro de las pruebas experimentales se realizó seguimiento con termogravimetría (TG), medición de oxígeno en el espacio de cabeza y titulación para medir el índice de peróxidos. Adicionalmente, se propone un modelo cinético para la oxidación térmica con base en el esquema básico de descomposición de hidroperóxidos. El modelo se extrapoló a películas de polipropileno (PP) con cargas de aceite de linaza y se estudió el consumo de oxígeno con diferentes espesores, bajo la suposición de dispersión homogénea en el polímero y difusión de oxígeno determinada por la matriz de polipropileno.

**Palabras clave:** Empaques activos, absorbentes de oxígeno, aceite de linaza, oxidación térmica, modelado cinético, predicción de consumo de oxígeno.



# **Introduction (in French language)**

---

La thèse porte sur l'utilisation d'adjuvants absorbeurs d'oxygène dans les emballages alimentaires plastiques, pour prévenir le rancissement et la dégradation du contenu. Le concept d' « emballage actif » qui date des années 1970, a connu un développement notable dans les pays industrialisés ; l'intérêt de l'utilisation d'absorbeurs d'oxygène y est reconnu (p.ex. Communauté Européenne 2008). Par contre, dans les pays à prédominance agricole, comme la Colombie, ces solutions sont encore peu connues. C'est la raison pour laquelle notre équipe de l'Université de los Andes a élaboré un projet intitulé : « Développement d'un composite thermoplastique basé sur une polyoléfine, ayant des propriétés d'absorption d'oxygène »

Il a été décidé d'étudier les propriétés d'absorption d'oxygène de la lécithine de soja (LC) et de l'erythorbate de sodium (EC) (activé par l'humidité, 99%HR pendant une heure). Ces adjuvants sont incorporés dans du polyéthylène basse densité (PEbd), mis en œuvre sous forme de film d'emballage. Cependant les adjuvants n'étaient pas stables dans les conditions usuelles d'extrusion (160°C), ce qui a conduit à la recherche d'autres méthodes de préparation.

Parmi les méthodes étudiées, l'encapsulation sol-gel de l'absorbeur d'oxygène s'est avérée la plus prometteuse et a fait l'objet d'un brevet (Medina Perilla et al. 2012). Des recherches ultérieures ont mis en évidence l'intérêt éventuel d'une activation par irradiation UV ou par catalyse par sulfate de fer, et d'un ajout d'huile de lin particulièrement riche en doubles liaisons.

L'objectif de la présente thèse est de proposer un modèle cinétique du phénomène d'absorption d'oxygène par les films d'emballage contenant les absorbeurs d'oxygène en question, pour donner une base scientifique aux données technologiques déjà obtenues par notre équipe. Pour cela nous sommes associés à l'équipe TemPO de l'ENSAM pour bénéficier de son expérience dans le domaine de la cinétique d'oxydation.

# **Introduction**

---

According to the Food and Agriculture Organization of the United Nations (FAO) the post-harvest losses in developed countries oscillate between 5% and 25%. This value can reach about 50% in the case of developing countries (FAO & IICA/PRODAR, 2005).

On average, about one third of horticultural crops produced are never consumed by humans due to diverse reasons including genetic factors, climatic conditions, cultural practices, and failures in post-harvest management practices. Packaging technologies are considered to play a key role between these last, being critical to maintain quality and safety of food products (Kader & Rolle, 2004). New technologies in this field may help to increase shelf life of perishables and reduce food losses.

Since 1970s, active packaging has been proposed as a technology able to improve quality and shelf life of products by means of components that might interact with the packaged food by releasing to, or absorbing from the surrounding, environment substances directly related to the degradation process, such oxygen scavengers which avoid oxidation (Comision Europea, 2009; Day., 2008; M. Ozdemir, 2004; P. Suppakul, 2003).

However, in developing countries with a large agricultural base, active packaging still remains unexplored both in terms of application and research. Prospective reports of flexible and semi rigid packaging in Colombia from 2004 and 2011 regarding the flexible and semi rigid packaging industry in Colombia made evident a lack of development and technology transfer in this field (Noriega et al., 2011)

The global market of active packaging is worth \$8.8 bn. USD, and it is set to grow by 5.2% annually to \$11.9 bn. USD in 2017 (Addy, 2013), with a share of 35% of applications that include oxygen scavengers (Visiongain, 2010). According to own market analysis around 2.3% of the total market of flexible packaging will be introduce oxygen scavengers which corresponds to \$1bn. USD in 2019, and 8.5% of semi-rigid packaging could introduce this technology with equals to \$2.35 bn. USD in 2019 (ITUANGO, 2015).

Taking into account such a growing, and that all the new knowledge about oxygen scavengers is concentrated in USA, Japan , China and Europe (ITUANGO, 2015), it is imperative to study and control the effect of oxygen scavengers in different environments, and contribute to the local research, in order to be able to scale-up such knowledge and reach an optimal, safe, and cost-effective package design. The lack of technical criteria is especially acute on O<sub>2</sub> scavenging films, labels, sheets, and trays (Miltz J & MR., 2000; Miltz, Passy, & Mannheim, 1995).

With the aim to set forth the research in new active ingredients for oxygen scavengers and to introduce the active packaging in Andean countries, the *Grupo de Materiales y Manufactura* (CIPP-CIPEM) of *Universidad de los Andes* and *Instituto de Capacitación e Investigación del Plástico y del Cauchó* (ICIPC) collaborated under the project titled “Development of a thermoplastic composite based on polyolefin and with oxygen scavengers properties”(Sierra & Medina, 2009).

Blends of Soybean Lecithin/CuCl<sup>1</sup> (L-C) and Sodium Erythorbate/CuCl (E-C) proposed as oxygen scavengers, (activated at humidity of 99% HR during one hour) brought promising results. L-C and E-C blends were mixed in Low density polyethylene (LDPE) to form a composite that could be processed into packages, however the composite presented browning due to incipient thermo-oxidation of L-C and E-C (Figure I. 1)



**Figure I. 1: Browning in blend of LDPE + (E-C) processed at 160°C.**

New forms to introduce oxygen scavengers into polymer matrixes were explored, avoiding early thermo-oxidation because processing conditions. There was proposed impregnation in carbon matrix before to blend with polymers (Cardona, Noriega, & Sierra, 2012; Joven, Garcia, Arias, & Medina, 2014), use of super critics fluids(Sierra, Cardona, & Noriega, 2009), and sol – gel encapsulation before blend with polymers(A. García, 2010)

Sol-gel encapsulation emerged as one promising and then was explored deeply by CIPP-CIPEM. As result, a method to encapsulate active ingredients for oxygen scavengers and include them in polymer matrix has been patented in Colombia and waiting for granted in United States(Medina, García, Arias, & Joven, 2012).

Subsequent Master thesis (A. García, 2010; Salas, 2011) proposed activation by means of UV radiation, and added linseed oil as a possible ingredient for oxygen scavengers because its high content of unsaturated fatty acids (UFA). Also sulphate ferrous was incorporated as catalyst to make compositions: Soybean Lecithin/Sulphate ferrous (L-Fe) and Linseed oil/Sulphate ferrous (O-Fe).

This thesis has two main objectives, one oriented to technological application of oxygen scavengers in active packaging and the second one which seeks give scientific support to the data previously collected.

Technological objective is to evaluate the effect of processing variables over the scavenger efficiency of linseed oil encapsulated. Scientific main objective is to propose and validate a kinetic model for the thermo-oxidation of linseed oil which allows evaluate its oxygen uptake capacity under different oxygen concentrations and temperatures.

---

<sup>1</sup> CuCl: Copper (I) chloride.

Kinetic model will be validated mainly by two experimental tests , first usual headspace oxygen measurements proposed by other authors (Charles, Sanchez, & Gontard, 2006) and thermogravimetric analyses (TGA) proposed as a new method to measure oxygen scavenging capacity.

The collaboration between CIPP-CIPEM (Universidad de los Andes) and TemPO (Ecole Nationale Supérieure d'Arts et Métiers) intend to take advantage of the experience of the latter research group in modelling of oxidation of polymers and molecules of low molecular weight (Richaud et al., 2012; Richaud, Fayolle, Verdu, & Rychly, 2013).

Along the thesis, advances have been presented in events as the Conference of the Polymer Processing Society PPS(Á. García, Salas, & Medina, 2012), Latin-American Symposiums of Polymers(Á. García, Medina, Verdu, & Fayolle, 2014b), national colloquiums (Garcia, Medina, Aguilar, Fayolle, & Verdu, 2013) and packaging conferences(Á. García, Medina, Verdu, & Fayolle, 2014a)<sup>2</sup>.

In parallel with the research, CIPP-CIPEM has advanced in the path for future commercialization of oxygen scavengers for active packaging, bring forward in the market study, product presentation and business model with the project “Absorbedores De Oxígeno para uso en Empaques de Alimentos (Oxylife Packaging )” accepted and co-financed by Colciencias and Universidad de los Andes as a product of innovation based in scientific knowledge(Medina & García, 2015).

---

<sup>2</sup> All the papers mentioned are in Annex 1 of the thesis.

## References

- Addy, R. (2013). Strong growth forecast for active, controlled and intelligent packaging. *Food Production daily.com.* Retrieved from <http://www.foodproductiondaily.com/Markets/Strong-growth-forecast-for-active-controlled-and-intelligent-packaging>
- Cardona, E. D., Noriega, M. d. P., & Sierra, J. D. (2012). Oxygen scavengers impregnated in porous activated carbon matrix for food and beverage packaging applications. *Journal of Plastic Film and Sheeting*, 28(1), 63-78.
- Charles, F., Sanchez, J., & Gontard, N. (2006). Absorption kinetics of oxygen and carbon dioxide scavengers as part of active modified atmosphere packaging. *Journal of Food Engineering*, 72(1), 1-7. doi:10.1016/j.jfoodeng.2004.11.006
- Comision Europea. (2009). REGLAMENTO (CE) No. 450/2009 sobre materiales y objetos activos e inteligentes destinados a entrar en contacto con alimentos (pp. 9). Diario Oficial de las Comunidades Europeas.
- Day., B. P. F. (2008). *Active Packaging of Food. Smart Packaging Technologies for Fast Moving Consumer Goods*: John Wiley & Sons, Ltd.
- FAO, & IICA/PRODAR. (2005). Curso de Gestión de Agronegocios en empresas asociativas rurales en América Latina *Poscosecha y servicios de apoyo a la comercialización* (Hernando Riveros; Pilar Santacoloma; Florence Tartanac ed., Vol. Módulo 4).
- Garcia, Á., Medina, J., Aguilar, R., Fayolle, B., & Verdu, J. (2013). *Modelamiento de la vida de anaquel en películas de polímeros reactivos*. Paper presented at the ICIPC Colloquium 2013, Medellín, Colombia.
- García, A. (2010). *Evaluación térmica y cinética de una capa activa, en estructuras de empaques con propiedades de absorción de oxígeno*. Universidad de los Andes, Bogotá.
- García, Á., Medina, J., Verdu, J., & Fayolle, B. (2014a). *Methodology to Evaluate Performance of Active Ingredients as Oxygen Scavengers*. Paper presented at the 19th IAPRI World Conference on Packaging, Melbourne, Australia.
- García, Á., Medina, J., Verdu, J., & Fayolle, B. (2014b). *Metodología para Evaluar el Desempeño de Absorbentes de Oxígeno para ser Utilizados en Empaques Activos*.

Paper presented at the XIV Latin American Symposium of Polymers, XII Ibero American Congress of Polymers, Porto de Galinhas, PE, Brazil.

García, Á., Salas, J., & Medina, J. (2012). *Linseed oil as active ingredient in active packaging*.

Paper presented at the Polymer Processing Society Americas Conference, Niagara, Ontario.

ITUANGO, S. C. (2015). *Primer Informe- Fase dos. Entendimiento de Mercado de absorbentes de oxígeno*. UNIVERSIDAD DE LOS ANDES.

Joven, R., Garcia, A., Arias, A., & Medina, J. (2014). Development of an Active Thermoplastic Film with Oxygen Scavengers Made of Activated Carbon and Sodium Erythorbate. *Packaging Technology and Science*.

Kader, A. A., & Rolle, R. S. (2004). *The role of post-harvest management in assuring the quality and safety of horticultural produce* (Vol. 152): Food and Agriculture Organization of the United Nations.

M. Ozdemir, J. D. F. (2004). Active Food Packaging Technologies. *Critical Reviews in Food Science and Nutrition*, 185-193.

Medina, J., & García, Á. (2015). *ABSORBEDORES DE OXÍGENO PARA USO EN EMPAQUES DE ALIMENTOS. (OxyLife Packaging )*. Accepted project for Colciencias funded in the call 642, 2014: "Locomotora de la Innovación". Universidad de los Andes.

Medina, J., García, Á., Arias, A., & Joven, R. (2012). 167.(WO2012020287) OXYGEN-ABSORBING COMPOUND ENCAPSULATED IN A SILICA MATRIX AND METHOD FOR THE PRODUCTION THEREOF.

Miltz J, & MR., P. (2000, June 14-18). *Active packaging technologies:oxygen scavenging* Paper presented at the Intl. Assoc. of Packaging Res Inst. Annual Symposium., San Jose State Univ., San Jose, Calif.

Miltz, J., Passy, N., & Mannheim, C. H. (1995). Trends and applications of active packaging systems. *Special Publications of the Royal Society of Chemistry*, 162, 201-210.

Noriega, M., Naranjo, A., Sierra, J., Medina, J., Cárdenas, A., Mojica, F., & Mahecha, C. (2011). ESTUDIO PROSPECTIVO DE LOS EMPAQUES PLÁSTICOS FLEXIBLES Y SEMIRRÍGIDOS EN COLOMBIA. *Escenarios y estrategias al horizonte del año 2020*.

P. Suppakul, J. M., K. Sonneveld and S.W. Bigger. (2003). Active Packaging Technologies with an Emphasis on Antimicrobial Packaging and its Applications. *Journal of food science*, 408-420.

- Richaud, E., Audouin, L., Fayolle, B., Verdu, J., Matisová-Rychlá, L., & Rychlý, J. (2012). Rate constants of oxidation of unsaturated fatty esters studied by chemiluminescence. *Chemistry and Physics of Lipids*, 165(7), 753-759.  
[doi:http://dx.doi.org/10.1016/j.chemphyslip.2012.09.002](http://dx.doi.org/10.1016/j.chemphyslip.2012.09.002)
- Richaud, E., Fayolle, B., Verdu, J., & Rychlý, J. (2013). Co-oxidation kinetic model for the thermal oxidation of polyethylene-unsaturated substrate systems. *Polymer Degradation and Stability*, 98(5), 1081-1088.
- Salas, J. C. (2011). *Processability of polyolefinic films filled with oxygen scavengers.* . (M.Sc Engineering), Universidad de los Andes, Bogotá.
- Sierra, J. D., Cardona, E. D., & Noriega, M. d. P. (2009). Colombia Patent No. SIC: ICIPC.
- Sierra, J. D., & Medina, J. A. (2009). *INFORME TÉCNICO FINAL. Desarrollo de un compuesto termoplástico con base en Poliolefinas y con propiedades de absorción de oxígeno.* Retrieved from Informe entregado a Colciencias:
- Visiongain. (2010). *The Active, Intelligent and Smart Food & Drink Packaging Market 2011-2021* Retrieved from [www.visiongain.com](http://www.visiongain.com)

# I

# Bibliographic Review and Strategy

## CONTENT

---

**INDEX OF FIGURES 22**

**INDEX OF TABLES 22**

**RESUME DU CHAPITRE I 23**

---

INTRODUCTION	26
1.1 ACTIVE PACKAGING	26
1.2 OXYGEN SCAVENGERS (OS)	26
1.3 OXIDATION OF LINSEED OIL	29
1.4 OXIDATION OF UNSATURATED FATTY ACIDS AND ESTERS	30
1.5 MODELS TO PREDICT OXYGEN IN THE HEADSPACE	31
1.6 INCORPORATION OF OS IN POLYMER MATRICES	38
1.7 SUMMARY OF BIBLIOGRAPHIC INFORMATION	40
1.8 OBJECTIVES	41
1.9 STRATEGY	41
1.9.1 To evaluate the effect of processing variables over the scavenger efficiency of linseed oil encapsulated.	41
1.9.2 Calculate a theoretical oxygen uptake capacity (OC) of Linseed oil based in its chemical compositions.	41
1.9.3 Validate TGA as a method to follow scavenging capability of OS.	42
1.9.4 Comparison of theoretical and experimental oxygen uptake of Linseed oil, under different experimental methods.	42

### 1.9.5 Kinetic modelling of thermo-oxidation of Linseed oil. 42

## REFERENCES 44

## INDEX OF FIGURES

FIGURE 1.1: CRYOVAC OS1000 OXYGEN SCAVENGING FILM .....	28
FIGURE 1.2: CHANGE OF HYDROXYL AND UNSATURATION INDEXES IN LINSEED OIL UNDER THERMO-AGEING (A) AND PHOTO AGEING (B).....	30
FIGURE 1.3: HEADSPACE OXYGEN ANALYSIS IN SOY BREAD WITH AND WITHOUT PRESERVATIVE INITIALLY PACKAGED WITH AIR, TESTED BY THE EXPERIMENTAL AND MATHEMATICAL MODEL METHODS (PASCALL ET AL., 2008).....	32
FIGURE 1.4: PLOT OF LN K VS. E/R OF THE VALUES OBTAINED BY ADAPTED FROM TEWARI ET AL. (2002).....	34
FIGURE 1.5: (A) OXYGEN INGRESS THROUGH A PE/PA MULTILAYER FILM (ENTPLATER, 30°C). (B). PREDICTED VERSUS OBSERVED VALUES FOR THE PE/PA MULTILAYER FILM (VAN BREE ET AL., 2010). .....	35
FIGURE 1.6: EVOLUTION OF INTERFACIAL CONCENTRATION AT THE REACTIVE SIDE ( $C_1$ ) IN THE REACTIVE-PASSIVE (RP) FILM: THIELE MODULUS $\Phi_0=3.16$ , SOLUTE PARTITION COEFFICIENT $H_{12}=1$ , AND DIMENSIONLESS PARAMETER OF SIZE $Z=1$ (SOLOVYOV & GOLDMAN, 2006b). .....	36
FIGURE 1.7: COMPARISON OF (A) DOWNSTREAM FLUX PLATEAU IN LOG SCALE AND (B) TIME LAG $\Theta$ IN LINEAR SCALE AS A FUNCTION OF PARTITION COEFFICIENT $H$ , FOR A FILM WITH THREE LAYERS VERSUS A POLYMER BLEND (ANALYTICAL PREDICTIONS). (A) THE MULTILAYER PLATEAU IS EVALUATED FOR TWO BULK REACTION RATES $K_R$ . ALL PARAMETER VALUES ARE THE SAME FOR THE BLEND AND MULTILAYER FILMS AND ARE GIVEN IN TABLE 1.2 (CARRANZA, PAUL, & BONNECAZE, 2012). .....	37
FIGURE 1.8: PROCESSING TEMPERATURES OF LOW DENSITY POLYETHYLENE (LDPE), HIGH DENSITY POLYETHYLENE (HDPE), POLYPROPYLENE (PP) AND POLYETHYLENE TEREPHTHALATE (PET). DATA EXTRACTED FROM (STRONG, 2006) .....	39
FIGURE 1.9: RESULTS FOR ADSORPTION ISOTHERM FOR GRANULAR ACTIVATED CARBON. ....	40

## INDEX OF TABLES

TABLE 1.1: ARRHENIUS EQUATIONS FOR DIFFERENT OXYGEN SCAVENGERS (TEWARI, JAYAS, JEREMIAH, & HOLLEY, 2002).....	33
TABLE 1.2: LIST OF PARAMETERS FOR COMPARISON BETWEEN HOMOGENEOUS, BLEND AND MULTILAYER FILM (CARRANZA ET AL., 2012). .....	37

# Résumé du chapitre I

Ce chapitre est dédié à une revue bibliographique sur le sujet d'étude.

La première partie est une vue panoramique sur les emballages « actifs ». Il s'agit d'incorporer dans l'emballage des adjuvants permettant de contrôler le transport de gaz et vapeurs de l'environnement vers l'intérieur de l'emballage (par exemple l'humidité) ou de l'intérieur vers l'extérieur (par exemple éthylène).

La deuxième partie est consacrée aux absorbeurs d'oxygène (OS) en général. Leur utilisation est justifiée par la sensibilité de nombreux produits alimentaires à l'oxydation (Cooksey, 2002). Les OS fonctionnent généralement par voie chimique en capturant les molécules d'oxygène diffusant à travers l'emballage. Ils peuvent être incorporés au produit alimentaire sous forme de sachets, ou à l'emballage sous forme de couche adhésive ou d'adjvant dissous dans la matrice polymère. Cette dernière solution est la plus intéressante du point de vue industriel. La première application d'OS date de 1950 en Finlande, mais le premier développement notable date de 1977 (Mitsubishi).

Diverses voies d'activation ont été étudiées : catalytique par le fer, photochimique sur des colorants photosensibles, enzymatique, etc.

L'utilisation du fer, peu coûteux, résulte de l'effet catalytique bien connu des métaux de transition sur l'oxydation. Le problème est que ce processus nécessite la présence d'humidité, indésirable dans certaines applications. Il en est de même pour l'acide ascorbique, qui a été commercialisé mais dont le pouvoir absorbant est faible. Les autres modes d'activation n'ont pas connu de développement commercial.

En ce qui concerne les cinétiques d'absorption d'oxygène, on note l'utilisation fréquente de modèles du premier ordre avec des constantes de vitesse de  $10^{-3}$  à  $10^{-1} \text{ h}^{-1}$ . Il s'agit évidemment de simplifications sans lien avec le mécanisme réel.

La troisième partie est consacrée à l'huile de lin (HL) dont le processus d'oxydation a fait l'objet d'études liées à l'application des huiles siccatives. L'oxydation de l'HL se traduit par l'accumulation de groupements oxygénés, la disparition des insaturations et une réticulation liée aux additions de radicaux sur les doubles liaisons. Il apparaît que l'HL subit d'abord un phénomène d'autoxydation de la partie insaturée. La partie saturée n'évolue qu'à long terme. L'étude citée (Lazzari et Chiantore, 1999) ne rapporte pas de valeurs de constantes de vitesse.

La quatrième partie est consacrée aux composants élémentaires de l'huile de lin : acides et esters gras. L'oxydation de ces produits a fait l'objet d'études depuis longtemps en raison de l'importance des processus de rancissement dans l'industrie alimentaire. On a montré que la sensibilité à l'oxydation augmentait avec le nombre de doubles liaisons : linolenique > linoléique > oléique. Les

acides s'oxydent plus vite que les esters correspondants car les acides catalysent ou assistent la décomposition des hydro peroxydes.

La cinquième partie est consacrée à la modélisation cinétique du phénomène. van Bree et al. (2010) ont proposé un modèle sophistiqué basé sur le bilan d'oxygène diffusant au travers de l'emballage et l'oxygène absorbé à la fois par le produit alimentaire et par l'OS. D'autres modèles sont basés sur l'hypothèse d'une cinétique du premier ordre, sans justifier cette simplification. Tewari et al (2002) publient ainsi les valeurs de constantes de vitesse et les énergies d'activation de quatre OS différents. Nous montrons que ces données obéissent à une loi de compensation dont les paramètres suspects semblent indiquer que les valeurs n'ont pas de sens physique. Solovyov et Goldman (2006) ont proposé un modèle inspiré de la chimie des solides, faisant appel à des couches actives et passives (Solovyov & Goldman, 2006a). Cette approche est contestable, à notre avis, dans le cas étudié où le milieu réactionnel est plus proche d'un liquide (du point de vue de la solubilité et de la diffusivité de l'oxygène) que d'un solide. D'autre part l'oxydation procède d'un mécanisme radicalaire en chaîne qui ne se réduit pas à une réaction par stades d'ordre déterminé . Il en est de même du modèle de Ferrari et al. (2009) et de la résolution numérique de ce modèle par Carranza et al. (2012).

La sixième partie est dédiée au problème de l'incorporation de l'OS dans le polymère constitutif de l'emballage. On s'attend à ce qu'aux températures de mise en œuvre du polymère, l'OS soit rapidement consommé ou, peut-être, migre rapidement hors de l'emballage. Ces problèmes justifient l'étude de procédés tels que l'encapsulation sol-gel de l'OS.

La septième partie justifie le programme de la thèse à partir des lacunes révélées par l'analyse bibliographique. Le point le plus important est l'élaboration d'un modèle cinétique fondé sur le mécanisme réel d'oxydation de l'OS. Ce dernier est un produit naturel complexe mais la détermination de ses paramètres cinétiques s'appuiera sur l'étude parallèle de l'oxydation de molécules modèles comme les linoléates et linolénates de méthyle. Ce modèle fera l'objet de tests de validation dans des configurations expérimentales décrites dans la neuvième partie et dans le chapitre suivant.

La huitième partie définit les objectifs de l'analyse cinétique.

La neuvième partie décrit les méthodes mises en œuvre pour cette analyse. L'HL, qui est l'OS le plus important de cette étude, fera l'objet d'une caractérisation préalable très complète, en particulier par IR et GC dans le but d'identifier et quantifier les groupements réactifs à l'oxydation (carbones allyliques). L'étude de la vitesse d'oxydation de l'HL permettra ensuite de tester la valeur prédictive du modèle. Cette vitesse d'oxydation sera déterminée quasi directement par thermogravimétrie isotherme et indirectement par mesure de la consommation d'oxygène dans une cellule fermée par l'emballage contenant l'OS. La validité des constantes de vitesse d'oxydation de l'HL sera appréciée par comparaison avec celles déterminées sur les esters insaturés modèles. La

structure du modèle sera identique à celle proposée par Richaud et al. (2012) dans laquelle on considère que les espèces réactives sont les CH allyliques.

Enfin on tentera d'évaluer l'intérêt d'une méthode d'encapsulation de l'OS dans le silicagel. Le système sera incorporé dans une matrice polyoléfine pour les essais d'absorption d'oxygène.

## Introduction

This chapter presents the review relevant to the thesis subject. A bibliographic survey of Active packaging and Oxygen scavengers (OS) is presented in Sections 1.1 and 1.2, respectively. The Section 1.3 addressed the oxidation of Linseed oil which is the innovator ingredient studied in this research as OS, along with bibliographic background about unsaturated fatty acids (UFA) and unsaturated fatty esters (UFE) in Section 1.4.

The next two sections show information about two issues of the research: first, the importance of modelling of oxygen concentration in a packaging without and with the presence of OS, where relevant models to predict oxygen concentration in headspace are explored; and second, the incorporation processes of thermally sensitive OS into a packaging structure. Section 1.7 contains a coherent integration of the bibliographic review.

Finally, Section 1.8 presents the objectives of the doctoral thesis followed by the strategy proposed to approach these in Section 1.9.

### 1.1 Active packaging

Since the very beginning of packaging development, this has maintained a passive role in preservation of goods. Flexible and rigid packaging have worked as an inert barrier to all detrimental external elements and conditions. However, since the late 1970's active packaging appeared as a new way to preserve sensitive products.

Active packaging improve quality and shelf life of products by means of components that might interact with the packaged food by releasing to or absorbing from the surrounding environment substances directly related to the degradation process, modifying gases content and flavours, or adding antioxidants and antimicrobials (Comision Europea, 2009; F. Soares et al., 2009; Miltz J & MR., 2000; Rooney, 1992). Carbon dioxide, water, antimicrobial and aroma releasers, as well as oxygen, ethylene, radicals, humidity and taints scavengers are examples of active packaging (Day., 2008).

Between all the active components to be added into the packaging, two kinds can be distinguished: oxygen scavengers and moisture absorbers. They are estimated to grow at a compound annual growth rate (CAGR) of 8 and 11,9%, respectively (Plastemart, 2011).

### 1.2 Oxygen scavengers (OS)

Oxidative degradation is one of the major pathways for degradation of goods (Krämer, 2006). Oxygen participates in microbial growth, nutritional loss, changes in flavour and aroma, and alteration of texture and colour of foods (Cooksey, 2002; Pascall, Fernandez, Gavara, & Allafi, 2008). The

purpose of an oxygen scavenger is to limit the amount of oxygen available for deteriorative reactions that can lead to reduced functionality of the product (Cooksey, 2002).

Oxygen scavengers (OS) are substances incorporated deliberately to package, and may combine with oxygen to effectively remove it from the inner package environment (Brody, Strupinsky, & Kline, 2001; Charles, Sanchez, & Gontard, 2006; Cooksey, 2002).

OS can be added as sachets and layer adhesives, or can be into the packaging structure, for example including one layer rich in OS in a multilayer structure. In 2002, oxygen scavengers in bottles made up 43,8% of the market, followed by cap/liner/lidding representing 31,5%, sachets with 22,6%, and oxygen-absorbing film with 2% (Cooksey, 2002).

Oxygen scavengers can be used in conjunction with other means of preservation, such as chemical preservatives, reduced water activity, reduced pH, vacuum packaging, or modified atmosphere packaging (Cooksey, 2002).

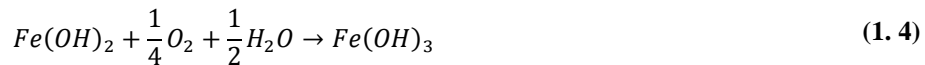
First oxygen scavengers were patented since 1930s in Finland and the UK, becoming widely used after the introduction of the commercial product Ageless® from Mitsubishi Gas Chemical's, which was available in the United States in 1977 (Cooksey, 2002; F. Soares et al., 2009; Krämer, 2006).

Sachets are the first presentation that appears for oxygen scavengers, mostly commercialized in eastern countries, but in the 1990s, work focused to incorporate oxygen scavengers directly into film and other package forms such as closure liners, thermo-formed cups, tubs, and trays rather than sachets. However, this incorporation has been slowly because the high packaging requirements, only 2% of the oxygen scavengers are immersed into the films (Cooksey, 2002).

Oxygen scavengers are the most patented of all active packaging technologies (Cooksey, 2002) and have proven to be efficient in prevention of discoloration of cured meats and tea, rancidity problems in food with high fat content, mold spoilage of medium to moisture content in bakery products, and oxidative flavour changes in coffee (Berenzon & Saguy, 1998; Gill & McGinnis, 1995; Smith, Hoshino, & Abe, 1995).

Active ingredients explored for oxygen scavengers utilize one or more of the following concepts: iron powder oxidation, ascorbic acid oxidation, photo-sensitive dye oxidation, enzymatic oxidation, unsaturated fatty acids, or immobilized yeast on a solid material (Floros, Dock, & Han, 1997).

Iron-base sachets are the type of oxygen scavenging system that has been used commercially for many years(Cooksey, 2002); in them iron powder reacts with oxygen as is presented in equations (1. 1) to (1. 4)**Erreur ! Source du renvoi introuvable.** (Brody & Budny, 1995; Charles et al., 2006).



The main drawback of metal based systems is that the absorption of oxygen only works with humidity and therefore they are not suitable for dry applications. Furthermore, transition metals used are strong catalysts for oxidation of polymers used in packaging, and they are inconvenient if there are systems of metal detection.

Ascorbic acid is safe and is a well-known preserving agent. W.R. Grace holds several patents and offers commercial products as Darex® and DarEval®, but reactivity and absorption capacity are low. Similar to metal based scavengers, ascorbic acid needs humidity to react with oxygen and may not be used for dry applications (Rooney, 1992).

In the development of oxygen scavenging polymers, the most commercially successful materials have been homogeneous blends of reactive substances with polymers, activated by light and including photosensitizing dye. Another approach was based on transition-metal-catalysed oxidation of an aromatic nylon (Trade name Oxbar) which can be blended with polyester and formed for packaging of wine and beer in plastic bottles. Amoco Chemicals introduced Amosorb, which blended polyester and polybutadiene and was catalysed by a transition metal salt. Other polymer materials are OS1000 (Figure 1.1) and 2000 by Cryovac Division of sealed air (Cooksey, 2002).



**Figure 1.1: Cryovac OS1000 oxygen scavenging film**

Other concepts for formulations of oxygen scavengers like photo-sensitive dye oxidation, enzymatic oxidation, unsaturated fatty acids, or immobilized yeast on a solid material are still at the research and development state of advance and they are not commercialized in the same quantities than metal based scavengers.

About OS kinetics, is frequently described by first order models, with magnitudes of the rate constant between  $10^{-3}$  and  $10^{-1} \text{ h}^{-1}$  (Berenzon & Saguy, 1998; Charles et al., 2006; F. Soares et al., 2009). However these models are usually obtained by regression of experimental data, and do not show direct correspondence between the specific reactions and the oxygen scavenging capacity.

### 1.3 Oxidation of Linseed oil

A herbaceous plant, *Linum usitatissimum*, linseed (also called flax) produces seeds oval and pale to dark brown colour. The oil prepared by crushing these seeds is denominated Linseed or Flaxseed Oil (Dlugogorski, Kennedy, & Mackie, 2012).

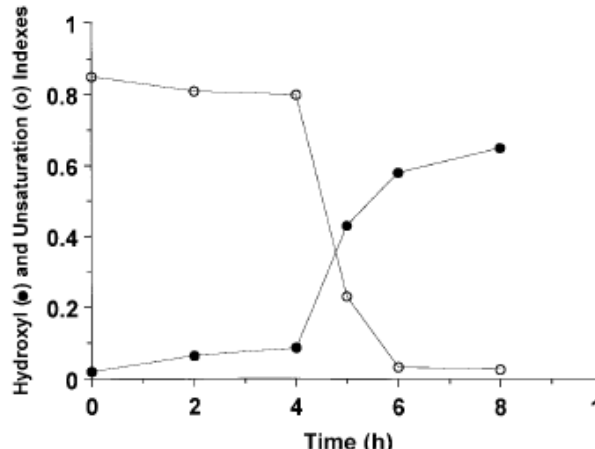
Lazzari & Chiantore 1999, presented an interesting research about drying and oxidative degradation of linseed oil, where the autoxidation of its unsaturated components was analysed, including oxidative cross-linking properties which give to the oil the denomination of “drying oil”. They used films of linseed oil  $80\pm10 \mu\text{m}$  thick at different ageing conditions<sup>1</sup>, and followed the reaction with Fourier Transform infrared spectroscopy (FTIR), thermogravimetric analyses (TGA), differential Scanning Calorimetry (DSC), determination of chloroform soluble and size exclusion chromatography (SEC).

They concluded that thermo-ageing and photo ageing simply produce an acceleration of the natural processes of drying and degradation at ambient temperature, with the same structural variations detected during all treatments (Figure 1.2).

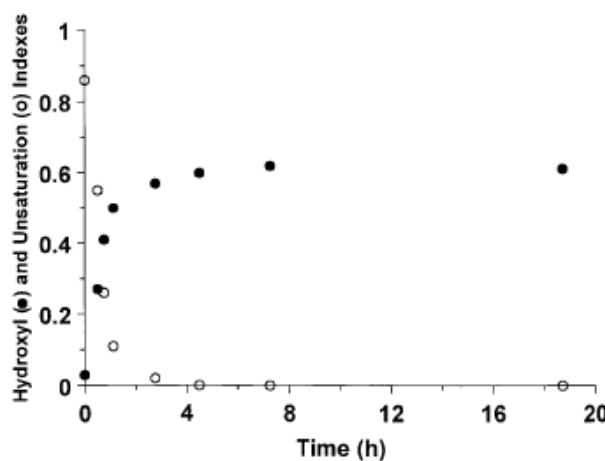
Their conclusions about photo-ageing can appear surprising. Photo-ageing is expected to have qualitative differences with thermal ageing. For example, the pseudo-first order rate constant of hydro peroxide decomposition is more than  $10^6$  times higher in photo than in thermal ageing at moderate temperatures ( $< 100^\circ\text{C}$ ). As a consequence, no induction period is observed in photo-ageing whereas it can be observed in thermal ageing (Figure 1.2). Due to this very high initiation rate, irradiation creates high concentrations of alkyl radicals which cannot be scavenged by oxygen (diffusion controlled oxidation). These radicals can disappear in bimolecular processes among which coupling can generate crosslinking with yields considerably higher than thermal ageing. Another difference is related to the existence of photolytic secondary reactions, for instance ketone photolysis which do not exist in thermal ageing.

---

<sup>1</sup> Samples were exposed to indoor laboratory conditions, accelerated weathering with temperature ( $80^\circ\text{C}$  for 20hours) and photo ageing UV  $> 295 \text{ nm}$  (Lazzari & Chiantore, 1999)



(a) Change of hydroxyl (●) and unsaturation concentrations (○) in linseed oil treated at 80°C.



(b) Change of hydroxyl (●) and unsaturation concentrations (○) in photo-aged linseed oil.

**Figure 1.2: Change of hydroxyl and unsaturation indexes in linseed oil under thermo-ageing (a) and photo ageing (b).**

The authors concluded that oxidation could be described by three well-differentiated stages. Early stage, corresponding to the drying phase, consist of the autoxidation of the unsaturated fatty acid components, which is followed by a crosslinking stage, characterized for the formation of a highly stable network as a consequence of the slow consumption of the labile cross-links. In the late stage, only at ageing times corresponding to years of natural ageing, a progressive oxidation on the alkyl saturated segments takes place, leading to partial fragmentation of the structure together with the formation of larger amounts of oxygenated groups.

Lazzari & Chiantore, 1999 not determine values for the rate constants of the scheme proposed.

#### 1.4 Oxidation of unsaturated fatty acids and esters

Because thermo-oxidation of linseed oil is directly related with its content of unsaturated fatty acids, literature about their oxidation was consulted.

In 1947, Holman & Elmer made a comparative study of a series of pure acids and esters under the same conditions of temperature and oxygen flux, with the aim of give a light upon effects of fatty acid composition upon their oxidation rates. They studied acids and esters from one to four unsaturations finding that as the number of unsaturations increases the maximum rate of autoxidation increases markedly. The oxidation rates for oleic acid, linoleic acid and linolenic acid were 0.08, 2.20 and 6.18 moles of O<sub>2</sub> per acid equivalent per 100 hours, respectively.

They found that the oxidation rates of unsaturated acids were greater than the corresponding esters; unfortunately, the authors proposed neither chemical pathways nor kinetic expressions useful for modelling of the autoxidation of these unsaturated substances.

It can be reasonably assumed that the difference between esters and acids is linked on the fact that acid groups are considerably more polar than ester groups and are able to establish stronger hydrogen bonds with the OH group of hydro peroxides. These hydrogen bonds are responsible for a decrease of the –O-O- bond energy in hydro peroxides and then favour their decomposition into radicals. Acids appear thus as efficient catalysts of POOH decomposition, i.e. of initiation of the radical chain oxidation. The catalytic effect of esters is considerably less marked and perhaps nonexistent.

## 1.5 Models to predict oxygen in the headspace

One of the most used methods to follow the oxygen uptake, in the case of OS, is to measure directly the oxygen concentration inside the packaging were the OS has been included; apart from experimental results some models to predict oxygen in the headspace has been consulted, finding two interesting papers: Pascall et al, 2008 and van Bree et al, 2010.

Pascall (2008) proposed a model to predict headspace oxygen concentration of soy bread packaged at different storage times; they included as independent variables the initial headspace composition, transmission rate of oxygen (O<sub>2</sub>) and carbon dioxide (CO<sub>2</sub>) through packaging materials, and rate of the oxygen consumption and CO<sub>2</sub> emission from moulds and bacteria. They solved the model by a finite increment method and compare their model results with gas chromatographic data, obtaining reliable agreement (Figure 1. 3). The model proposed was restricted to passive packages and therefore oxygen scavengers were out of the model scope.

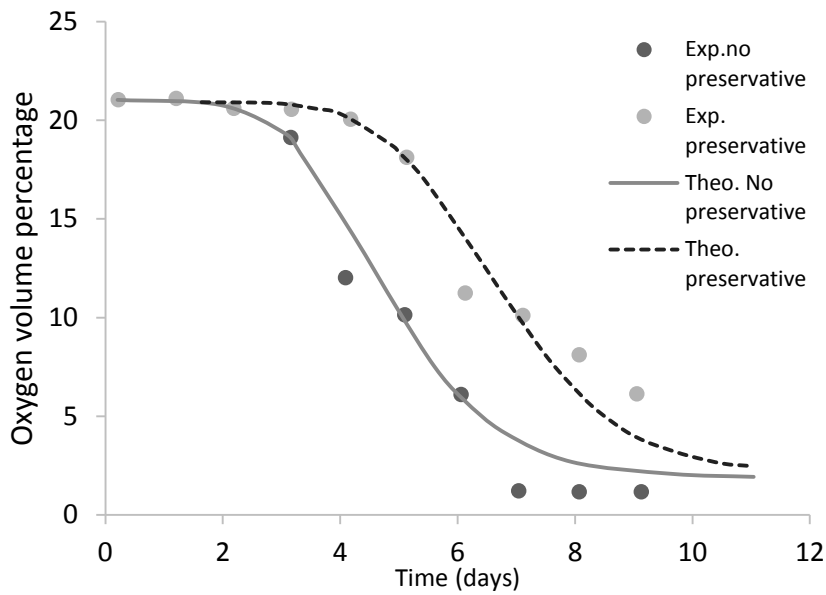


**Figure 1.3: Headspace oxygen analysis in soy bread with and without preservative initially packaged with air, tested by the experimental and mathematical model methods (Pascall et al., 2008).**

On the other hand, van Bree (2010) proposed a simulation tool to predict and compare the amount of oxygen that permeates through various multilayer packaging configurations i.e. films, trays with top foils and bottles with caps. The model takes into account the influence of factors such as the time-temperature profile, type of polymer, film layer composition, film thickness, volume of the headspace and residual oxygen level at the start of storage.

The permeability model is just a transfer of the molecules through the film by a sorption-diffusion-desorption mechanism, driven by the difference in partial pressure across the film, thus this calculation just takes into account oxygen that enters to the package. To include oxygen that is consumed they include two options: respiration by fresh-cut vegetables or oxygen scavengers.

To predict the consumption of oxygen by fresh-cut vegetables, the model designed by Jacxsens, et al 200 was used. To predict the effect of oxygen scavengers, the software has an option to consider active packaging material and is based in results presented by Tewari et al. (2002), where was reported for different commercial oxygen scavengers, mostly based on iron oxidation, a first order absorption kinetic. Then consumption of oxygen by the oxygen scavengers and the remaining concentration in the headspace is given by Equation 1.5.

$$\ln(O_2) = -k*t + \ln(O_2)_{init} \quad (1.5)$$

where  $k [h^{-1}]$  is the absorption rate constant and  $(O_2)_{init}$  the initial oxygen concentration (%). Tewari et al.(2002) propose the values presented in the table 1.1 for various commercial oxygen scavengers to evaluate the effect of temperature based in a model of Arrhenius (Equation 1.6).

$$k = K e^{-E/RT} \quad (1.6)$$

**Table 1.1: Arrhenius equations for different oxygen scavengers (Tewari, Jayas, Jeremiah, & Holley, 2002)**

<b>Scavenger-name</b>	<b>Scavenger-reaction</b>	<b>Atmosphere</b>	<b>Arrhenius equation for the absorption rate constant k<sup>a</sup></b>
Ageless® FX-100	Iron oxidation	Air N <sub>2</sub> +air	k=484077.4 exp <sup>(-6004.03/T)</sup> k=0.005 exp <sup>(-1118.23/T)</sup>
Bioka® S-100	Enzyme mediated oxidation	Air N <sub>2</sub> +air	k=13082.1 exp <sup>(-5379.43/T)</sup> k=2.04 exp <sup>(-3169.74/T)</sup>
FreshPax® M-100	Iron oxidation	Air N <sub>2</sub> +air CO <sub>2</sub> +air	k=1636 exp <sup>(-5301.5/T)</sup> k=7404511.2 exp <sup>(-7703.6/T)</sup> k=1480.3 exp <sup>(-5129.87/T)</sup>
FreshPax® R-300	Iron oxidation	Air N <sub>2</sub> +air	k=0.006 exp <sup>(-881.25/T)</sup> k=0.41 exp <sup>(-2487.72/T)</sup>

<sup>a</sup> k :rate constant (s<sup>-48</sup>) ; T :Temperature (K)

The atmospheric condition “air” in Table 1,1 refers to high oxygen concentration (20.9%), while “N<sub>2</sub>+air” refers to initial concentration of 0.05%. In the case of van Bree et al (2010), they only include k-values of the scavenger materials for the high oxygen levels and affirm that low concentrations (0.05%) are already considered by many food companies to be equal to zero and the packaging limit for residual oxygen is often considered to be above 0.5%. This exclusion could be not totally appropriate because highly sensitive-oxygen products are affected even by these low concentrations and oxygen scavengers can exert their function to enlarge shelf life and to improve quality to this type of products.

Plotting Ln (K) against E/R (Figure 1.4) is obtained a straight line of slope (a) 0.0035. This means that the results obey a compensation law with a compensation temperature T<sub>C</sub> = a<sup>-1</sup> = 285.7 K (12.6 °C). The fact that the compensation temperature is so close to the experiment temperature, the unexplained differences of activation energies between air and nitrogen + air, and the fact that activation energies are so sharply linked with pre-exponential factors despite the apparent absence of coherence in the results indicate that Arrhenius parameter values are probably not significant.

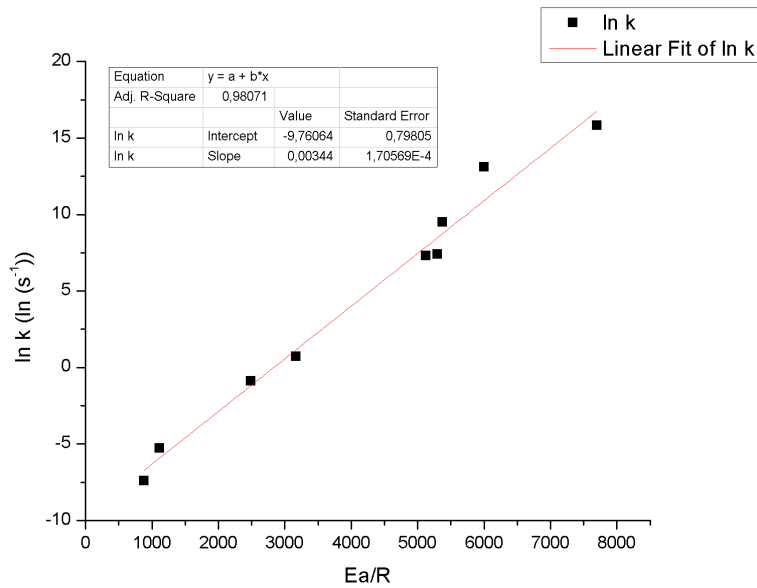


**Figure 1.4: Plot of ln K vs. E/R of the values obtained by Adapted from Tewari et al. (2002)**

The work of van Bree et al. (2010) obtained good agreement between the model and experimental data from non-invasive measures with OxySense® T210 for passive barriers (Figure 1.5).

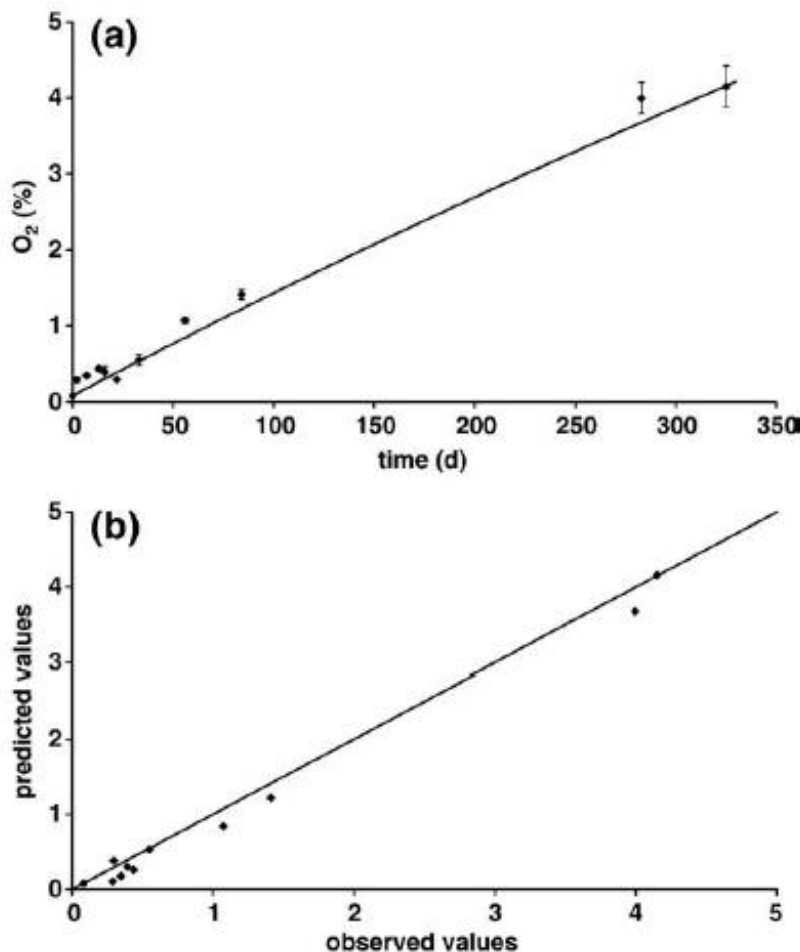


**Figure 1.5: (a) Oxygen ingress through a PE/PA multilayer film (Entplater, 30°C). (b). Predicted versus observed values for the PE/PA multilayer film (van Bree et al., 2010).**

Summarizing, the simulation tool of van Bree et al. (2010) is mostly centred in permeation of passive barriers and there is a lack of depth study about the reactions for oxygen scavengers, which can be useful to incorporate in the option of active packaging in the simulation tool.

In the present thesis, models for oxygen scavengers composed by unsaturated fatty acids are proposed. The model proposed is based on the chemical reactions involved in the oxidation of C-H bonds adjacent to double bonds as active sites. This is a different approach than those used by van Bree et al. (2010) in their simulation tool and done by Tewari et al. (2002) who determined the order of reaction from the experimental data, using plots of the natural logs of volume of oxygen remaining in the pack atmosphere  $[A]_0$  vs. time and plots of the reciprocals of  $[A]_0$  vs. time. In all the commercial scavengers studied by Tewari et al. (2002) the  $\log_n$  plot was approximated to a straight line, then first order was assumed.

Experimental approaches like done by Tewari et al. (2002) are not extrapolated to other oxygen scavengers, even if they have the same mechanism because there is no direct relationship with the chemical reactions involved.

Concerning modelling of permeation through active packaging, one relevant analysis was presented by Solovyov & Goldman, 2006a from Alcoa Closure Systems International, Inc. They proposed a theory of transient permeation through homogeneous and multilayer reactive polymeric structures in two stages: first, at steady state for homogeneous passive and reactive media assuming catalytic scavenger<sup>2</sup>; and a second stage, without the assumption of catalytic scavenger and including transient permeation theory across multilayer structures with active and passive layers.

They obtained profiles of flux and concentration of solutes with respect to film thickness, and they presented practical analytical solutions for systems with reactive-diffusive transport in solids (Figure 1.6).

Other mathematical model for predicting transient barrier properties of polymer oxygen scavengers in a matrix of a barrier polymer was presented by Ferrari et al, 2009. They considered a shrinking core model for oxygen consumption by the particles of the oxygen scavenger, and treat oxygen diffusion in the matrix polymer by a one-dimensional approximation.

With the shrinking core model, Ferrari considered the reaction of scavenging being fast compared to the diffusion process in the particle shell, so when oxygen reaches the surface of the core it reacts immediately and diffusion of oxygen in the matrix can be approximated as a function only of the coordinate axis in the thickness direction and time.

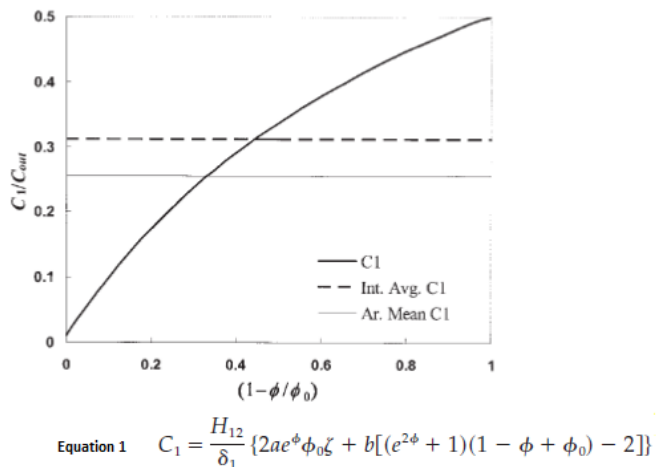


**Figure 1.6: Evolution of interfacial concentration at the reactive side ( $C_1$ ) in the reactive-passive (RP) film: Thiele modulus  $\phi_0=3.16$ , solute partition coefficient  $H_{12}=1$ , and dimensionless parameter of size  $\zeta=1$  (Solovyov & Goldman, 2006b).**

Ferrari (2009) assumes spherical particles and a continuum, where all the properties and variables are averages over a particular film volume and in terms of kinetics assumes a simple first order surface reaction between the polymer-scavenger and the oxygen. Let us notice that this kind of

<sup>2</sup> Catalytic scavenger means that concentration of active scavenging sites  $R$  is in excess of the stoichiometric amount of oxygen and therefore  $R$  remains constant.

model would not apply to the case where the oxygen absorber would be miscible with the polymer i.e. would form a single phase with this latter.

Carranza, et al (2012) solved the model proposed by Ferrari et al. (2009) analytical and numerically using an explicit finite difference method, and as result they obtained profiles of concentration and flux with respect to time and space. They began with a monolayer model and extended their research to multilayer structures and polymer blends (Figure 1. 7)(Ferrari et al., 2009).

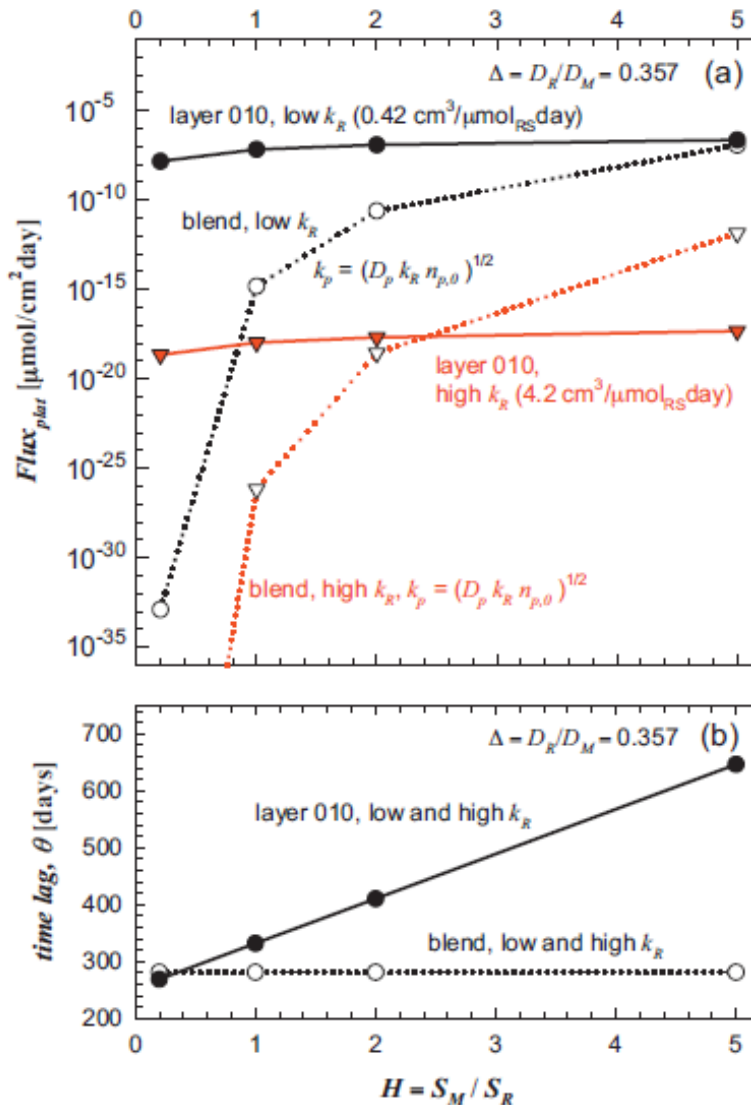


**Figure 1.7:** Comparison of (a) downstream flux plateau in log scale and (b) time lag  $\theta$  in linear scale as a function of partition coefficient  $H$ , for a film with three layers versus a polymer blend (analytical predictions). (a) The multilayer plateau is evaluated for two bulk reaction rates  $k_R$ . All parameter values are the same for the blend and multilayer films and are given in Table 1.2 (Carranza, Paul, & Bonnecaze, 2012).

**Table 1.2:** List of parameters for comparison between homogeneous, blend and multilayer film (Carranza et al., 2012).

Name	Symbol	Value
------	--------	-------

Partition coefficient	H	$H = S_m/S_p$ for polymer blend, $H = S_M/S_R$ for multilayer films, dimensionless.
Total film thickness	L	0.025 cm (250μm)
Volume fraction of reactive layers	ϕ	0.1
Initial concentration of reactive sites in reactive layers or particles	$n_{R,0}$ for reactive layers; $n_{P,0}$ for reactive particles	8000 μmol <sub>RS</sub> /cm <sup>3</sup>
Initial concentration of reactive sites in homogeneous film	$n_0 = \phi n_{P,0}$ to match content of blend	800 μmol <sub>RS</sub> /cm <sup>3</sup>
Stoichiometric coefficient	û	2μmol <sub>RS</sub> /μmol <sub>O<sub>2</sub></sub>
Oxygen solubility coefficient for the inert matrix layers or inert matrix in blend	$S_M$ for inert matrix layer $S_m$ for inert matrix in polymer blend	4.38 μmol <sub>O<sub>2</sub></sub> /cm <sup>3</sup> atm
Oxygen diffusion coefficient for the inert matrix layers or inert matrix in blend	$D_M$ for inert matrix layer	4.84×10 <sup>-4</sup> cm <sup>2</sup> /day
Oxygen solubility coefficient for the reactive layers or particles	$S_R$ for reactive layers	4.38 μmol <sub>O<sub>2</sub></sub> /cm <sup>3</sup> atm
Oxygen diffusion coefficient for the reactive layers or particles	$D_R$ for reactive layers	1.73×10 <sup>-4</sup> cm <sup>2</sup> /day
Bulk reaction rate constant for particles	$k_R$	0.42 and 4.2 cm <sup>3</sup> /μmol <sub>RS</sub> day, as indicated
Surface reaction rate constant for particles	$k_p = \sqrt{k_R D_p n_{P,0}}$ to match the rate for multilayer film	

In general, the models for permeation in active layers establish reactions of first order for the oxygen scavenger, and do not evaluate possibilities of more complex kinetics, or the effect of variables, as temperature, over the rate reaction. Furthermore, other properties of the active layer will be influenced for the reaction oxygen-scavenger, as for example diffusivity, solubility, and properties related with polymer degradation.

## 1.6 Incorporation of OS in polymer matrices

Thermal degradation, migration and oxygen scavenging effect are some of the most important phenomena that must be taking into account by adding OS in polymer matrices to form active packaging structures.

For the case of linseed oil as OS, exothermic thermo-oxidation occurs between 150°C and 250°C (Lazzari & Chiantore, 1999) coinciding with processing temperatures of most of polymers used in the packaging sector as LDPE, HDPE, PP and PET (Figure 1.8).

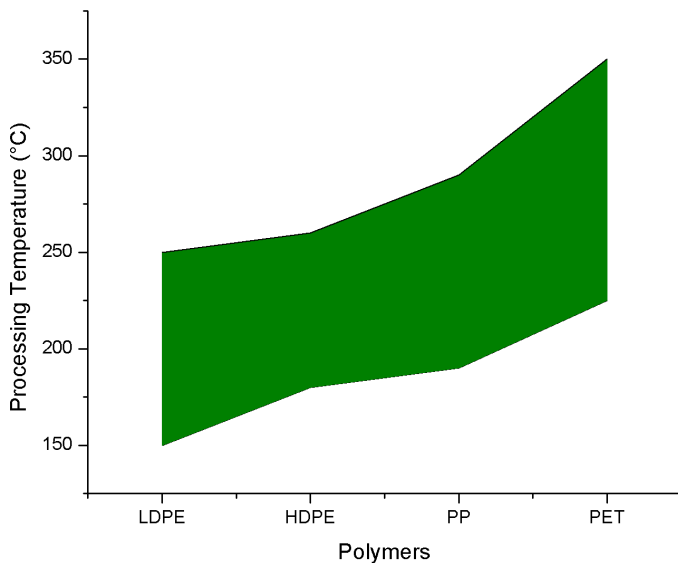


**Figure 1.8: Processing temperatures of low density polyethylene (LDPE), high density polyethylene (HDPE), polypropylene (PP) and polyethylene terephthalate (PET). Data extracted from (Strong, 2006)**

Two ways were proposed by the *Grupo de Materiales y Manufactura* (CIPP-CIPEM) of *Universidad de los Andes* to insert OS in polymers: adsorption in powdered activated carbon (Joven, Garcia, Arias, & Medina, 2014) and encapsulation in silica-gel (Medina, García, Arias, & Joven, 2010).

Pore size and pore volume of two types of activated carbon were characterized by means of an adsorption isotherm of nitrogen (adjust BET) in a Quantachrome Autosorb-1, obtaining in the best case an superficial area of  $986.4 \text{ m}^2/\text{g}$  for granular activated carbon, results are presented in Figure 1.9.

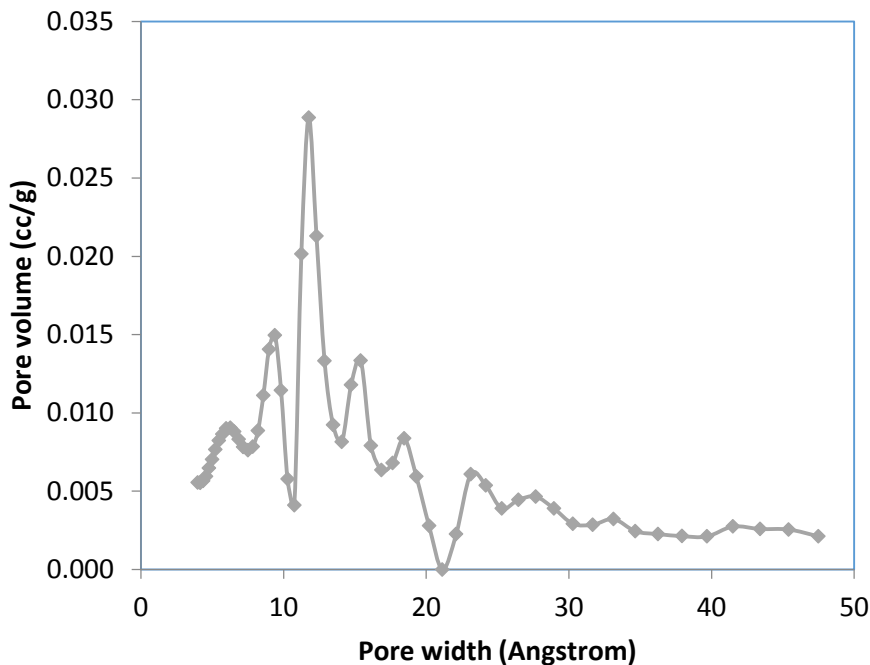


**Figure 1.9: Results for adsorption isotherm for granular activated carbon.**

Sol-gel encapsulation in silica was proposed because has been effective to protect organic compounds of the effect of temperature (Brinker, Ashley, Bhatia, & Singh, 2002; Cestari & Airolidi, 1997) and also because its porous characteristics can support the initial load of OS and its oxidation products (Baez Q., Sáenz G., & Rodriguez N., 2007).

Sol-gel encapsulation of organic molecules and biomolecules route proposed in US Patent 6495352 (Brinker et al., 2002) can improve hardness, optical clarity and chemical durability of the encapsulated substances and to provide defined porosity and give heat resistance.

## 1.7 Summary of bibliographic information

Kinetic information of OS only comes from experimental data regression (Berenzon & Saguy, 1998; Charles et al., 2006; F. Soares et al., 2009), and there is a lack between experimental data and oxidation reactions, and their corresponding kinetic rates (Section 1.2). On the other hand, even though oxidation path reaction of linseed oil has been proposed there is no values of the kinetic constants, and less information is found at low or moderate temperatures (<150°C) (Lazzari & Chiantore, 1999).

In this thesis, thermo-oxidation of linseed oil, including kinetic rates, will be studied and modelled at moderate temperatures, with the aim to solve the questions about the efficiency of linseed oil as OS thermo-activated ; in addition to the technique of measurements of oxygen concentration in

confined spaces (HS-O<sup>3</sup>) normally used for OS, an alternative of TGA is proposed. Also, the sol-gel reaction to encapsulate linseed oil will be studied in order to analyse its effect over oxygen uptake capacity.

## 1.8 Objectives

Based on the review and previous work, this doctoral thesis has two objectives. One technological objective oriented to evaluate the effect of processing variables over the scavenger efficiency of linseed oil encapsulated, and a scientific main objective to propose a kinetic model for the thermo-oxidation of unsaturated fatty substances. The latter objective will be divided in the following specific objectives:

- Calculate a theoretical oxygen uptake capacity (OC) of Linseed oil based in its chemical compositions.
- Validate TGA as a method to follow scavenging capability of OS.
- Comparison of theoretical and experimental oxygen uptake of Linseed oil, under different experimental methods.
- Kinetic modelling of thermo-oxidation of Linseed oil.

## 1.9 Strategy

At following the strategy to accomplish each specific objective.

### 1.9.1 To evaluate the effect of processing variables over the scavenger efficiency of linseed oil encapsulated.

#### *Strategy*

1. Evaluate effect of catalyst in oxygen uptake capacity of linseed oil encapsulated.
2. Evaluate process variables of milling (mass ratio ball/sample, time) and particle size over oxygen uptake capacity of linseed oil encapsulated.
3. Evaluate process variables of film manufacturing over oxygen uptake capacity of linseed oil encapsulated.

### 1.9.2 Calculate a theoretical oxygen uptake capacity (OC) of Linseed oil based in its chemical compositions.

#### *Strategy*

---

<sup>3</sup> HS-O = Notation used for experiments of HeadSpace Oxygen concentration

1. Chemical characterization of Linseed oil: this oil is a complex compound whose composition varies in function of method of extraction, main source and location. Specific oil used in this thesis will be characterized by Infrared spectroscopy (FTIR) and gas chromatography (GC) to identify functional groups susceptible to oxidation.
2. Potential oxidation capacity of linseed oil will be calculated based on its content of double bonds and corresponding adjacent allylic carbons (Richaud et al., 2012).

#### **1.9.3 Validate TGA as a method to follow scavenging capability of OS.**

Isothermal tests in a thermogravimetric device are proposed to follow the weight increase because oxygen-uptake in thermo-oxidation. These experiments will be done at linseed oil but also to unsaturated fatty esters (UFE) similar, in carbon length, to components of linseed oil, they will be *model substances* to understand thermogravimetric results in oxidative and non-oxidative atmospheres. Data from model substances will be useful for simulation stage and avoid possible synergic effects that can occur in a complex substance like linseed oil which can have in its composition metals, water or other substances not identified.

Headspace measurements (HS-O) will be done to linseed oil, in order to compare with TGA data.

#### **1.9.4 Comparison of theoretical and experimental oxygen uptake of Linseed oil, under different experimental methods.**

##### *Strategy*

1. Measurement of presence of hydro peroxides: Besides results of TGA and headspace, iodometric titrations will be made to measure peroxide concentration at different times and temperatures because hypothesis of path reaction include their formation.
2. Comparison between theoretical potential of oxidation, obtained by chemical characterization, and experimental results (HS-O and TGA).

#### **1.9.5 Kinetic modelling of thermo-oxidation of Linseed oil.**

A classical model of auto-oxidation mechanism based on active allylic hydrogens is proposed for the model substances (UFE). Kinetic equations will be statement and corresponding differential equation system will be solved in Matlab. Some parameters for oxygen excess atmospheres will be extracted from Richaud et al., 2012 , and others like kinetic rates of radicals reactions will be obtained from experimental data.

Kinetic rates of the model substance methyl linolenate will be used for linseed oil because is the molecule more approximate to linolenic acid (content of 52.6% in linseed oil) and oxygen uptake of active films containing linseed oil and polypropylene will be simulated, evaluating the effect of film thickness and headspace atmosphere (content of oxygen).

Results obtained in this thesis will give more information about thermo-oxidation of linseed oil and UFE to be used in active packaging, but will be also helpful for the field of food conservation, in themes of oxidation of edible oils, additives, and efficiency of antioxidants.

## References

- Baez Q., C. A., Sáenz G., M. C., & Rodriguez N., G. (2007). Estudio de las condiciones de reacción para la obtención de Sílica Gel Adsorbente (SGA). *Ingeniería e investigación*, 44-50.
- Berenzon, S., & Saguy, I. S. (1998). Oxygen Absorbers for Extension of Crackers Shelf-life. *Lebensmittel-Wissenschaft und-Technologie*, 31(1), 1-5. doi:10.1006/fstl.1997.0286
- Brinker, C. J., Ashley, C. S., Bhatia, R., & Singh, A. K. (2002). *Sol-gel method for encapsulating molecules* (US Patent 6495352). Retrieved from
- Brody, A. L., & Budny, J. A. (1995). Enzymes as active packaging agents *Active food packaging* (pp. 174-192): Springer.
- Brody, A. L., Strupinsky, E. R., & Kline, L. R. (2001). Active Packaging for Food Applications. . Pennsylvania: Technomic Publishing Company. .
- Carranza, S., Paul, D. R., & Bonnecaze, R. T. (2012). Multilayer reactive barrier materials. *Journal of Membrane Science*, 399–400(0), 73-85. doi:<http://dx.doi.org/10.1016/j.memsci.2012.01.030>
- Cestari, A. R., & Airoldi, C. (1997). Diamine Immobilization on Silica Gel through the Sol-Gel Process and Increase in the Organic Chain by Using Glutaraldehyde followed by Ethylenediamine. *Langmuir*, 2681-2686.
- Charles, F., Sanchez, J., & Gontard, N. (2006). Absorption kinetics of oxygen and carbon dioxide scavengers as part of active modified atmosphere packaging. *Journal of Food Engineering*, 72(1), 1-7. doi:10.1016/j.jfoodeng.2004.11.006
- Comision Europea. (2009). REGLAMENTO (CE) No. 450/2009 sobre materiales y objetos activos e inteligentes destinados a entrar en contacto con alimentos (pp. 9). Diario Oficial de las Comunidades Europeas.
- Cooksey, K. (2002). Oxygen Scavenging Packaging Systems *Encyclopedia of Polymer Science and Technology*: John Wiley & Sons, Inc.
- Day., B. P. F. (2008). *Active Packaging of Food. Smart Packaging Technologies for Fast Moving Consumer Goods*: John Wiley & Sons, Ltd.
- Dlugogorski, B. Z., Kennedy, E. M., & Mackie, J. C. (2012). Low temperature oxidation of linseed oil: a review. *Fire science reviews*, 1(1), 1-36.

- F. Soares, N. d. F., S. Pires, A. C., Camilloto, G. P., Santiago-Silva, P., P. Espitia, P. J., & A. Silva, W. (2009). Recent patents on active packaging for food application. *Recent patents on food, nutrition & agriculture*, 1(2), 171.
- Ferrari, M. C., Carranza, S., Bonnecaze, R. T., Tung, K. K., Freeman, B. D., & Paul, D. R. (2009). Modeling of oxygen scavenging for improved barrier behavior: Blend films. *Journal of Membrane Science*, 329(1-2), 183-192. doi:10.1016/j.memsci.2008.12.030
- Floros, J. D., Dock, L. L., & Han, J. H. (1997). Active packaging technologies and applications. *Food Cosmetics and Drug Packaging*, 20(1), 10-17.
- Gill, C. O., & McGinnis, J. C. (1995). The use of oxygen scavengers to prevent the transient discoloration of ground-beef packaged under controlled, oxygen-depleted atmospheres (Vol. 41, pp. 19-27): Meat Science.
- Joven, R., Garcia, A., Arias, A., & Medina, J. (2014). Development of an Active Thermoplastic Film with Oxygen Scavengers Made of Activated Carbon and Sodium Erythorbate. *Packaging Technology and Science*.
- Krämer. (2006). New Packaging Technology for IVD - Dealing with Oxygen. [www.s-cpp.com:](http://www.s-cpp.com/) Süd-Chemie Performance Packaging.
- Lazzari, M., & Chiantore, O. (1999). Drying and oxidative degradation of linseed oil. *Polymer degradation and stability*, 65(2), 303-313.
- Medina, J., García, Á., Arias, A., & Joven, R. (2010). Colombia Patent No. SIC: S. d. I. y. C. SIC.
- Miltz J, & MR., P. (2000, June 14-18). *Active packaging technologies:oxygen scavenging* Paper presented at the Intl. Assoc. of Packaging Res Inst. Annual Symposium., San Jose State Univ., San Jose, Calif.
- Pascall, M. A., Fernandez, U., Gavara, R., & Allafi, A. (2008). Mathematical modeling, non-destructive analysis and a gas chromatographic method for headspace oxygen measurement of modified atmosphere packaged soy bread. *Journal of Food Engineering*, 86(4), 501-507. doi:10.1016/j.jfoodeng.2007.11.001
- Plastemart. (2011). Global active, smart and intelligent packaging for food and beverages: trends and forecasts to 2015. Retrieved from <http://www.plastemart.com/Plastic-Technical-Article.asp?LiteratureID=1679&Paper=global-active-smart-intelligent-packaging-food-beverages-trends-packaging-manufacturers>
- Richaud, E., Audouin, L., Fayolle, B., Verdu, J., Matisová-Rychlá, L., & Rychlý, J. (2012). Rate constants of oxidation of unsaturated fatty esters studied by chemiluminescence.

*Chemistry and Physics of Lipids*, 165(7), 753-759.  
doi:<http://dx.doi.org/10.1016/j.chemphyslip.2012.09.002>

Rooney, M. L. (1992). *Reactive packaging materials for food preservation* Paper presented at the First Japan–Australia workshop on Food Processing Tsukuba, Japan.

Smith, J. P., Hoshino, J., & Abe, Y. (1995). *Interactive packaging involving sachet technology*. (B. A. a. Professional Ed.). London.

Solovyov, S. E., & Goldman, A. Y. (2006a). Optimized design of multilayer barrier films incorporating a reactive layer. I. Methodology of ingress analysis. *Journal of Applied Polymer Science*, 100(3), 1940-1951. doi:10.1002/app.23433

Solovyov, S. E., & Goldman, A. Y. (2006b). Optimized design of multilayer barrier films incorporating a reactive layer. II. Solute dynamics in two-layer films. *Journal of Applied Polymer Science*, 100(3), 1952-1965. doi:10.1002/app.23439

Strong, A. B. (2006). *Plastics. Materials and processing*: Pearson Prentice Hall.

Tewari, G., Jayas, D. S., Jeremiah, L. E., & Holley, R. A. (2002). Absorption kinetics of oxygen scavengers. *International journal of food science & technology*, 37(2), 209-217.

# III

## Materials and methods

---

### INDEX OF FIGURES 48

### RESUME DU CHAPITRE II 49

---

INTRODUCTION	50
2.1 MATERIALS	50
2.2 SOL-GEL ENCAPSULATION	50
2.3 MANUFACTURING OF ACTIVE FILMS	53
2.4 OXYGEN CONCENTRATION IN HEADSPACE	53
2.5 CHEMICAL CHARACTERIZATION	54
2.5.1 <i>Gas chromatography (GC)</i> .....	54
2.5.2 <i>Fourier Transform Infrared spectroscopy (FTIR)</i> .....	54
2.6 TGA AS TECHNIQUE TO EVALUATE OXYGEN UPTAKE CAPABILITY	54
2.7 DETERMINATION OF THE PEROXIDE VALUE BY IODOMETRIC TITRATION METHOD	55
2.7.1 <i>Principle</i> .....	55
2.7.2 <i>Calculation of Peroxide value (PV)</i> .....	55
2.7.3 <i>Reagents</i> .....	56
2.7.4 <i>Procedure</i> .....	56
2.8 KINETIC MODEL	56
REFERENCES	57

## **INDEX OF FIGURES**

FIGURE 2.1 BLOCK DIAGRAM OF SOL-GEL ENCAPSULATION .....	51
FIGURE 2. 2. LABORATORY MATERIALS TO DO SOL-GEL ENCAPSULATION.....	52
FIGURE 2.3: BALL MILL USED TO DIMINISH THE BULK SIZE OF MATERIALS ENCAPSULATED IN SILICA GEL .....	52
FIGURE 2.4: ATR ACCESSORY USED TO COLLECT SPECTRA OF LIQUIDS. ....	54

## Résumé du chapitre II

Le deuxième chapitre est consacré à la description des matériaux et substances étudiés et aux méthodes de caractérisation utilisées.

L'encapsulation sol-gel de l'OS était réalisée par une méthode partant du silicate de sodium. L'OS encapsulé était ensuite incorporé au polypropylène (PP) par extrusion.

Pour la caractérisation de l'Huile de Lin on a utilisé la chromatographie gazeuse (GC) qui permet de séparer les différents esters gras. On a également utilisé la spectrophotométrie infra-rouge (IR) pour l'analyse des groupements résultant de l'oxydation ou détruits par l'oxydation (doubles liaisons).

L'analyse thermique différentielle (DSC) a été utilisée pour caractériser les transitions éventuelles à  $T < 250^{\circ}\text{C}$  et les évènements exothermiques en présence d'oxygène. La thermogravimétrie (TGA) a été utilisée pour caractériser les pertes par évaporation en atmosphère neutre et la prise de masse liée à l'oxydation en présence d'oxygène.

Les performances d'OS ont été caractérisées par des mesures de consommation d'oxygène dans des cellules fermées contenant l'OS. L'oxygène résiduel est dosé par voie électrochimique. L'état d'oxydation de l'OS est également caractérisé par dosage des hydro peroxydes par la méthode classique utilisant la réaction iodure  $\rightarrow$  iode.

## Introduction

In this chapter, techniques proposed in strategy section are described. At the beginning, techniques related with technological objective are presented; it means, methods to obtain, characterize and include sol-gel encapsulates in polymer matrices are described. Section 2.4 describes the method to measure oxygen concentration in headspace, which is used to measure scavenger performance in both objectives.

In section 2.5 begins the explanation of tests related with the scientific objective, starting with methods used for chemical characterization, section 2.6 described the use of thermogravimetric analyses to following oxygen uptake, section 2.7 explains titration to calculate peroxide index, and section 2.8 makes reference to the software used for solve the model of thermo-oxidation.

### 2.1 Materials

Linseed oil double boiled (DISPROALQUIMICOS, Colombia) was used in this research, according bibliography this oil variety is produced by adding a mixture of hydrocarbon solvents and metallic dryers to the raw oil. Chemical characterization is explained in section 2.5.

As *models substances* were used three unsaturated fatty esters: methyl oleate, methyl linoleate and methyl linolenate, more described in chapter IV.

### 2.2 Sol-Gel Encapsulation

Encapsulation by sol-gel reaction initiates with the formation of the sol with industrial grade sodium silicate (Properties in Table 2.1, JADESI LTDA) and hydrochloric acid 1.55M. Process continues with agitation and pH control, when pH reaches values between 1 to 3<sup>1</sup> substances to be encapsulated are added, continuing stirring and adding sodium silicate until gel is obtained.

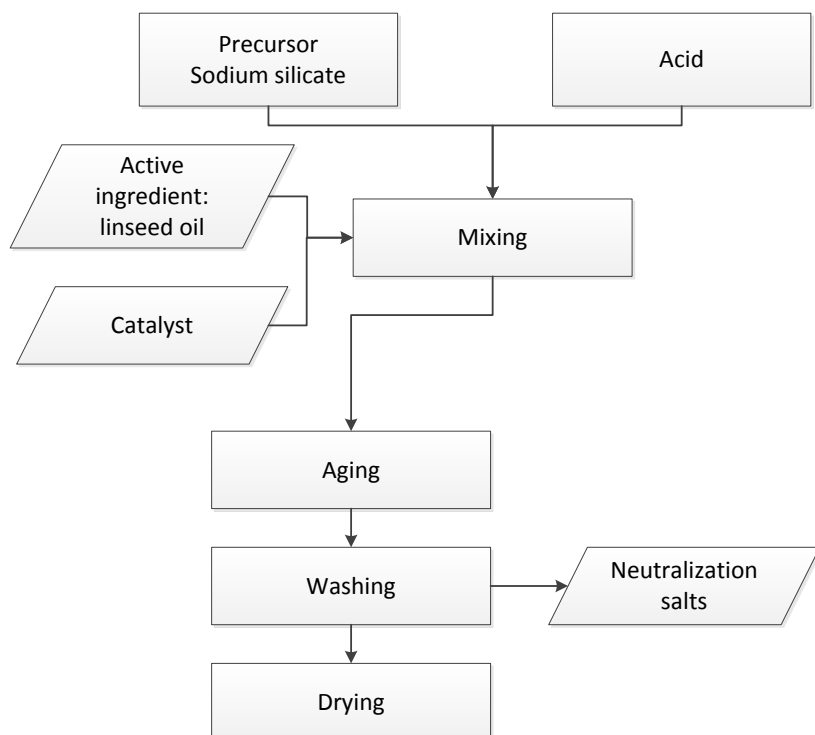
Gel is left at ambient conditions for 24 hours (aging) to facilitate the contraction of the bonds Si-O-Si, after is washed with distilled water to remove the salt produced by the reaction and filtered in vacuum and dried in a oven. Material is dried in a oven at atmospheric pressure and 60 °C until weight change of less of 1% is obtained. Figure 2.1 illustrates block diagram of the process.

---

<sup>1</sup> Study of the influence of pH of addition in the oxygen scavenging capacity was done in (Aguilar Palomo, Medina Perilla, & Garcia Mora, 2013).

**Table 2.1 Properties of sodium silicate, industrial grade.**

Property	Value
Density °Bé 20°C	50+/-1
Specific gravity	1.48 a 1.5
Alkalinity (%Na <sub>2</sub> O)	12.5+/-1
Silica content (%SiO <sub>2</sub> )	31.20 a 33.15
Ratio (Na <sub>2</sub> O:SiO <sub>2</sub> )	1:2.10 a 1:2.40 (Brinker, Ashley, Bhatia, & Singh, 2002) recommend ratio from 1:1.5 to 1:4
Viscosity	600 a 850 centipoise
pH	12±0.5

**Figure 2.1 Block diagram of sol-gel encapsulation**

For sol-gel manufacturing two different laboratory mounts were used, magnetic stirred to obtain small volumes and Ultraturrax agitation for bigger ones; illustrative pictures of the latter are presented in Figure 2.2.

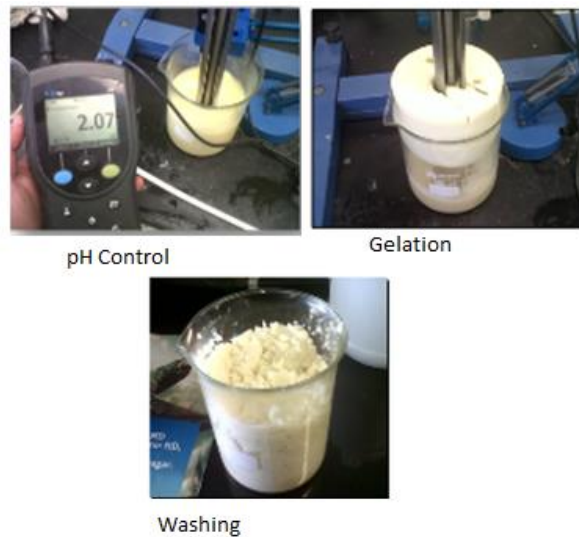


**Figure 2.2. Laboratory materials to do sol-gel encapsulation.**

Material dried is milled in a ball mill (US, STONEWARE) (Figure 2.3) at 48 RPM angular velocity, three different mass ratios sample/balls were studied: 1/5, 1/10, 1/15 and 1/20, and two milling times: 90minutes and 180 minutes. Each milling was done in batches of 30grams of sample. Sample milled is finally sieved and classified by size.



**Figure 2.3: Ball mill used to diminish the bulk size of materials encapsulated in silica gel.**

Sol-gel encapsulation of active ingredients, different from linseed oil, are presented in other publications: Aguilar Palomo et al., 2013; García, 2010; Salas, 2011 . In this thesis, linseed oil encapsulation is presented, and variables of milling, size and blending with polymers studied.

Oxygen scavengers encapsulated were analysed by infrared spectroscopy (FTIR)<sup>2</sup> to identify functional groups from active ingredients and from silica gel, also they were observed by scanning electron microscopy (JEOL-Model JSM 6490-LV) to measure the effect of processing, specifically milling, in the particle size.

<sup>2</sup> More description of FTIR is presented in section 2.5

## 2.3 Manufacturing of active films

Materials proposed as OS were encapsulated and after blended with Homo-polymer polypropylene (Ref 03H96), used in flexible packaging. Blends of 1% of OS<sub>E</sub><sup>3</sup> and 99% polypropylene, were done in a mixer brabender PlasticCorder, in a multipurpose single screw extruder (BRABENDER) which has L/D ratio 25:1, and in a twin screw extruder (BRABENDER, model TSE 30) which has compression ratio 1:3 and L/D 25:1. Temperature profiles oscillated between 160°C and 200°C, and they are specified in each experiment.

## 2.4 Oxygen concentration in headspace

Measurements of oxygen concentration in time into headspace are a usual technique established to follow performance of oxygen scavengers (Berenzon & Saguy, 1998; Durango, De FÁTIMA Soares, & Arteaga, 2011; Tewari, Jayas, Jeremiah, & Holley, 2002). In this research oxygen was followed with a portable spot check oxygen analyser Model 901 (Quantek) which takes a sample of the atmosphere contained in the headspace with a syringe type system and in its inner has a “fuel cell” type of oxygen sensor.

"Fuel cell" oxygen sensors consist of a diffusion barrier, a sensing electrode (cathode) made of a noble metal such platinum, and a working electrode made of a base metal such as lead or zinc immersed in a basic electrolyte (such as a solution of potassium hydroxide)(George, 1996).

Oxygen diffusing into the sensor is reduced to hydroxyl ions at the cathode:



Hydroxyl ions in turn oxidize the lead (or zinc) anode:



This yields an overall cell reaction of:



Fuel cell oxygen sensors are current generators. The amount of current generated is proportional to the amount of oxygen consumed (Faraday's Law). The instrument monitor the current output of the sensor (George, 1996).

Each composition studied: linseed oil, linseed oil/Catalyst, linseed oil encapsulated (LO-E) and active films (LO-E blended with polypropylene) was evaluated with the oxygen analyser; corresponding results are presented in the next chapter specifying sample mass and headspace volume.

---

<sup>3</sup> OS<sub>E</sub>= Oxygen Scavenger Encapsulated in silica.

Each sample was punctured once and the device was calibrated with the shortest time (2 seconds), because once punctured the sample can be affected by the outside atmosphere. Three replicates and two empty containers were measured each time to manage the bias error related with puncturing. The analyser Quantek model 901 has a resolution of 0.1% and accuracy  $\pm 1\%$  of reading. Currently, there are analysers which avoid errors caused by puncturing, which are non-invasive (See Dansensor® or ImPULSE® sensors).

## 2.5 Chemical characterization

### 2.5.1 Gas chromatography (GC)

The method (A.O.C.S) Ce1-62 by the American Oil Chemist's Society (Firestone, 2009) was used to determine the fatty acid profile of linseed oil. 2 ml. of NaOH dissolved in methanol are added to 100 mg of sample which is heated under reflux during 30 minutes, 2ml. of Boron trifluoride are added and heated under reflux during 30 minutes, after 4ml. of n-heptane added and heated under reflux for 5 minutes, 20 ml of a saturated solution NaCl added to eliminate aqueous phase, after the sample is washed with water, three times and dried with sodium sulphate. With the reaction described Methyl esters of fatty acids are obtained and separated to be determined quantitatively in Gas chromatography (Equipment: Agilent 7890 A) using a packed column (88% cianopropyl)-Aryl-Polysiloxane of 60m x 0.25mm x 0.2 $\mu$ m.

### 2.5.2 Fourier Transform Infrared spectroscopy (FTIR)

FTIR spectra of the linseed oil was acquired on a Nicolet 380 Fourier transform infrared spectrometer (Nicolet Instrument Inc., Madison, WI) in order to see functional groups susceptible to oxidation. The instrument was purged with nitrogen; all spectra were recorded from 4000 to 400  $\text{cm}^{-1}$ , co-adding 32 interferograms at a resolution of 4  $\text{cm}^{-1}$ . Attenuated total reflectance (ATR) accessory was used to analyse the liquid (Figure 2.4); three replicates were analysed and after the spectra were averaged in the software Essential FTIR.



**Figure 2.4: ATR accessory used to collect spectra of liquids.**

### 2.6 TGA as technique to evaluate oxygen uptake capability

TGA is proposed in this thesis as a method to evaluate oxygen-uptake efficiency of OS, alternative to usual Headspace measurements.

In the presence of oxygen, an increase in the mass of the oils caused by oxidative reactions is expected. Samples of UFE and linseed oil were analysed using TGA 500 (TA Instruments) with isothermal tests at 60°C, 80°C and 110°C and a heating rate of 20°C/min.

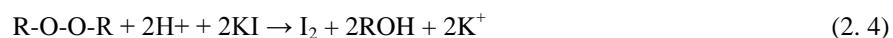
Thermal curves were obtained under nitrogen, air and pure oxygen atmospheres. In order to improve repeatability and reproducibility, and to avoid the effect of heat transmission by diffusion in TGA analysis, the mass in all the experiments was, in average, 4mg and duplicates were done in all cases.

## 2.7 Determination of the Peroxide value by Iodometric titration method

With the purpose to evaluate hydro peroxide concentration during thermo-oxidation of linseed oil, peroxide value (PV) was measured by iodometric titration method.

### 2.7.1 Principle

The reaction between a saturated solution of potassium iodide and an oil sample is the basis of the method. The method takes advantage of the ability of hydro peroxides to oxidize iodide ions ( $I^-$ ) to iodine ( $I_2$ ), as described in Equation 2.4



The iodine formed gives a quantitative measurement of the hydro peroxides present when titrated against sodium thiosulfate with starch as an endpoint indicator, as described in Equation 2.5:



### 2.7.2 Calculation of Peroxide value (PV)

The equation to report peroxide values is the following:

$$POV \left[ \frac{mmol}{L} \right] = \frac{(V_1 - V_0) * c * 1000}{V_s * 2} \quad (2.6)$$

where,

POV=peroxide value

$V_1$  = consumption of 0.01 mol/l or 0.1 mol/l sodium thiosulfate in the main test

$V_0$  = consumption of 0.01 mol/l or 0.1 mol/l sodium thiosulfate in the blank test.

c = molar concentration of the sodium thiosulfate solution

m = weighted portion of substance in grams

$V_s$  = volume portion of substance in ml

### 2.7.3 Reagents

#### *Starch (indicator)*

Soluble starch 5.0 g was dissolved in deionized water, 500 ml. formic acid, and 3 ml was added to stabilize the solution.

#### *Saturated potassium iodide solution*

Deionized water 50 ml, potassium iodide 74 g was added until to see undissolved crystals after shaking. The solution was kept in a dark bottle of 1 liter.

#### *Solvent Mixture*

Glacial acetic acid: chloroform (3:2). 30ml of Glacial acetic acid and 20 ml of chloroform (reagent type)

#### *Sodium thiosulfate solution*

Standard volumetric solution (0.01 N) was prepared dissolving 1.25 g of sodium thiosulfate until a volume of 500 ml.

### 2.7.4 Procedure

Transfer 3.0 g of linseed oil into a 250 ml Erlenmeyer flask with glass stopper. Add 50 ml of solvent mixture: Glacial acetic acid: chloroform (3:2) and saturated potassium iodide solution 1 ml and allow react for 60 seconds and shaking thoroughly (manually) during this period. Then add water, 100 ml and shake (manual). Titrate with 0.01 N solution of thiosulfate solution, using 1 ml starch solution.

### 2.8 Kinetic model

After to propose all the reactions involved in thermo-oxidation, corresponding differential equations were solved in MatLab software. Data obtained from the kinetic model was compared with TGA experimental results, and finally a simulation of thermo-oxidation process of a film of polypropylene containing linseed oil was done. More details about parameters and variables involved in the kinetic model is presented in chapter V.

## References

- Aguilar Palomo, R. H., Medina Perilla, J. A., & Garcia Mora, A. M. (2013). *Análisis y evaluación de los efectos de la reducción de tamaño de partícula de ingredientes con propiedades de absorción de oxígeno en el desempeño de películas poliméricas para la fabricación de empaques activos*: Bogotá : Uniandes, 2013.
- Berenzon, S., & Saguy, I. S. (1998). Oxygen Absorbers for Extension of Crackers Shelf-life. *Lebensmittel-Wissenschaft und-Technologie*, 31(1), 1-5. doi:10.1006/fstl.1997.0286
- Brinker, C. J., Ashley, C. S., Bhatia, R., & Singh, A. K. (2002). *Sol-gel method for encapsulating molecules* (US Patent 6495352). Retrieved from
- Durango, A. M., De FÁTIMA Soares, N., & Arteaga, M. R. (2011). FILMES Y REVESTIMIENTOS COMESTIBLES COMO EMPAQUES ACTIVOS BIODEGRADABLES EN LA CONSERVACIÓN DE ALIMENTOS. (Spanish). *EDIBLE FILMS AND COATINGS AS BIODEGRADABLE ACTIVE PACKAGING IN THE PRESERVATION OF FOOD PRODUCTS*. (English), 9(1), 122-128.
- Firestone, D. (2009). *Official methods and recommended practices of the AOCS*: AOCS.
- García, Á. (2010). *Evaluación térmica y cinética de una capa activa, en estructuras de empaques con propiedades de absorción de oxígeno*. Universidad de los Andes, Bogotá.
- George, E. (1996). Corporate Health and Safety: Managing Environmental Issues in the Workplace In R. E. Henderson (Ed.), *Assessment and Management of Air Quality in the Workplace*. Southampton, Pennsylvania: Ergonomics, Inc.
- Salas, J. C. (2011). *Processability of polyolefinic films filled with oxygen scavengers*. . (M.Sc Engineering), Universidad de los Andes, Bogotá.
- Tewari, G., Jayas, D. S., Jeremiah, L. E., & Holley, R. A. (2002). Absorption kinetics of oxygen scavengers. *International journal of food science & technology*, 37(2), 209-217.



# III

## Experimental results of linseed oil

### CONTENT

---

<b>INDEX OF FIGURES</b>	<b>60</b>
<b>INDEX OF TABLES</b>	<b>61</b>
<b>RESUME DU CHAPITRE III</b>	<b>62</b>
INTRODUCTION	63
3.1 SOL-GEL ENCAPSULATION FOR INCLUSION OF OS IN POLYMER-BASED ACTIVE PACKAGING	63
3.1.1 <i>FTIR characterization</i>	63
3.1.2 <i>Electron Microscopy (SEM)</i>	65
3.1.3 <i>Linseed oil encapsulation</i>	65
3.1.4 <i>Linseed oil encapsulated + Polypropylene (PP)</i>	68
3.2 LINSEED OIL CHEMICAL CHARACTERIZATION	68
3.2.1 <i>Gas- Liquid Chromatography (GLC)</i>	68
3.2.2 <i>Fourier Transform Infrared Spectroscopy</i>	70
3.3 TGA TO EVALUATE OXYGEN UPTAKE CAPABILITY	74
3.3.1 <i>TGA in non-oxidative atmosphere</i>	74
3.3.2 <i>TGA in oxidative atmospheres</i>	75
3.4 MEASUREMENTS OF OXYGEN IN HEADSPACE.	76
3.5 COMPARISON BETWEEN TGA AND HEADSPACE RESULTS	78
3.6 RELATIONSHIP BETWEEN PEROXIDE VALUE AND TGA.	80
REFERENCES	82

## INDEX OF FIGURES

FIGURE 3.1: FTIR OF LINSEED OIL DOUBLE BOILED.....	63
FIGURE 3.2 FTIR OF SILICAGEL .....	64
FIGURE 3.3. FTIR OF LINSEED OIL ENCAPSULATED IN SILICA GEL.....	64
FIGURE 3.4. LINSEED OIL ENCAPSULATED IN SILICA MILLED AND SIEVED UNTIL SIZES BETWEEN 20 $\mu$ M AND 45 $\mu$ M AFTER (A) 10 MINUTES, (B) 30 MINUTES AND (C) 60 MINUTES OF MILLING. X200. ....	65
FIGURE 3.5. LINSEED OIL ENCAPSULATED IN SILICA MILLED AND SIEVED UNTIL SIZES BETWEEN 20 $\mu$ M AND 45 $\mu$ M AFTER (A) 10 MINUTES, (B) 30 MINUTES AND (C) 60 MINUTES OF MILLING. X5000. ....	65
FIGURE 3.6 : EFFECT OF SOL-GEL ENCAPSULATION OVER OXYGEN UPTAKE OF A BLEND OF LINSEED OIL AND FERROUS SULFATE ACTIVATED BY HUMIDITY (90%RH) .....	66
FIGURE 3.7: RESULTS OF MEASUREMENTS OF OXYGEN CONCENTRATION INTO FLASKS OF 38ML CONTAINING 1 GRAM OF LO ENCAPSULATED IN SILICA GEL (■) AND LO-F ENCAPSULATED IN SILICA GEL (●), ACTIVATED BY HUMIDITY (99%RH , 1 HOUR) WITHOUT PREVIOUS MILLING. ....	67
FIGURE 3.8: RESULTS OF MEASUREMENTS OF OXYGEN CONCENTRATION INTO FLASKS OF 38ML CONTAINING 1 GRAM OF LO-F ENCAPSULATED IN SILICA GEL, MILLED AND SIEVED UNTIL SIZE LESS THAN 25 $\mu$ M , ACTIVATED BY HUMIDITY (99%RH , 1 HOUR). ....	67
FIGURE 3.9: OXYGEN UPTAKE OF BLENDS OF LINSEED OIL/FeSO <sub>4</sub> ENCAPSULATED + PP AT TWO DIFFERENT SCREW RATES.....	68
FIGURE 3.10: ILLUSTRATION OF TYPES OF REACTIVE SITES FOR AUTO-OXIDATION .....	70
FIGURE 3.11: INFRARED SPECTRUM OF LINSEED OIL DOUBLE BOILED PRESENTING THE PRINCIPAL PEAKS IDENTIFIED.....	71
FIGURE 3.12: INFRARED SPECTRUM OF METHYL LINOLENATE PRESENTING THE PRINCIPAL PEAKS IDENTIFIED.....	72
FIGURE 3.13 COMPARISON OF SPECTRA OF LINSEED OIL (—) AND METHYL LINOLENATE (—) IN THE ZONE BETWEEN 3100CM <sup>-1</sup> AND 2800CM <sup>-1</sup> .....	73
FIGURE 3.14 COMPARISON OF SPECTRA OF LINSEED OIL (—) AND METHYL LINOLENATE (—) IN THE ZONE BETWEEN 1800CM-1 AND 600CM-1.....	73
FIGURE 3.15 COMPARISON OF SPECTRA OF LINSEED OIL DOUBLE BOILED (—) AND VIRGIN LINSEED OIL (—). ....	74
FIGURE 3.16: THERMAL CURVE OF LINSEED OIL IN NITROGEN ATMOSPHERE AT 60°C, 80°C AND 110°C. ....	75
FIGURE 3.17 TGA RESULTS OF LINSEED OIL IN AIR ATMOSPHERE.....	75
FIGURE 3.18: TGA RESULTS OF TGA OF LINSEED OIL IN OXYGEN ATMOSPHERE .....	76
FIGURE 3.19: RESULTS OF MEASUREMENTS OF OXYGEN CONCENTRATION INTO FLASKS OF 20ML CONTAINING 1 ML OF LINSEED OIL AT 80°C. ....	77

FIGURE 3.20: RESULTS OF MEASUREMENTS OF OXYGEN CONCENTRATION INTO FLASKS OF 20ML, 60ML AND 110ML CONTAINING 1 ML OF LINSEED OIL AT 80°C.....	77
FIGURE 3.21 OXYGEN UPTAKE OF 1ML OF LINSEED OIL HEATED AT 80°C AT THREE HEADSPACE VOLUMES. ....	78
FIGURE 3.22: OXYGEN CONSUMED IN TGA EXPERIMENTS OF LINSEED OIL IN ATMOSPHERE OF AIR AT 80°C AND 110°C. ....	79
FIGURE 3.23: OXYGEN CONSUMED IN TGA EXPERIMENTS OF LINSEED OIL IN ATMOSPHERE OF 99% OXYGEN AT 60°C, 80°C AND 110°C .....	79
FIGURE 3.24: COMPARISON BETWEEN TGA RESULTS, ATMOSPHERE OF AIR (LEFT) AND HEADSPACE MEASUREMENTS (RIGHT) IN TERMS OF OXYGEN UPTAKE FOR LINSEED OIL .....	80
FIGURE 3. 25 COMPARISON BETWEEN TGA RESULTS, ATMOSPHERE OF AIR (Y AXIS) AND HEADSPACE MEASUREMENTS (X-AXIS) FOR LINSEED OIL IN TERMS OF OXYGEN UPTAKE AT 80°C.....	80
FIGURE 3.26: PEROXIDE VALUE AND THERMOGRAVIMETRIC RESULTS IN AIR ATMOSPHERE FOR LINSEED OIL AT 60°C.....	81

## INDEX OF TABLES

TABLE 3.1: COMPOSITION OF LINSEED OIL OBTAINED BY GAS LIQUID CHROMATOGRAPHY (METHOD AOCS Ce1-62).....	69
TABLE 3.2: INFRARED VIBRATIONAL ASSIGNMENTS FOR LINSEED OIL DOUBLE BOILED.....	71

## Résumé du chapitre III

La première partie porte sur l'encapsulation sol-gel de l'HL. L'encapsulation est vérifiée par IR ; les spectres montrent la coexistence des pics de l'huile et du silicagel. Du sulfate de fer a été ajouté à l'huile avant encapsulation et des essais d'absorption d'oxygène ont été réalisés sur le système à -60°C. La fraction molaire d'oxygène décroît lentement pendant les 5 premiers jours puis s'accélère fortement pour s'annuler après 10 jours. La réaction est légèrement plus rapide lorsque le système est activé par l'humidité (1h à 99%HR). Lorsque l'HL encapsulée est introduite dans du polypropylène, on observe le même type de comportement mais la consommation d'oxygène n'est plus totale après 10 jours.

La deuxième partie porte sur l'analyse de l'huile de lin. La GC exploitée selon la méthode de l'American Oil Chemist's Society, permet de déterminer la fraction massique des différentes espèces insaturées parmi lesquelles prédomine l'acide linolénique. La masse molaire moyenne en nombre est 285.6g/mol. On détermine également la moyenne du nombre de sites réactifs qui sera nécessaire pour les calculs de cinétique dans lesquels l'HL sera assimilée à une « molécule moyenne en nombre ». L'IR permet d'observer les similitudes et les différences entre l'HL et ses composés modèles, en particulier linolénate de méthyle.

La troisième partie porte sur la thermo-oxydation. Les mesures en cellule à 60°C ne permettent pas d'observer clairement la consommation d'oxygène dans l'échelle de temps de 2 heures. Par contre à 80 et 110°C, la consommation apparaît clairement même avant une heure.

La prise de masse prédomine pendant la période d'induction alors que la perte de masse (liée à la dégradation) prédomine après la fin de la période d'induction, ce qui permet, au moins à température modérée, de quantifier la prise de masse et de caractériser le taux de conversion de la consommation d'oxygène sachant qu'une prise de masse de 32g correspond à la fixation d'une mole de O<sub>2</sub>. Bien sûr la détermination de ces grandeurs n'est possible que lorsque l'on a déduit du bilan de masse la perte liée à l'évaporation. Cette dernière a été mesurée sous azote à 60°C, 80°C et 110°C. Les essais d'oxydation ont été réalisés dans l'air et dans l'oxygène pur aux trois températures.

L'ensemble des résultats montre que le comportement des substrats étudiés résulte d'une oxydation en chaîne radicalaire amorcée par décomposition des hydro peroxydes. Ces derniers s'accumulent durant la période d'induction d'où la prise de poids. Cependant, dès que leur concentration dépasse un certain seuil, ils se décomposent probablement par voie bimoléculaire, pour générer des radicaux alkoxyles responsables des coupures de chaînes à l'origine de la dégradation finale.

## Introduction

Experimental results of linseed oil are included in this chapter. In order to evaluate the effect of process variables into active films with oxygen scavenger capacity, oxygen uptake plots were obtained by means of headspace measurements at each step proposed, namely, encapsulation, milling and sieved, and blending of linseed encapsulated with polypropylene.

To start with the scientific objective, chemical information of linseed oil was obtained by Gas Chromatography (GC) and Fourier Transform Infrared Spectroscopy (FTIR). To follow thermo oxidation thermogravimetric analysis and oxygen headspace measurement (HS-O) were done, complementary peroxide value titrations were done and in the last two sections experimental results of TGA, Headspace and Peroxide value are compared.

### 3.1 Sol-gel encapsulation for inclusion of OS in polymer-based active packaging

#### 3.1.1 FTIR characterization

Encapsulation is verified by infrared spectroscopy. Figures below show corresponding spectra for pure linseed oil, silica gel and linseed oil encapsulated in silica gel. In the spectrum corresponding to linseed oil encapsulated (Figure 3.3) it is possible to see a broad band between 3700 - 3100  $\text{cm}^{-1}$  and a smaller 1651 $\text{cm}^{-1}$  corresponding to the vibrations of Si-OH group Silanol characteristics of silica band. Further, can be observed the presence of peaks at 2929 and 2856  $\text{cm}^{-1}$  corresponding to the CH bond extensions linseed oil and a strong band for the extension C = O of the ester group at 1747 $\text{cm}^{-1}$  oil which means that linseed oil is into the new compound developed.

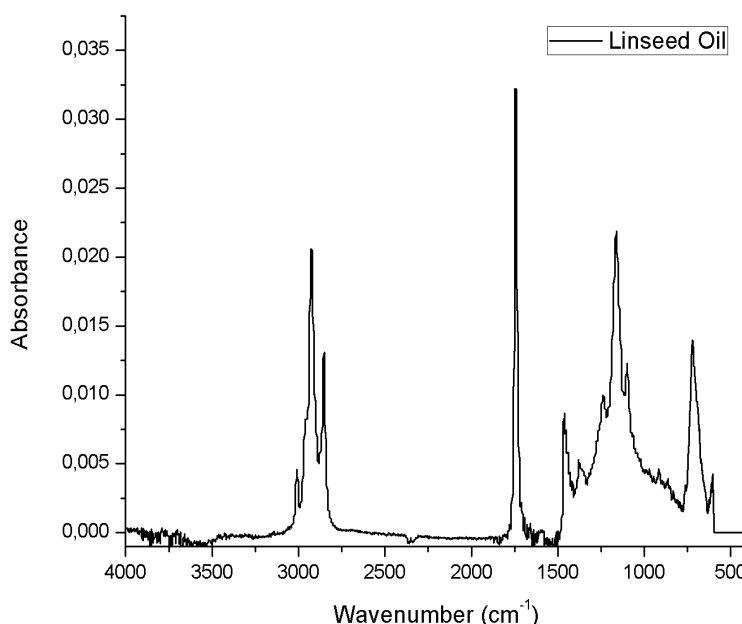
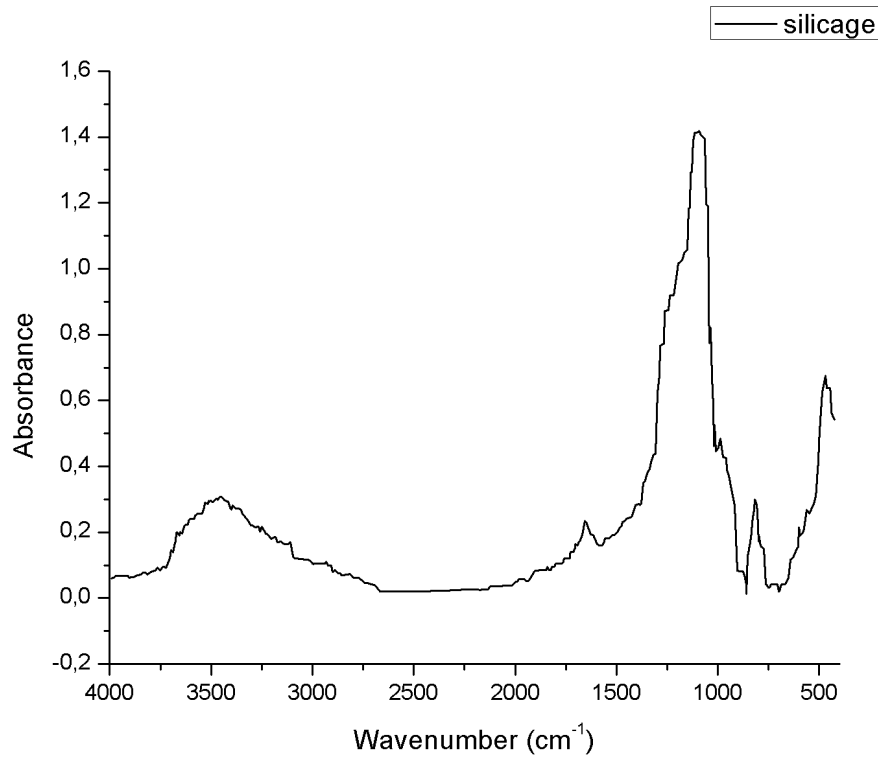
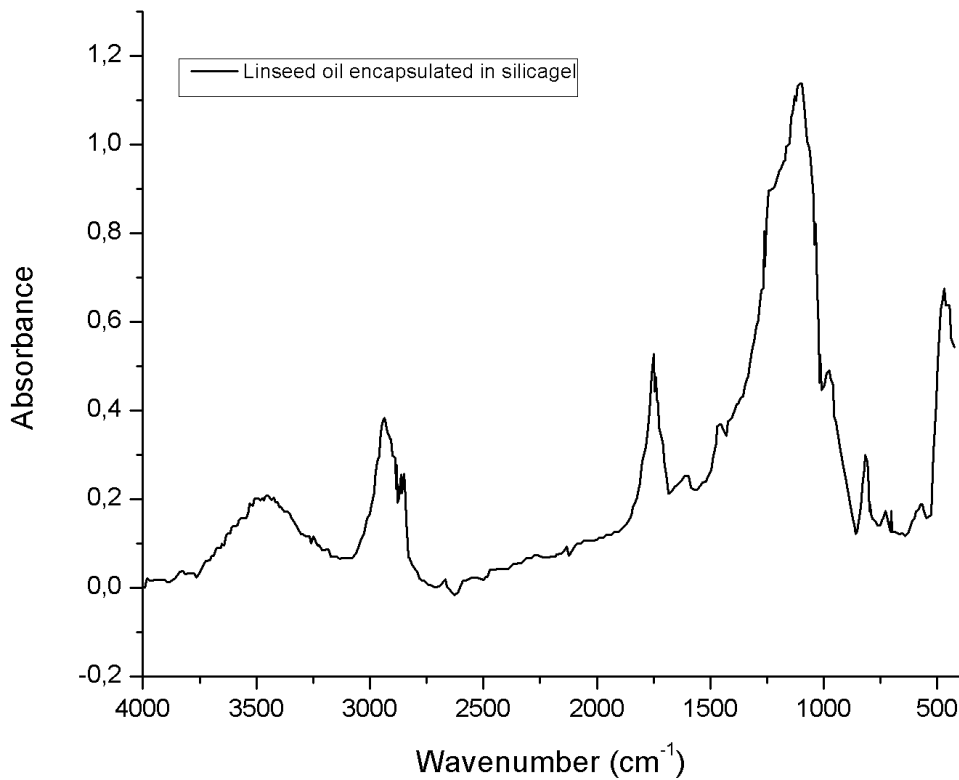


Figure 3.1: FTIR of linseed oil double boiled.



**Figure 3.2** FTIR of silica gel.



**Figure 3.3.** FTIR of linseed oil encapsulated in silica gel.

### 3.1.2 Electron Microscopy (SEM)<sup>1</sup>

After three different milling times, linseed oil encapsulated was sieved until sizes between 20 and 45 $\mu\text{m}$ . Product retained was observed in SEM (Figure 3.4).

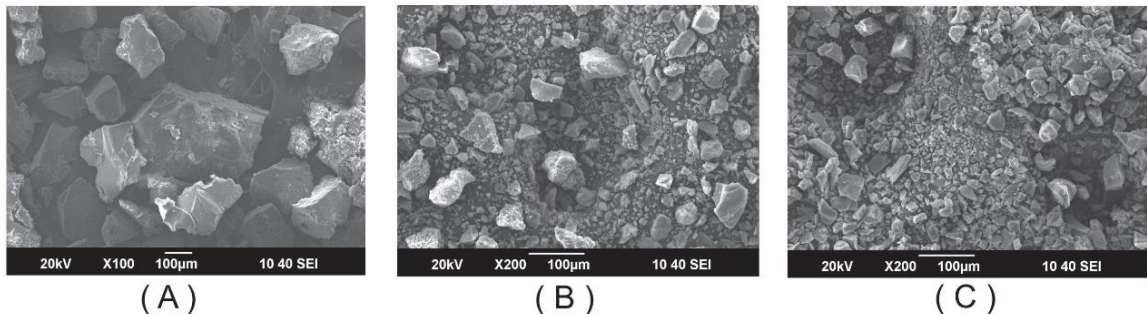


**Figure 3.4.** Linseed oil encapsulated in silica milled and sieved until sizes between 20 $\mu\text{m}$  and 45 $\mu\text{m}$  after (A) 10 minutes, (B) 30 minutes and (C) 60 minutes of milling. X200.

Size distribution changes with time milling as was expected, and just after short milling time (Figure 3.4-A) particles of around of 140  $\mu\text{m}$  are observed, even after sieved, this might be by agglomeration by water presence, indicating that a better drying must be done. In Figure 3.5 is more clear agglomeration with increased magnification, x5000.

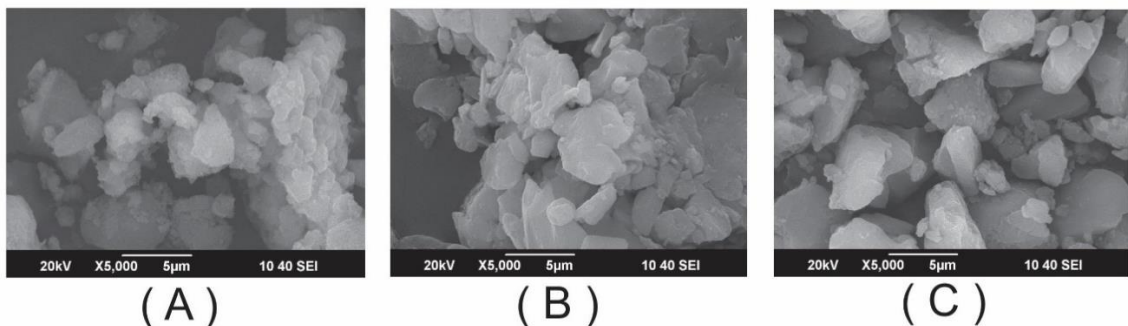


**Figure 3.5.** Linseed oil encapsulated in silica milled and sieved until sizes between 20 $\mu\text{m}$  and 45 $\mu\text{m}$  after (A) 10 minutes, (B) 30 minutes and (C) 60 minutes of milling. X5000.

### 3.1.3 Linseed oil encapsulation

Sol-gel encapsulation has been proved as an effective protection of active ingredients against early degradation (García, 2010) but has an effect over oxygen uptake capacity as shows Figure 3.6.

<sup>1</sup> Data obtained in collaboration with undergraduate student Rodrigo AGUILAR (Aguilar Palomo, Medina Perilla, & Ochoa Lleras, 2013).

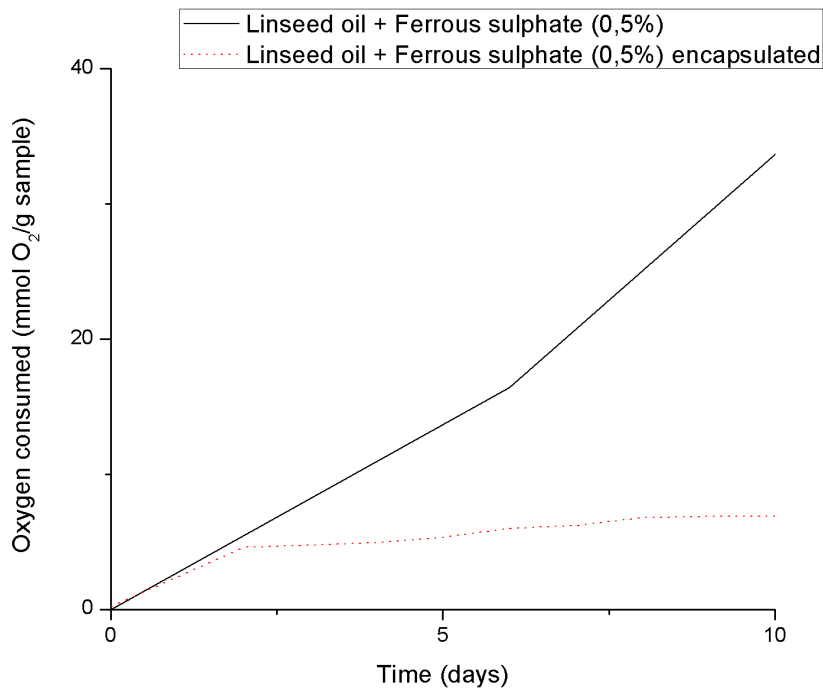


**Figure 3.6 : Effect of sol-gel encapsulation over oxygen uptake of a blend of linseed oil and ferrous sulfate activated by humidity (90%RH)**

From previous research (García, 2010; Salas, 2011) was proved the positive effect of metal catalysts in oxidation, activated by humidity, of compounds containing unsaturated fatty acids. Therefore, encapsulation of linseed oil was tested for solely the oil and also, for blends of oil with ferrous sulphate as catalyst.

Blends of linseed oil plus ferrous sulphate (LO-F) in a proportion of 0.5% w/w of catalyst, and solely Linseed oil (LO) without previous milling or sieving, were encapsulated in silica gel and dried at 60°C. Figure 3.7 shows oxygen uptake capacity of 1 g of encapsulated during 10 days, showing a slight improvement of oxygen scavenging with the addition of the metal catalyst.

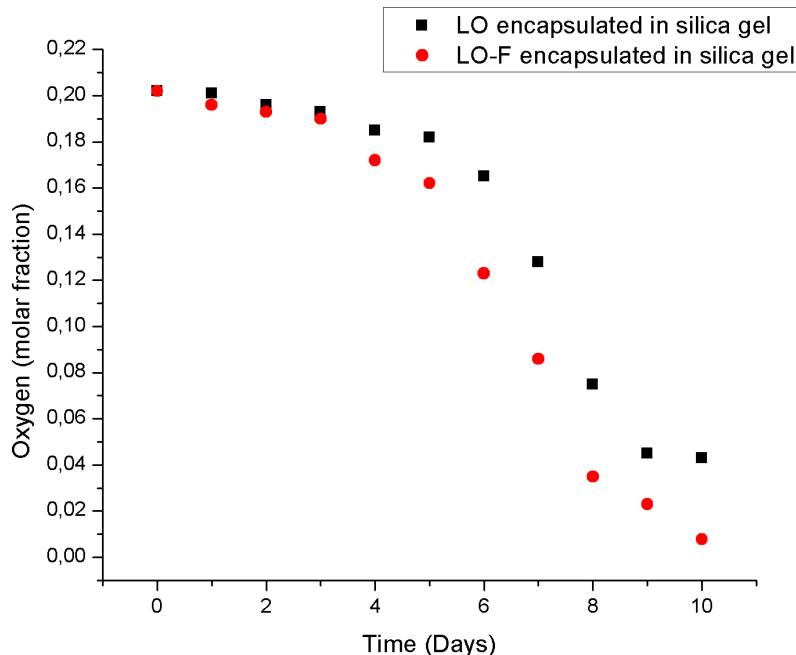


**Figure 3.7:** Results of measurements of oxygen concentration into flasks of 38ml containing 1 gram of LO encapsulated in silica gel (■) and LO-F encapsulated in silica gel (●), activated by humidity (99%RH , 1 hour) without previous milling.

To evaluate the effect of particle size, blends of linseed oil/0.5% ferrous sulphate (LO-F) were encapsulated in silica gel, dried, milled during 90 or 180 minutes and sieved. Particles with a size less than 25  $\mu\text{m}$ , were activated by humidity and tested by headspace measurements. Oxygen concentration in flasks of 38ml was monitored during 10 days obtaining data plotted in Figure 3.8 . Better oxygen uptake was observed at lower milling times, showing the effect of processing in the scavenger property of linseed oil, even after encapsulation.

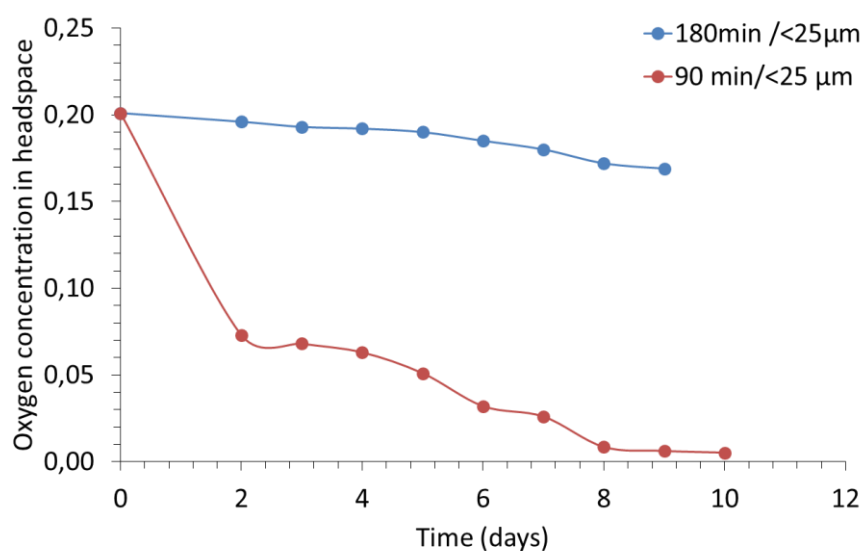


**Figure 3.8:** Results of measurements of oxygen concentration into flasks of 38ml containing 1 gram of LO-F encapsulated in silica gel, milled and sieved until size less than 25 $\mu\text{m}$  , activated by humidity (99%RH , 1 hour).

### 3.1.4 Linseed oil encapsulated + Polypropylene (PP)

A mix of linseed oil and ferrous sulphate was encapsulated and after blended at 190°C with PP in a multipurpose single extruder (C.W. Brabender Plasticorder) at two screw speeds, to obtain an active film of thickness less than 60 $\mu\text{m}$ . 100 grams of the film were packed in boxes of 38cm<sup>3</sup> and sealed with aluminium foil, oxygen concentration in the headspace was measured at different times. Figure 3.9 shows a delay in the oxygen uptake rate for the film manufactured at the higher screw rate.

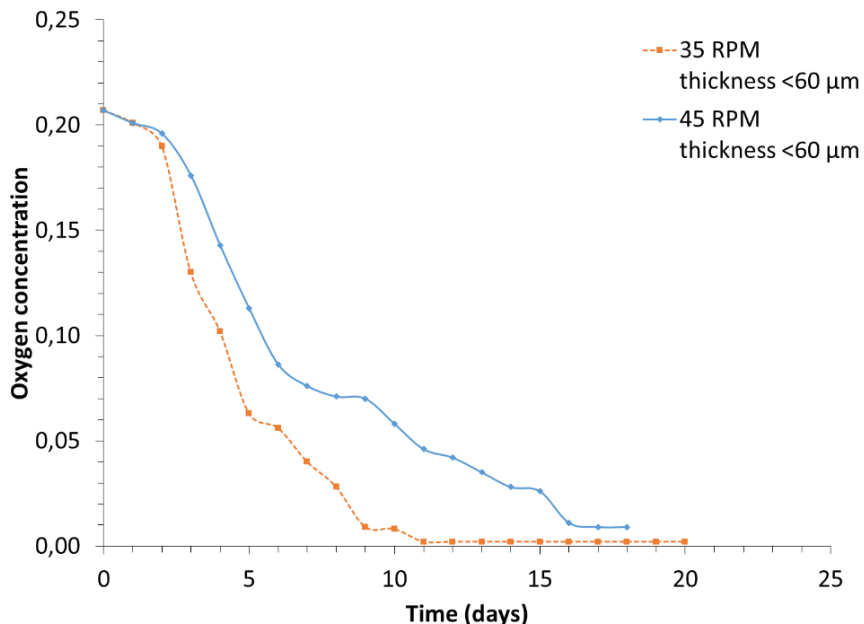


**Figure 3.9: Oxygen uptake of blends of linseed oil/FeSO<sub>4</sub> encapsulated + PP at two different screw rates.**

### 3.2 Linseed oil chemical characterization

In order to identify the functional groups susceptible to oxidation two tests were done: Determination of the fatty acid profile by Chromatography and infrared spectrometry.

#### 3.2.1 Gas- Liquid Chromatography (GLC)

Linseed oil double boiled was analysed by the method of American Oil Chemist's Society (A.O.C.S) Ce1-62, where methyl esters of fatty acids are separated and determined quantitatively by Gas liquid chromatography (GLC) using a packed column (Firestone, 2009).

The result of this analysis is a fatty acid profile with the corresponding weight fraction of each fatty acid calibrated. Table 3.1 presents results for linseed oil; the last row is the sum of weight percentage of the fatty acids unsaturated which are of interest because they are the major cause of oxidation.

**Table 3.1: Composition of linseed oil obtained by Gas liquid chromatography (Method AOCS Ce1-62)**

Component	Number of double bonds	Concentration ( $X_{\text{weight}}$ )
Palmitic acid	0	0.059
Stearic acid	0	0.034
Oleic acid	1	0.192
Linoleic acid	2	0.162
Linolenic acid	3	0.526
Unknown		0.027
<b>Total unsaturated fatty acids</b>		<b>0.880</b>

***Molecular weight calculated***

Based on results of fatty acid profile, a molecular weight can be calculated according with the equation 3.1.

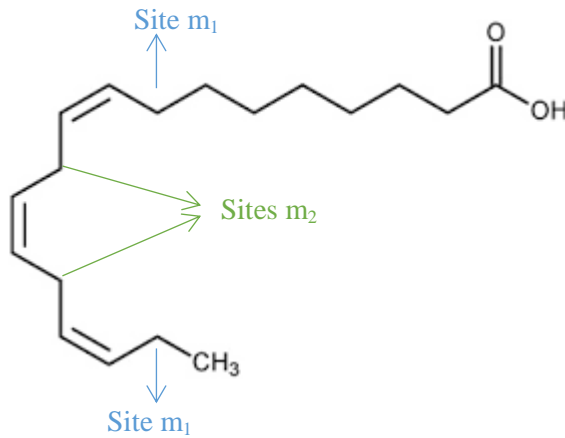
$$\bar{M} = \frac{1}{\sum_{i=1}^n \frac{X_i}{M_i}} \quad (3.1)$$

Where  $\bar{M}$  is the average molecular weight calculated,  $M_i$  is the molecular weight of each fatty acid  $n$  identified, and  $X_i$  is the weight fraction of each specie  $n$ . Applying equation 3.2 and using results presented in Table 3.1, molecular weight calculated of linseed oil is 285.6 g/mol.

***Oxidation potential based on GLC results***

GLC results are analysed in order to calculate a theoretical oxygen uptake capacity (OC) of Linseed oil. Auto-oxidation of unsaturated fatty acids is related with their reactive allylic hydrogens (next to a double bond). Two types of reactive allylic sites are identified, those that are just next to one double bond, named sites  $m_1$ , and those which are located between two double bonds which are sites  $m_2$ , and corresponding to the most reactive hydrogens in comparison with  $m_1$  sites in the case of molecules which have the two types.

Figure 3.10 illustrates these two types of reactive sites for the case of linolenic acid, in this case the most reactive hydrogens are those located in sites  $m_2$ .

**Figure 3.10: Illustration of types of reactive sites for auto-oxidation**

Concentration of reactive hydrogens can be calculated by Equation 3.2, based on fatty acid profile and will be equivalent to hydro peroxide concentration [PH].

$$[PH] \left( \text{mol/g} \right) = \sum m \text{ sites}_i \cdot (X_i/M_i) \quad (3.2)$$

Where  $i$  is each unsaturated fatty acid present in the fatty acid profile obtained by GLC,  $m$  sites the most reactive hydrogens ( $m_1$  or  $m_2$ ) for each acid  $i$ ,  $X_i$  the weight concentration of each  $i$ , and  $M_i$  the molar mass of each fatty acid  $i$ .

[PH] of linseed oil is 0.006 mol/g, a value similar of those obtained for neat unsaturated esters whose [PH] is 0.006 mol/g for methyl oleate , 0.003 for methyl linoleate and 0.006 for methyl linolenate (Richaud et al., 2012). Thus, if we consider that each allylic hydrogen will react with one mol of molecular oxygen, **consumption of oxygen by linseed oil will be of 0.006mol/g or 6mmol O<sub>2</sub> per gram of oil.**

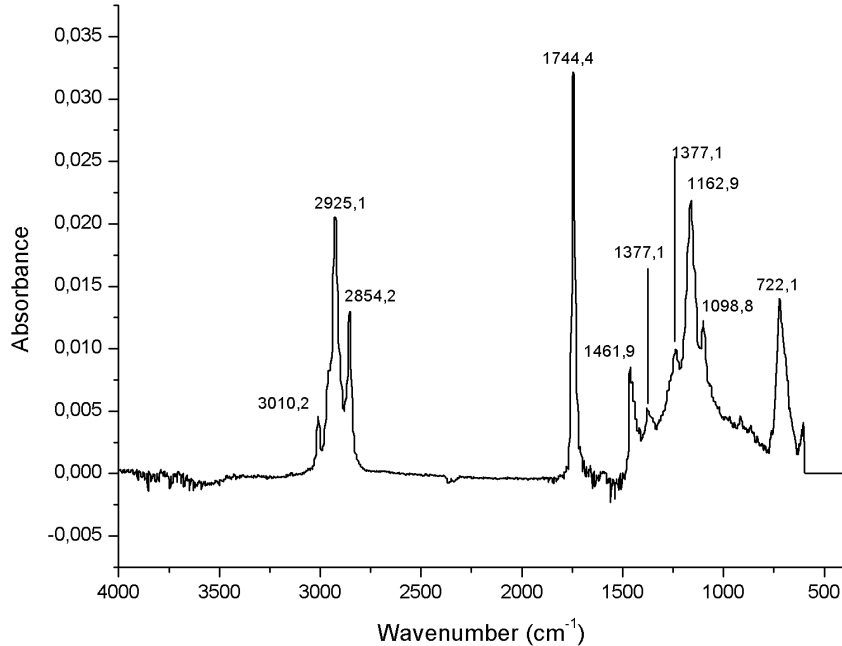
### 3.2.2 Fourier Transform Infrared Spectroscopy

Average spectra obtained for linseed oil is presented in Figure 3.11, Table 3.2 presents a summary of the principal peaks identified with the functional group assigned.

**Table 3.2: Infrared vibrational assignments for linseed oil double boiled.**

Band Position ( $\text{cm}^{-1}$ )	Intensity <sup>a</sup>	Assignment
3010	m	(C-H)=CH
2954	sh	(C-H)CH <sub>3</sub>
2925	s	(C-H)CH <sub>2</sub>
2854	s	(C-H)CH <sub>2</sub>
1744	s	C=O
1711	sh	C=O
1462	s	(CH <sub>2</sub> )
1377	m	(CH <sub>2</sub> )
1238	m	(C-C-O)
1163	s	(C-O)
1099	m	(O-CH <sub>2</sub> -C)
722	s	-(CH <sub>2</sub> )n and (C-H)=CH

<sup>a</sup> s: strong; m: medium; w: weak; sh: shoulder.

**Figure 3.11: Infrared Spectrum of linseed oil double boiled presenting the principal peaks identified.**

FTIR results agree with composition obtained by GLC (Table 3.1): band at  $3010\text{cm}^{-1}$  is related with double bonds, peaks from  $2954\text{cm}^{-1}$  to  $2854\text{cm}^{-1}$  with allylic carbon and bands at  $1744\text{cm}^{-1}$  and  $1711\text{cm}^{-1}$  are related with fatty acids oxidized; shoulder at  $1711\text{cm}^{-1}$  has been related with the presence of free fatty acids oxidized (Ismail, van de Voort, Emo, & Sedman, 1993).

Spectrum of methyl linolenate was collected (Figure 3.12) in order to compare it with linseed oil's spectrum. Subtraction shows than the peaks In the spectra of linseed oil, the peak at  $3011\text{cm}^{-1}$  is similar to methyl linolenate but in the zone between  $3000\text{cm}^{-1}$  and  $2800\text{cm}^{-1}$  the peaks of linseed oil have more absorbance (Figure 3.11). In the zone between  $1800\text{cm}^{-1}$  and  $600\text{cm}^{-1}$  linseed oil presents the same peaks than methyl linolenate with the exception of peaks at  $1435\text{cm}^{-1}$  which is assigned to the ester bond ( $\text{CO}-\text{O}-\text{CH}_3$ ) and  $1196\text{cm}^{-1}$  assigned to C-O (Figure 3.11).

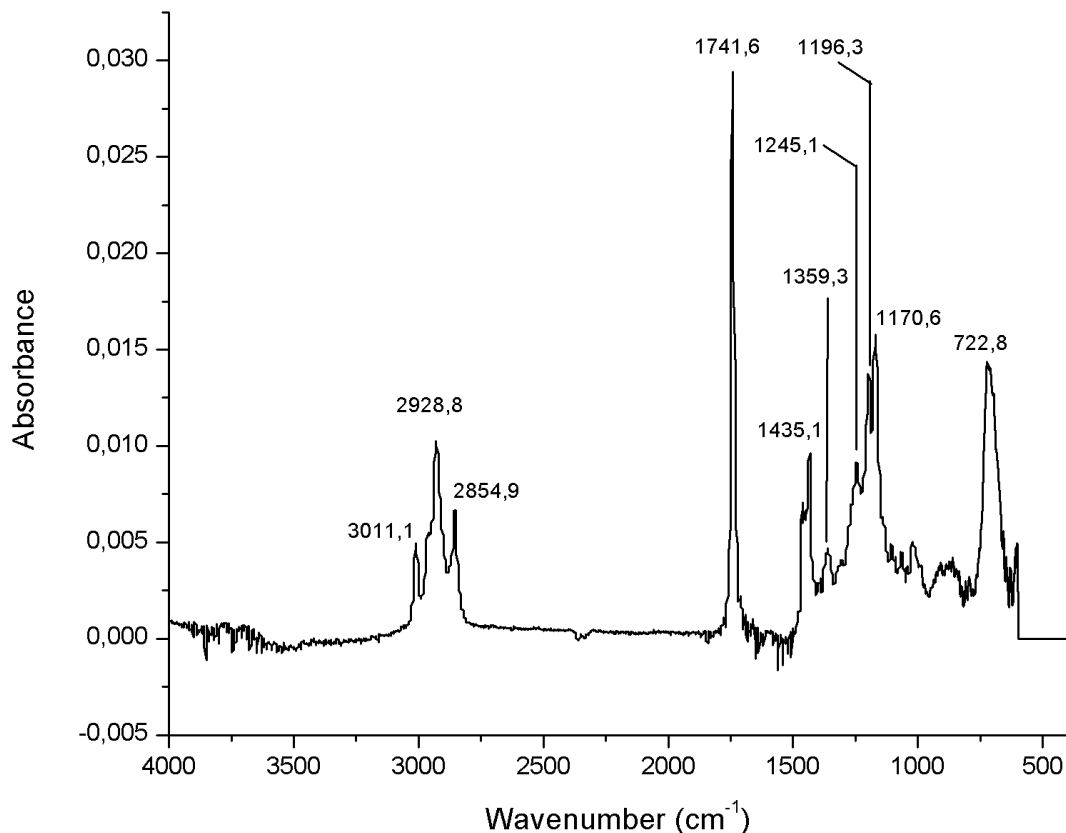


**Figure 3.12: Infrared Spectrum of methyl linolenate presenting the principal peaks identified.**

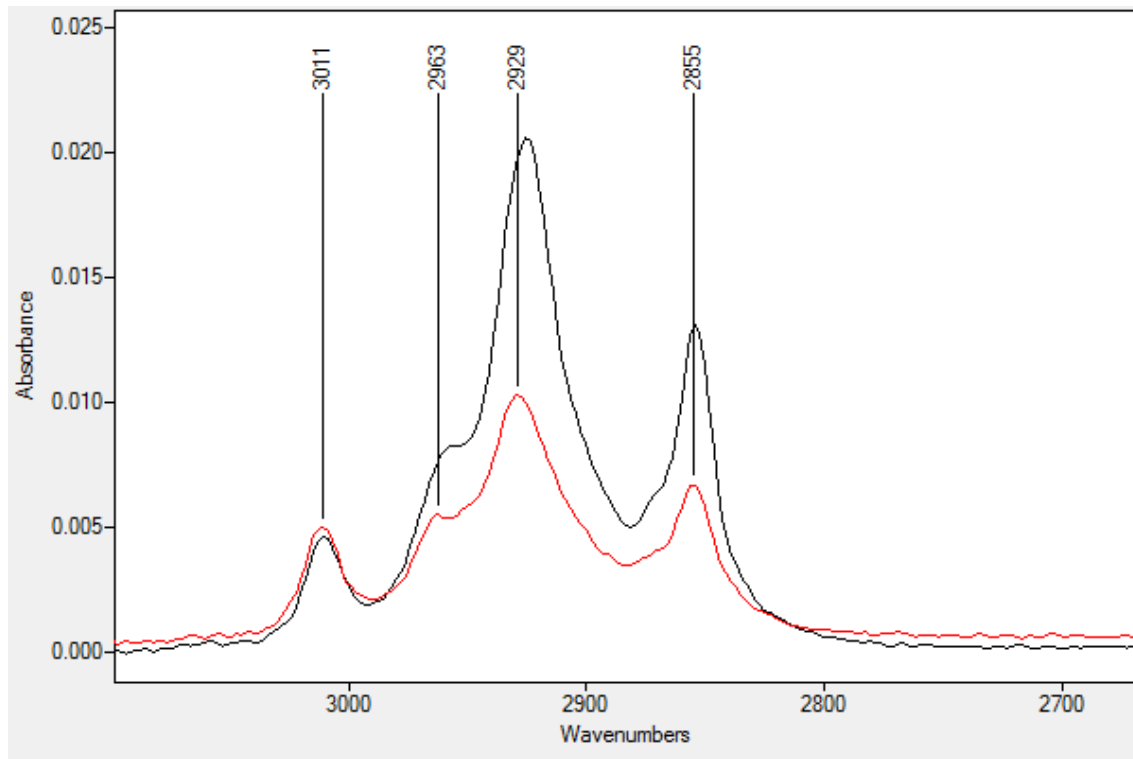


**Figure 3.13 Comparison of spectra of Linseed Oil (—) and Methyl linolenate (—) in the zone between  $3100\text{cm}^{-1}$  and  $2800\text{cm}^{-1}$ .**

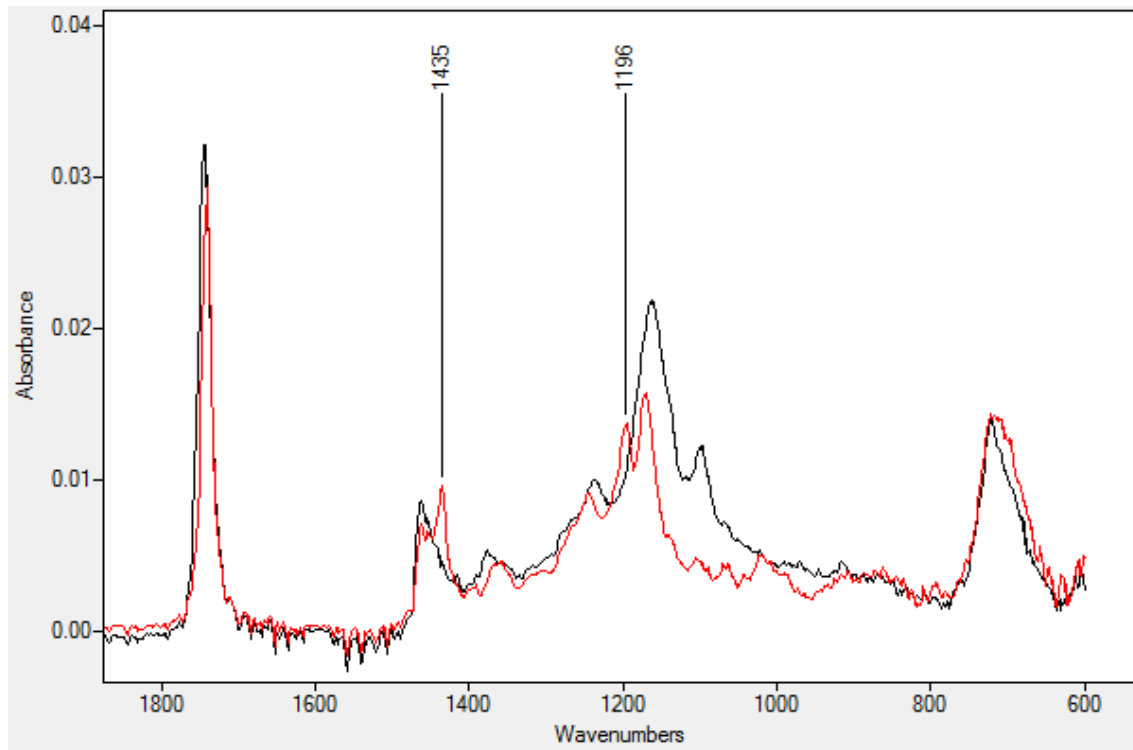


**Figure 3.14 Comparison of spectra of Linseed Oil (—) and Methyl linolenate (—) in the zone between  $1800\text{cm}^{-1}$  and  $600\text{cm}^{-1}$ .**

Spectrum of virgin linseed oil was collected obtaining essentially the same spectrum than for linseed oil double boiled (Figure 3.15), therefore hydrocarbon solvents added to speed drying time, in the case of boiled linseed oil cannot be differentiated in the spectrum (Dlugogorski, Kennedy, & Mackie, 2012).

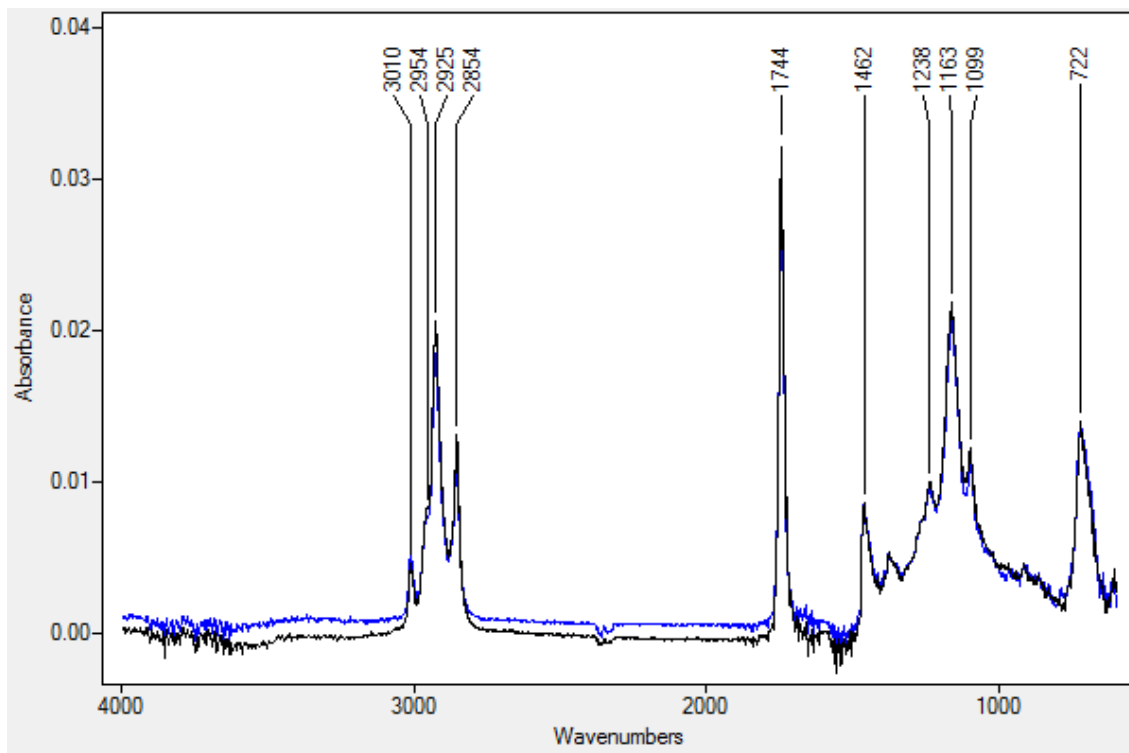


**Figure 3.15 Comparison of spectra of Linseed Oil double boiled (—) and Virgin Linseed Oil (—).**

### 3.3 TGA to evaluate oxygen uptake capability

Thermogravimetric analyses, which are usually utilized to evaluate thermal behaviour, were proposed as an alternative technique to evaluate the change in the mass of each active ingredient during thermo-oxidation at moderate temperatures (40°C to 110°C); isothermal analyses were done under non-oxidative and oxidative atmospheres, in order to separate effects of evaporation and oxidation.

#### 3.3.1 TGA in non-oxidative atmosphere

Isothermal experiments in nitrogen atmosphere were done for linseed oil at 60°C. In this non-oxidative atmosphere linseed oil reveals two stages; in the first 30 minutes (2000 s) there is a fast weight decrease and after in a second stage, the weight decrease slower. However, the total weight decrease is low; the minimum weight after 100 minutes (6000s) is 99.2% of the initial weight (Figure 3.16). It can be reasonably hypothesized that this relatively fast initial weight loss is due to the

evaporation of a volatile impurity of which the nature is unknown. The linseed oil itself remains stable in the timescale of the experiments.

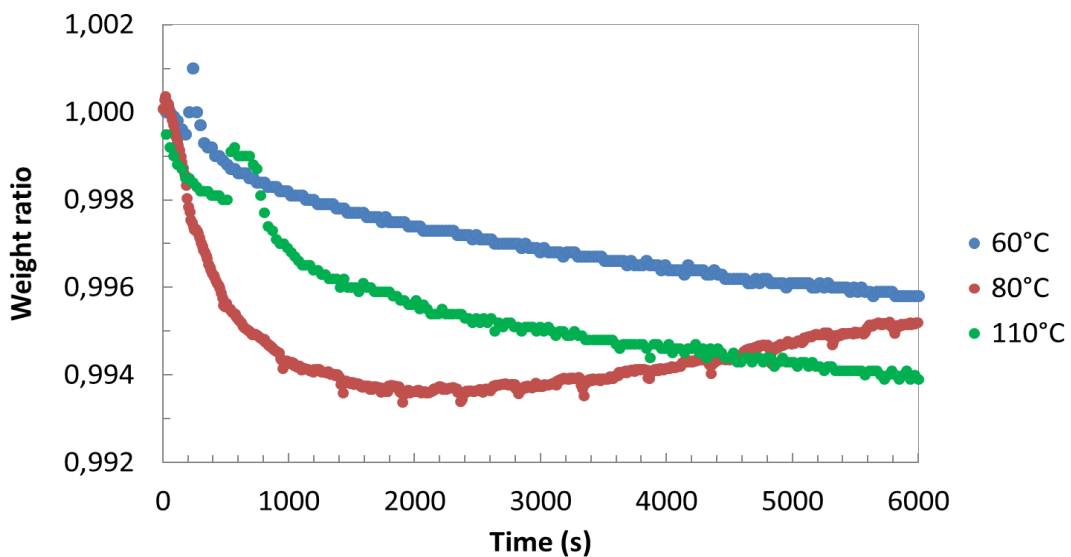


**Figure 3.16: Thermal curve of Linseed Oil in Nitrogen atmosphere at 60°C, 80°C and 110°C.**

### 3.3.2 TGA in oxidative atmospheres

Linseed oil in both oxidative atmospheres, air and oxygen, reveals increase of weight because oxygen grafting. The higher the oxygen concentration, the faster the initial weight increases but also the faster the final weight decreases. The maximum weight was about 2% in air (Figure 3.17) and 4% in pure oxygen (Figure 3.18).

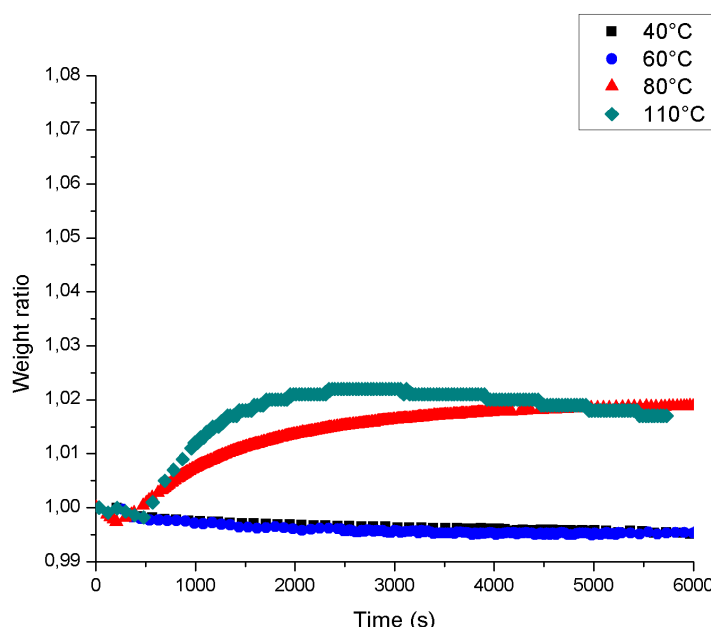


**Figure 3.17 TGA Results of Linseed Oil in Air atmosphere<sup>2</sup>**

<sup>2</sup> Tests done in Bogota, atmospheric pressure 564mm Hg.

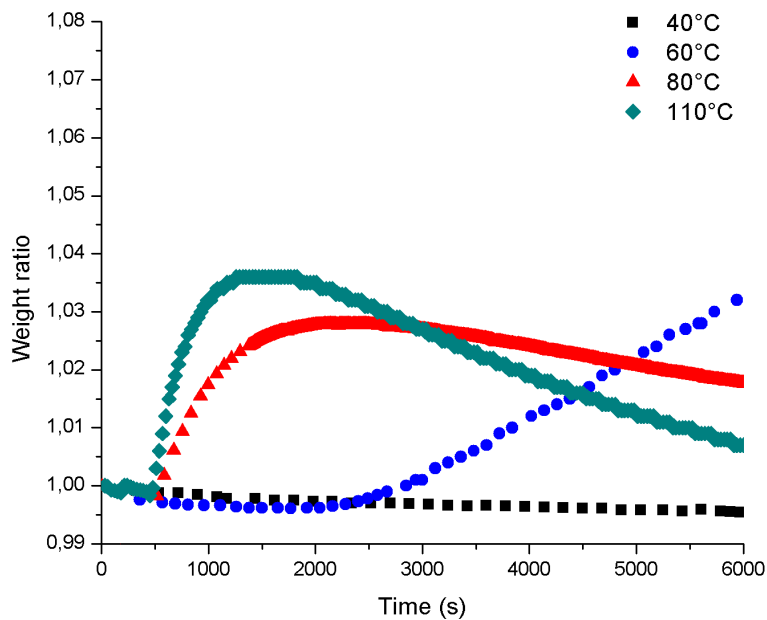


**Figure 3.18: TGA Results of TGA of Linseed Oil in Oxygen atmosphere<sup>3</sup>**

### 3.4 Measurements of oxygen in headspace.

Headspace measurements of oxygen are frequent in the evaluation of oxygen scavengers (Charles, Sanchez, & Gontard, 2006; Frydrych, Foltynowicz, Kowalak, & Janiszewska, 2007; Oms-Oliu, Odriozola-Serrano, Soliva-Fortuny, & Martín-Belloso, 2008), with this technique is possible to replicate real headspace into a packaging.

With the aim to compare TGA results with headspace measurements, 1ml of linseed oil was pouring in glass containers containing air to measure change in oxygen concentration during isothermal heating at 60°C, 80°C and 110°C. First tests were done in a glass containers of 20ml (Figure 3.19), but in order to doing an appropriate comparison with TGA, must ensure enough oxygen available for thermo-oxidation, then tests were extended to bigger glass containers : 60ml. and 110ml. (Results for 80°C are presented in Figure 3.20).

<sup>3</sup> Idem

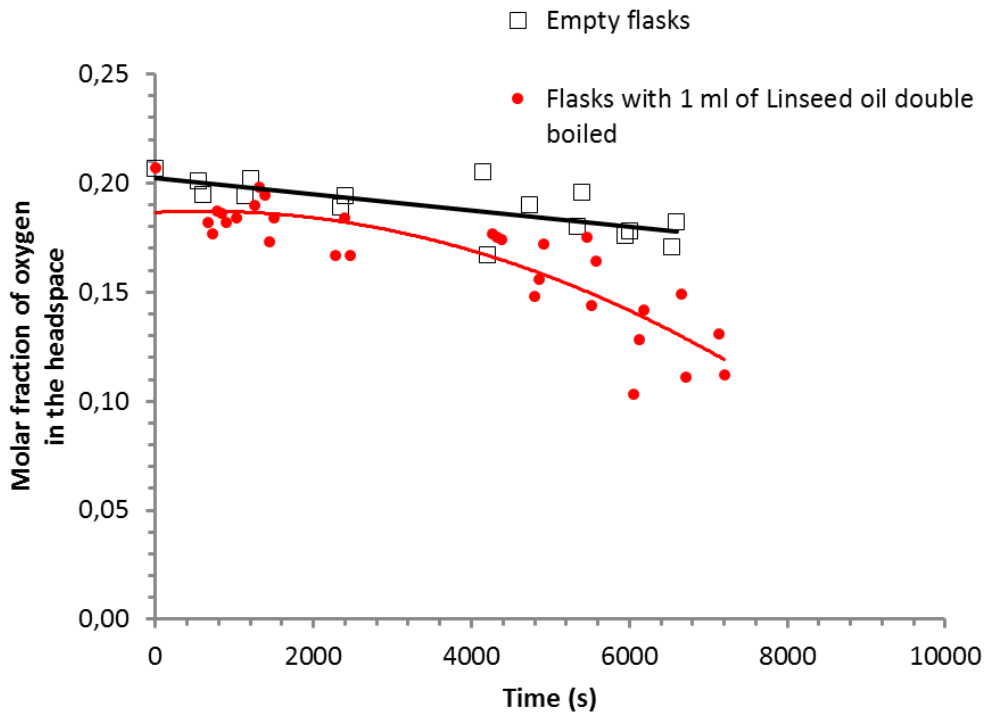


Figure 3.19: Results of measurements of oxygen concentration into flasks of 20ml containing 1 ml of linseed oil at 80°C.

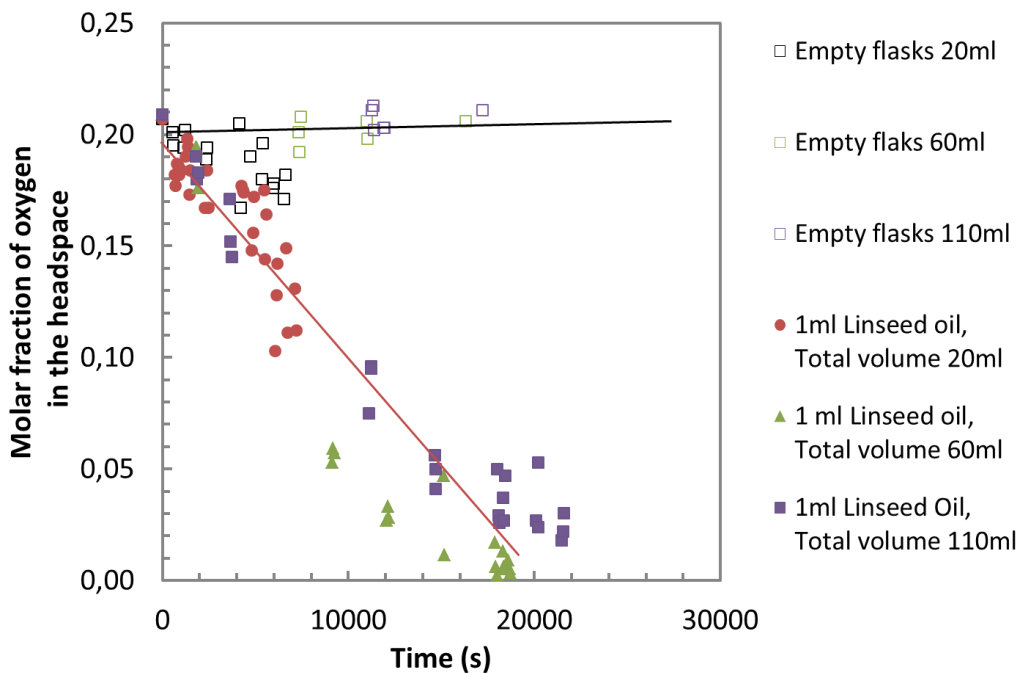


Figure 3.20: Results of measurements of oxygen concentration into flasks of 20ml, 60ml and 110ml containing 1 ml of linseed oil at 80°C.

In fact, when data is transformed according to equation 3.4., can be observed how oxygen uptake increase with volume, because there is more oxygen available (Figure 3.21).

$$x_{\text{oxygen consumed}} = \frac{1000PV(x_{\text{headspace oxygen}_0} - x_{\text{headspace oxygen}_t})}{RTm} \quad (3.4)$$

In equation 3.4,  $P$  is the atmospheric pressure of the test,  $V$  the headspace volume,  $x_{\text{headspace oxygen}_0}$  the Molar fraction of oxygen in the headspace in the time zero,  $x_{\text{headspace oxygen}_t}$  Molar fraction of oxygen in the headspace in the time  $t$ ,  $R$  the universal constant of ideal gases,  $T$  the temperature of the test and  $m$  the mass linseed oil sample.

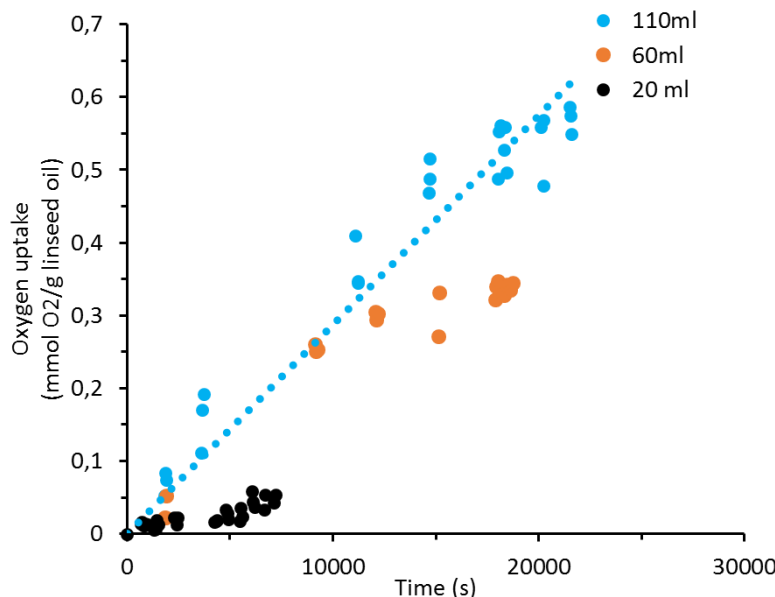


Figure 3.21 Oxygen uptake of 1ml of linseed oil heated at 80°C at three headspace volumes.

### 3.5 Comparison between TGA and headspace results

Results of TGA and headspace experiments were compared after data conversion of weight or oxygen concentration to oxygen grafted (mmol oxygen/gram of linseed oil).

TGA results were transformed by means the equation 3.3, only were analysed isothermal assays at 80°C and 110°C because in both increase of weight was observed in the first hours.

$$x_{\text{oxygen consumed}} = \frac{1000(X - 1)}{32} \quad (3.3)$$

Where  $x_{\text{oxygen consumed}}$  is the oxygen grafted (mmol of oxygen/gram of linseed oil) and  $X$  is the weight ratio obtained in TGA. Results are plotted in Figure 3.22 for atmosphere of Air and Figure 3.23 for atmosphere of 99% of oxygen.

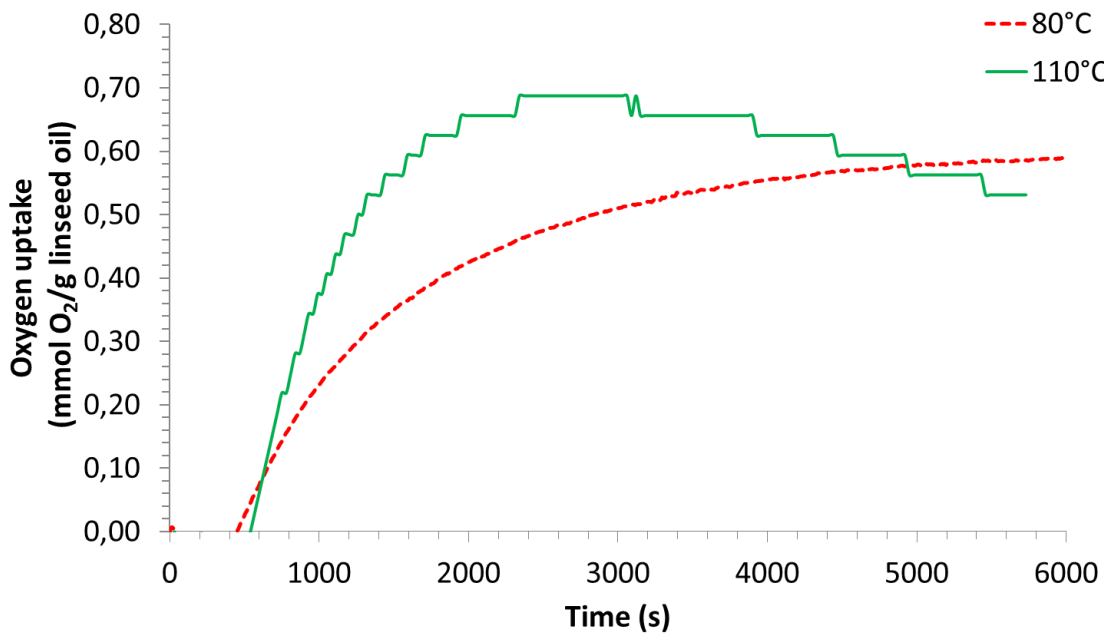


Figure 3.22: Oxygen consumed in TGA experiments of Linseed Oil in atmosphere of Air at 80°C and 110°C.

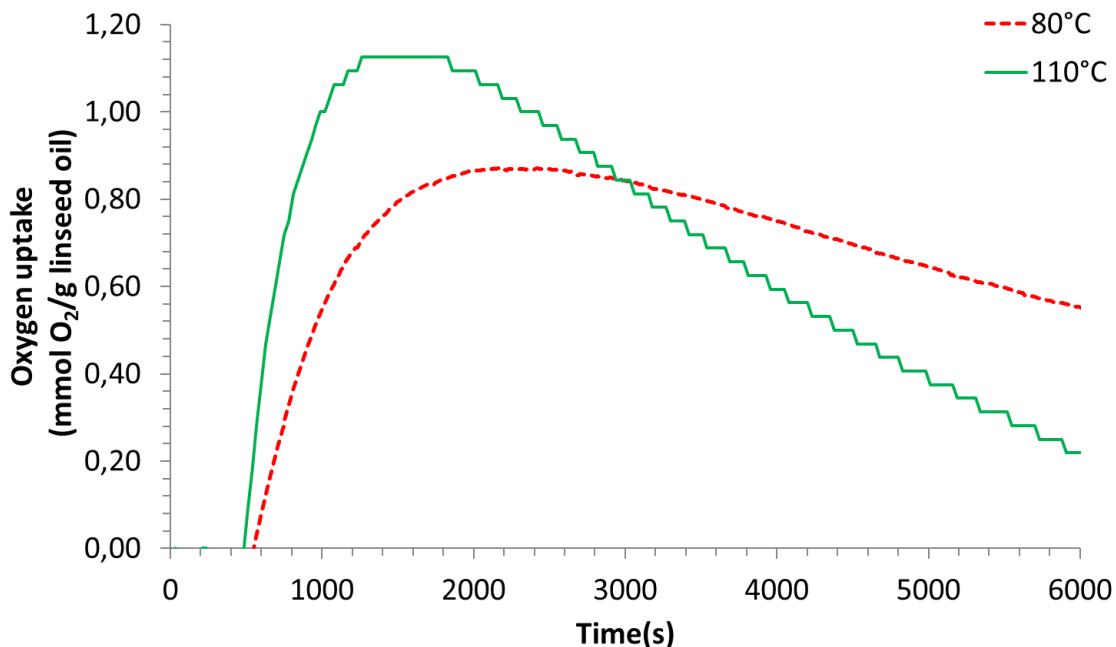
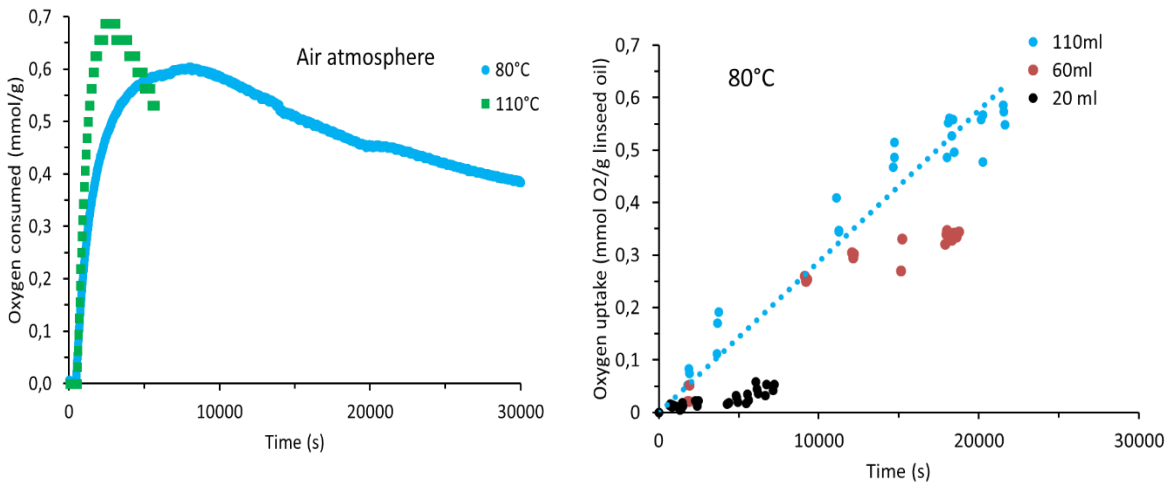


Figure 3.23: Oxygen consumed in TGA experiments of Linseed Oil in atmosphere of 99% Oxygen at 60°C, 80°C and 110°C

The observable difference in the amount of oxygen consumed is coherent with oxygen concentration in each atmosphere.

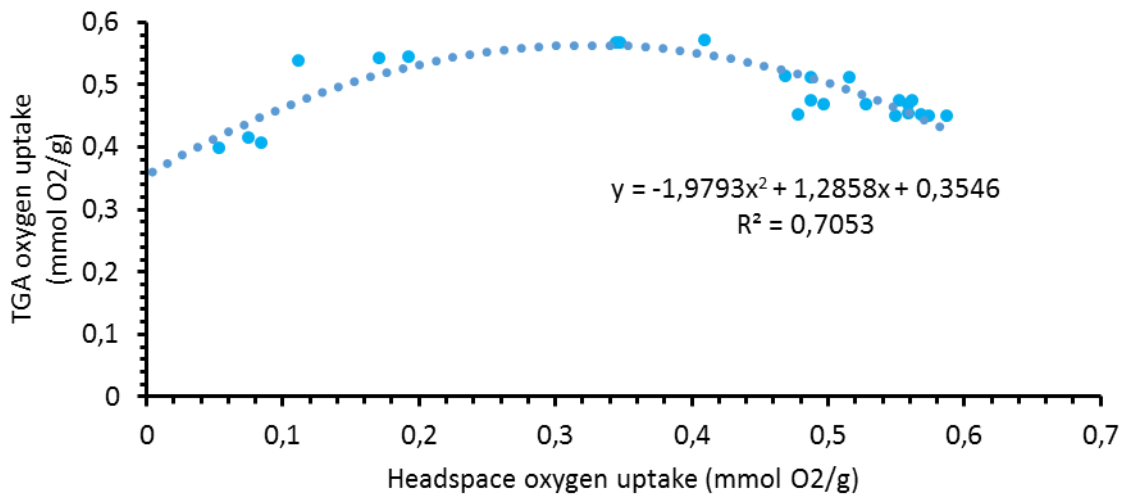
Values of oxygen consumed are very similar between the two experimental techniques (

Figure 3.24) and a correlation can be done when data from two techniques is plotted as can



be observed in Figure 3. 25.

**Figure 3.24: Comparison between TGA results, atmosphere of air (left) and headspace measurements (right) in terms of oxygen uptake for linseed oil.**



**Figure 3. 25 Comparison between TGA results, atmosphere of air (y axis) and headspace measurements (x-axis) for linseed oil in terms of oxygen uptake at 80°C.**

### 3.6 Relationship between Peroxide Value and TGA.

As was discussed before, at the beginning of the oxidation propagation products, i.e. hydro peroxides and peroxides, will predominate and the mass will increase. Then, a correlation between the initial rate of mass gain and the hydro peroxide concentration could be expected.

Figure 3.26, shows results of TGA and peroxide value for linseed oil at 60°C. In the plot is possible to see how when peroxide concentration tends to increase the weight increase rate is also the higher.

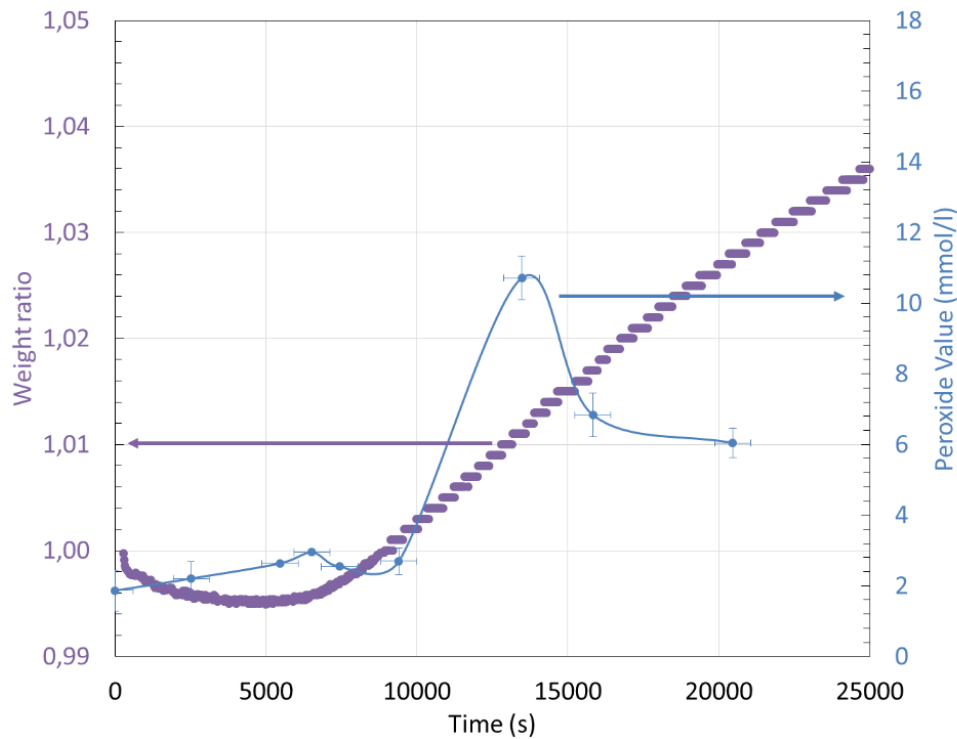


**Figure 3.26: Peroxide value and Thermogravimetric results in Air atmosphere for Linseed oil at 60°C**

## References

- Aguilar Palomo, R. H., Medina Perilla, J. A., & Ochoa Lleras, N. (2013). *Análisis y evaluación de los efectos de la reducción de tamaño de partícula de ingredientes con propiedades de absorción de oxígeno en el desempeño de películas poliméricas para la fabricación de empaques activos*: Bogotá : Uniandes, 2013.
- Charles, F., Sanchez, J., & Gontard, N. (2006). Absorption kinetics of oxygen and carbon dioxide scavengers as part of active modified atmosphere packaging. *Journal of Food Engineering*, 72(1), 1-7. doi:10.1016/j.jfoodeng.2004.11.006
- Dlugogorski, B. Z., Kennedy, E. M., & Mackie, J. C. (2012). Low temperature oxidation of linseed oil: a review. *Fire science reviews*, 1(1), 1-36.
- Firestone, D. (2009). *Official methods and recommended practices of the AOCS*: AOCS.
- Frydrych, E., Foltynowicz, Z., Kowalak, S., & Janiszewska, E. (2007). *Oxygen scavengers for packing system based on zeolite adsorbed organic compounds*. Paper presented at the Zeolites to Porous MOF Materials – the 40th Anniversary of International Zeolite Conference.
- García, Á. (2010). *Evaluación térmica y cinética de una capa activa, en estructuras de empaques con propiedades de absorción de oxígeno*. Universidad de los Andes, Bogotá.
- Ismail, A. A., van de Voort, F. R., Emo, G., & Sedman, J. (1993). Rapid quantitative determination of free fatty acids in fats and oils by fourier transform infrared spectroscopy. *Journal of the American Oil Chemists' Society*, 70(4), 335-341. doi:10.1007/BF02552703
- Oms-Oliu, G., Odriozola-Serrano, I., Soliva-Fortuny, R., & Martín-Belloso, O. (2008). Antioxidant Content of Fresh-Cut Pears Stored in High-O<sub>2</sub> Active Packages Compared with Conventional Low-O<sub>2</sub> Active and Passive Modified Atmosphere Packaging. *Journal of Agricultural and Food Chemistry*, 56(3), 932-940. doi:10.1021/jf071210z
- Richaud, E., Audouin, L., Fayolle, B., Verdu, J., Matisová-Rychlá, L., & Rychlý, J. (2012). Rate constants of oxidation of unsaturated fatty esters studied by chemiluminescence. *Chemistry and Physics of Lipids*, 165(7), 753-759. doi:<http://dx.doi.org/10.1016/j.chphyslip.2012.09.002>

Salas, J. C. (2011). *Processability of polyolefinic films filled with oxygen scavengers.* . (M.Sc Engineering), Universidad de los Andes, Bogotá.



# IV

## Experimental results of UFE

### CONTENT

---

EXPERIMENTAL RESULTS OF UFE	85	
INDEX OF FIGURES	86	
INDEX OF TABLES	86	
RÉSUME DU CHAPITRE IV	87	
INTRODUCTION	88	
4.1	TGA IN NON-OXIDATIVE ATMOSPHERE OF UNSATURATED ESTERS	89
4.2	TGA IN OXIDATIVE ATMOSPHERE	90
4.3	DISCUSSION OF RESULTS FOR TGA OF UNSATURATED ESTERS	93
4.3.1	<i>TGA in non-oxidative atmosphere</i>	93
4.3.2	<i>TGA in oxidative atmosphere</i>	94
4.3.3	<i>Calculating oxygen scavenging capacity based on TGA</i>	95
REFERENCES	100	

## INDEX OF FIGURES

FIGURE 4.1: ILLUSTRATION OF TYPES OF REACTIVE SITES FOR AUTO-OXIDATION	89
FIGURE 4.2: TGA OF METHYL OLEATE IN NITROGEN ATMOSPHERE	89
FIGURE 4.3: TGA OF METHYL LINOLEATE IN NITROGEN ATMOSPHERE	90
FIGURE 4.4: TGA OF METHYL LINOLENATE IN NITROGEN ATMOSPHERE	90
FIGURE 4.5: TGA OF METHYL OLEATE IN ATMOSPHERE OF AIR.	90
FIGURE 4.6: TGA OF METHYL LINOLEATE IN ATMOSPHERE OF AIR.	91
FIGURE 4.7: TGA OF METHYL LINOLENATE IN ATMOSPHERE OF AIR.	91
FIGURE 4.8: TGA OF METHYL LINOLENATE IN ATMOSPHERE OF AIR. ZOOM FOR TEMPERATURES FROM 40°C TO 80°C.	91
FIGURE 4.9: TGA OF METHYL OLEATE IN ATMOSPHERE OF OXYGEN (99%)	92
FIGURE 4.10: TGA OF METHYL LINOLEATE IN ATMOSPHERE OF 99% OXYGEN.	92
FIGURE 4.11: TGA OF METHYL LINOLENATE IN ATMOSPHERE OF OXYGEN 99%.	92
FIGURE 4.12: COMPARISON OF TGA RESULTS OF METHYL OLEATE IN AIR ATMOSPHERE (LEFT) AND OXYGEN ATMOSPHERE (RIGHT)	93
FIGURE 4.13: $\text{Ln}(\text{d}m/\text{dt})\text{T}$ vs. $1/T$ FOR ESTERS AND LINSEED OIL.	94
FIGURE 4.14: OXIDATION WEIGHT RATIO CALCULATED FOR METHYL LINOLENATE IN ATMOSPHERE OF AIR.	96
FIGURE 4.15: OXIDATION WEIGHT RATIO CALCULATED METHYL OLEATE IN ATMOSPHERE OF 99% OXYGEN.	96
FIGURE 4.16: OXIDATION WEIGHT RATIO CALCULATED FOR METHYL LINOLEATE IN ATMOSPHERE OF 99% OXYGEN.	97
FIGURE 4.17: OXIDATION WEIGHT RATIO CALCULATED FOR METHYL LINOLENATE IN ATMOSPHERE OF 99% OXYGEN.	98
FIGURE 4.18: COMPARISON BETWEEN OXIDATION WEIGHT RATIO CALCULATED FOR METHYL LINOLEATE IN ATMOSPHERE OF 99% OXYGEN (LEFT) AND METHYL LINOLENATE IN ATMOSPHERE OF 99% OXYGEN (RIGHT).	99
FIGURE 4.19: COMPARISON BETWEEN OXIDATION WEIGHT RATIO CALCULATED FOR METHYL LINOLENATE IN AIR ATMOSPHERE (LEFT) AND METHYL LINOLENATE IN ATMOSPHERE OF 99% OXYGEN (RIGHT).	99

## INDEX OF TABLES

TABLE 4.1: CHEMICAL STRUCTURE OF UNSATURATED ESTERS (ANALYTICAL REAGENTS FROM SIGMA-ALDRICH, SAN LUIS, MO, USA).....	88
TABLE 4.2: SLOPES CALCULATED FOR UNSATURATED ESTERS IN NITROGEN ATMOSPHERE.....	94

## Résumé du chapitre IV

Les substances modèles sont au nombre de trois : oléate de méthyle, linoléate de méthyle et linolenate de méthyl.

La première partie porte sur la thermo-oxydation. Les mesures en cellule à 60°C ne permettent pas d'observer clairement la consommation d'oxygène dans l'échelle de temps de 2 heures. Par contre à 80 et 110°C, la consommation apparaît clairement même avant une heure.

La prise de masse prédomine pendant la période d'induction alors que la perte de masse (liée à la dégradation) prédomine après la fin de la période d'induction, ce qui permet, au moins à température modérée, de quantifier la prise de masse et de caractériser le taux de conversion de la consommation d'oxygène sachant qu'une prise de masse de 32g correspond à la fixation d'une mole de O<sub>2</sub>. Bien sûr la détermination de ces grandeurs n'est possible que lorsque l'on a déduit du bilan de masse la perte liée à l'évaporation. Cette dernière a été mesurée sous azote à 60°C, 80°C et 110°C. Les essais d'oxydation ont été réalisés dans l'air et dans l'oxygène pur aux trois températures.

L'ensemble des résultats montre que le comportement des substrats étudiés résulte d'une oxydation en chaîne radicalaire amorcée par décomposition des hydro peroxydes. Ces derniers s'accumulent durant la période d'induction d'où la prise de poids. Cependant, dès que leur concentration dépasse un certain seuil, ils se décomposent probablement par voie bimoléculaire, pour générer des radicaux alkoxyles responsables des coupures de chaînes à l'origine de la dégradation finale.

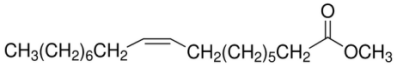
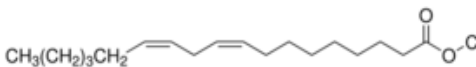
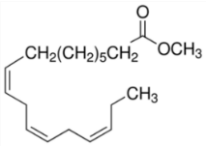
## Introduction

Experimental results for unsaturated fatty esters (UFE), called *model substances* are included in this chapter. The main objective is to use this substances to study thermo-oxidation of unsaturated fatty substances by means of thermogravimetric analysis (TGA). Using neat UFE avoids synergic or parallel effects which can occur in linseed oil for being a natural oil containing components different from unsaturated fatty acids.

Three UFE were selected as model substances because their similarity to fatty acids found in linseed oil and because there are a reliable research which can be complemented with TGA experiments (Richaud et al., 2012).

Because UFE are of reactive grade, TGA results can be analysed in depth and data treatment can be proposed to calculate oxygen uptake from thermo-oxidation. Table 4.1 shows structure, molecular weight and number of double bonds of each UFE.

**Table 4.1: Chemical structure of unsaturated esters (Analytical reagents from SIGMA-ALDRICH, San Luis, MO, USA)**

N ame	M olecular weight (g/mol)	Structure	M olecular weight (g/mol)	N umber of double bonds	[ PH] mol/g
ethyl oleate C1	96.49		96.49	2	1 (Type m <sub>1</sub> )
ethyl linoleate C2	94.47		94.47	2	3 (Type m <sub>2</sub> )
ethyl linolenate C3	92.46		92.46	2	6 (Type m <sub>2</sub> )

Based in the molecular structure of UFE, reactive sites explained in chapter III (Section 3.2.1) can be calculated for each one (column [PH] in Table 4.1), illustration of reactive sites is presented again in Figure 4.1

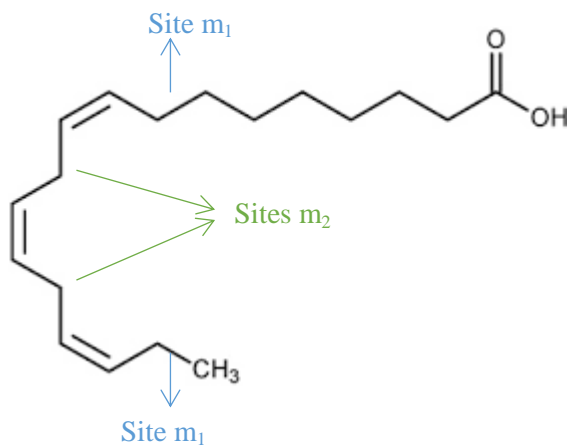


**Figure 4.1: Illustration of types of reactive sites for auto-oxidation**

Thermogravimetric analyses, which are usually utilized to evaluate thermal behaviour, were proposed as an alternative technique to evaluate the mass change caused by thermo-oxidation at moderate temperatures (from 40°C to 110°C); isothermal analyses were done at 40°C, 60°C, 80°C and 110°C under non-oxidative and oxidative atmospheres, in order to separate evaporation effects of oxidation ones.

#### 4.1 TGA in non-oxidative atmosphere of unsaturated esters

Thermogravimetric tests in nitrogen atmosphere show a slight decrease of weight (less than 5%) probably caused by equilibrium between ester-acid (Equation 4.1) or just by evaporation. Figures 4.2 to 4.4 show the same behaviour for the three UFE, because they have very similar molecular weight (Table 4.1).

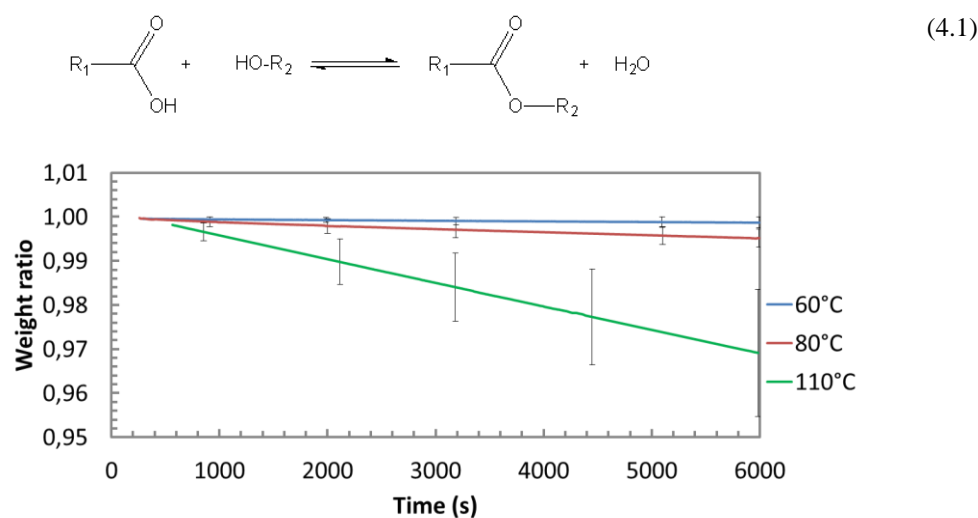


**Figure 4.2: TGA of Methyl Oleate in Nitrogen atmosphere**

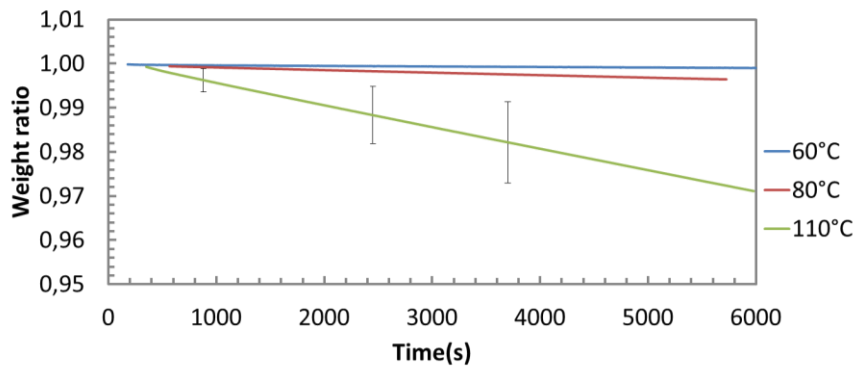


Figure 4.3: TGA of Methyl Linoleate in nitrogen atmosphere

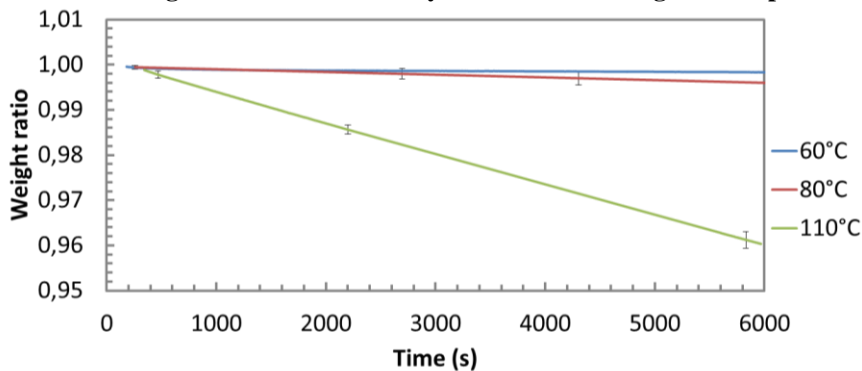


Figure 4.4: TGA of Methyl Linolenate in nitrogen atmosphere

For all the esters the decrease of weight is clearly different at each temperature.

#### 4.2 TGA in oxidative atmosphere

Oxidative atmospheres were air (21% oxygen concentration) and oxygen (99% oxygen concentration).

For methyl oleate (Figure 4.5) and methyl linoleate (Figure 4.6) was observable weight decrease during all the experimental time and temperatures. In the case of methyl linolenate (Figure 4.7) there is a slightly weight increase at 40°C, 60°C and 80°C attributable to oxygen grafting (Figure 4.8).

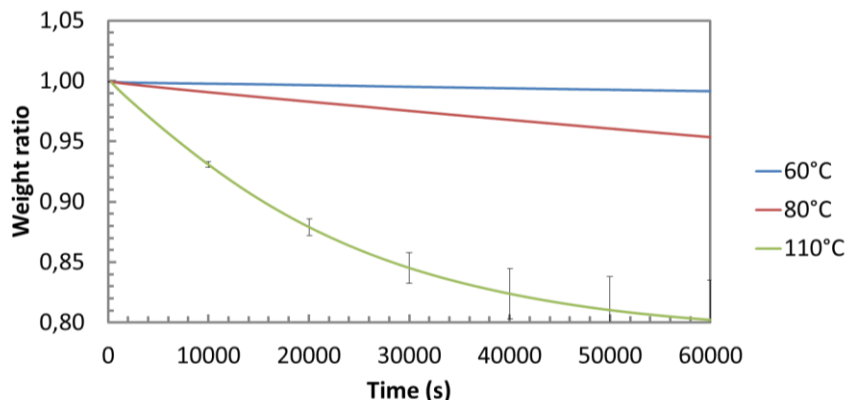


Figure 4.5: TGA of Methyl oleate in atmosphere of Air.

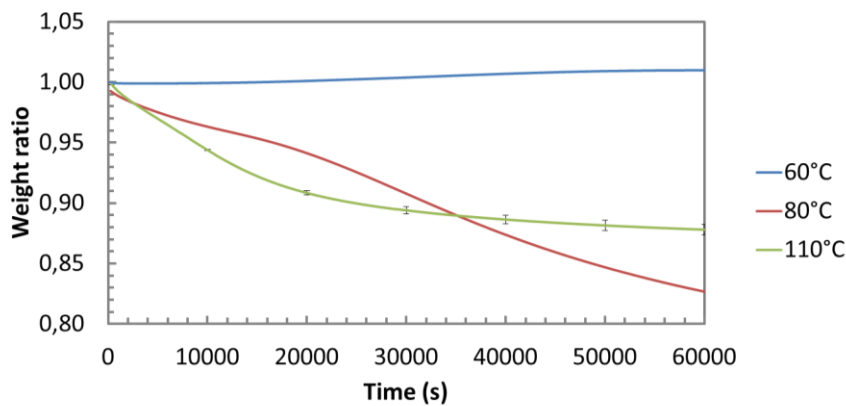


Figure 4.6: TGA of methyl Linoleate in atmosphere of Air.

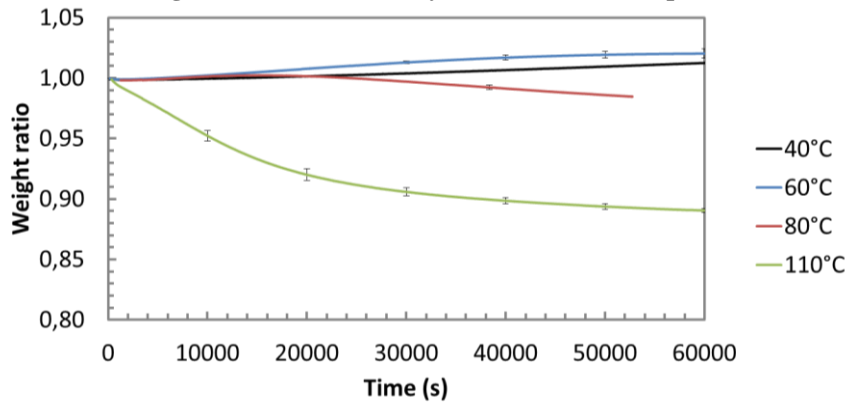


Figure 4.7: TGA of Methyl Linolenate in atmosphere of Air.

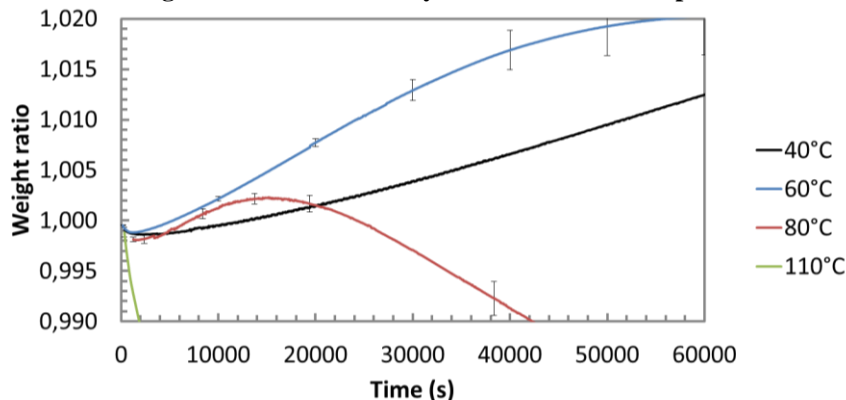


Figure 4.8: TGA of Methyl Linolenate in atmosphere of Air. Zoom for temperatures from 40°C to 80°C.

In the atmosphere with high oxygen concentration (c.a. 99% of dry oxygen), methyl oleate still exhibits decrease of weight at all temperatures studied (Figure 4.9). However, oxygen grafting is observable for methyl linoleate in the first 100 minutes at 60°C and 80°C (Figure 4.10) and for methyl linolenate at all the temperatures studied (Figure 4.11).

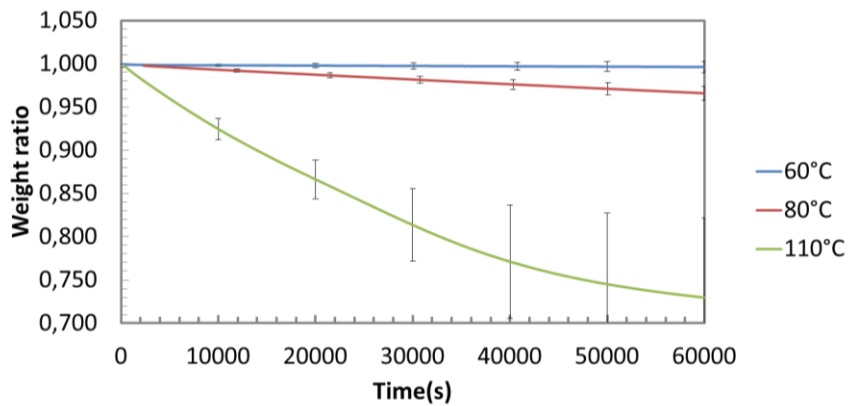


Figure 4.9: TGA of methyl oleate in atmosphere of Oxygen (99%)

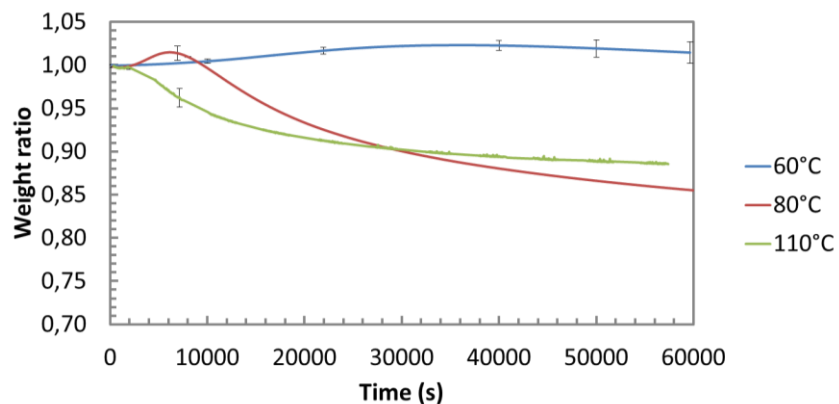


Figure 4.10: TGA of Methyl Linoleate in atmosphere of 99% Oxygen.

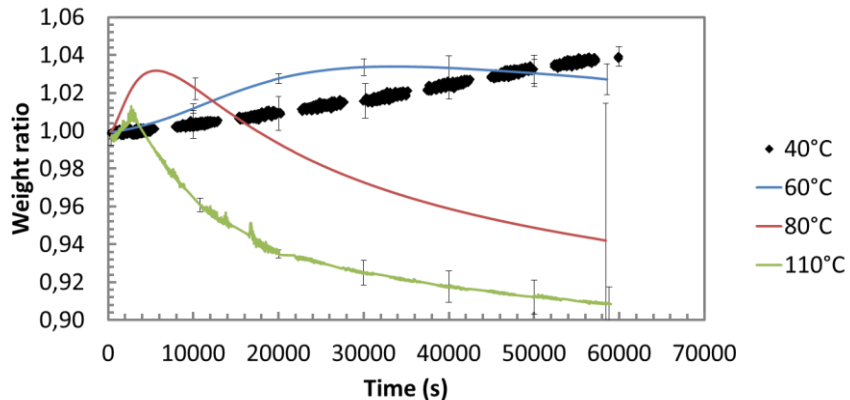
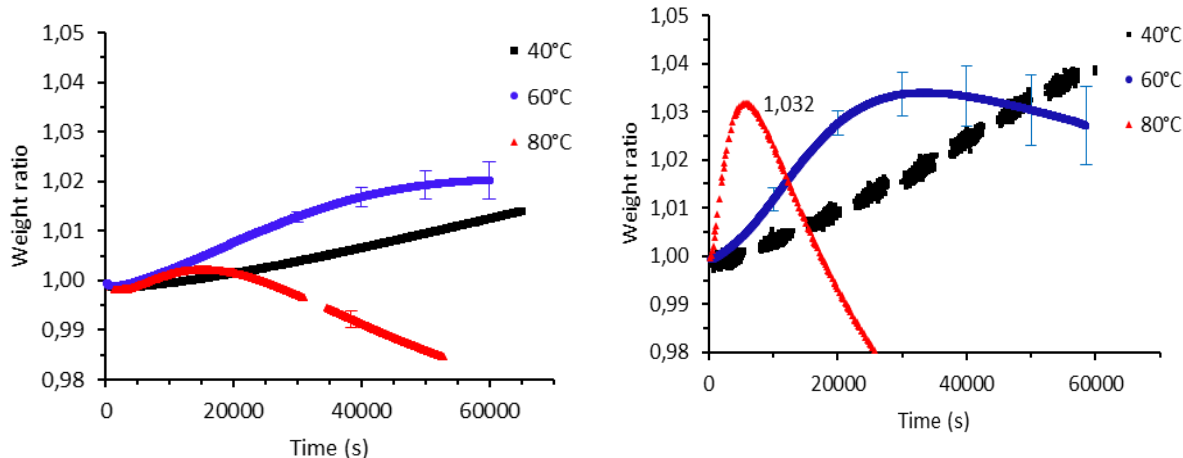


Figure 4.11: TGA of Methyl Linolenate in atmosphere of Oxygen 99%. About the differences in weight ratio with oxygen concentration, it is possible compare results for methyl linolenate (

Figure 4.12). At 110°C and air atmosphere, methyl oleate has weight decrease after 60000 s of 2% while in oxygen atmosphere the decrease was about 2.7%.



**Figure 4.12: comparison of TGA results of methyl oleate in air atmosphere (left) and oxygen atmosphere (right)**

### 4.3 Discussion of results for TGA of unsaturated esters

#### 4.3.1 TGA in non-oxidative atmosphere

To evaluate the decrease of weight in non-oxidative atmospheres, slopes  $\left(\frac{dm}{dt}\right)$  were calculated from TGA in nitrogen atmosphere and it was plotted  $\ln\left(-\frac{dm}{dt}\right)$  vs  $\frac{1}{T}$  to obtain values for an Arrhenius model (Equation 4.2)

$$\frac{dm}{dt}_T = \frac{dm}{dt}_0 e^{\frac{-E_a}{RT}} \quad 4.2)$$

$$\ln\left(-\frac{dm}{dt}_T\right) = \ln\frac{dm}{dt}_0 - \frac{E_a}{RT} \quad 4.3)$$

Plotting  $\ln\left(-\frac{dm}{dt}\right)$  vs  $\frac{1}{T}$  (Figure 4.13) is obtained a straight line which gathers all the esters studied, and then unique values for the Arrhenius expression were calculated. This coincidence can be explained by the similar molecular weight of the esters

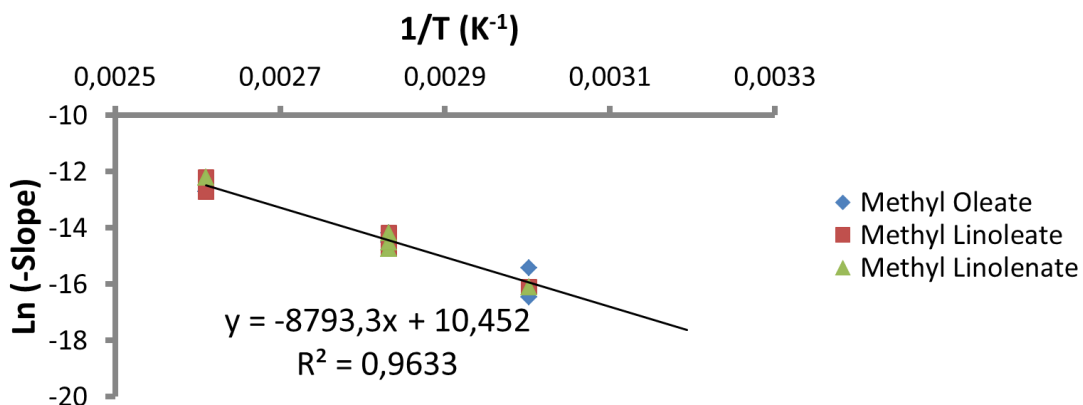


Figure 4.13:  $\ln \left( \frac{dm}{dt} \right)_T$  vs.  $1/T$  for esters and linseed oil.

Replacing values in equation 4.3, activation energy of 73kJ/mol is obtained

$\frac{dm}{dt}_0$  was also calculated (Equation 4.3)

$$10.452 = \ln \left( -\frac{dm}{dt}_0 \right) \quad 4.4)$$

$$\frac{dm}{dt}_0 = -e^{10.452} = -3.46 \times 10^4 s^{-1} \quad 4.5)$$

Replacing in equation 4.2, the expression below is obtained

$$\frac{dm}{dt}_T = -3.46 \times 10^4 e^{\frac{-73112}{RT}} \quad 4.6)$$

$\frac{dm}{dt}_T$  was calculated at the analysis temperatures, results are presented in Table 4.2

Table 4.2: Slopes calculated for unsaturated esters in nitrogen atmosphere.

Temperature °C	40	60	80	110
$dm/dt \text{ (s}^{-1}\text{)}$	$-2.21 \times 10^{-8}$	$-1.19 \times 10^{-7}$	$-5.31 \times 10^{-7}$	$-3.73 \times 10^{-6}$

### 4.3.2 TGA in oxidative atmosphere

Based on results presented in section 4.3.1, it appears clearly that mass changes result from two opposite phenomena: first oxygen grafting to the substrate molecules. This process leads to mass gain, for instance for a molecule of molar mass 300g/mol, the oxidation into hydro peroxide:  $\text{PH} + \text{O}_2 \rightarrow \text{POOH}$  would lead to a mass increase of 10.66%. If oxidation resulted only from this process, the mass would increase continuously until an asymptotic value corresponding to the full conversion of

oxidizable sites. But the observed decrease indicates the existence of a second process, responsible for mass loss, which becomes predominant after a time which is a decreasing function of temperature. This phenomenon results from the release of volatile molecules resulting from oxidative chain scissions in fatty ester molecules. Both (opposite) phenomena are thus manifestations of the same process i.e. the radical chain oxidation. It remains to explain why mass loss becomes competitive only after a certain time. Indeed the first explanation which comes in mind is that volatile products are only formed in secondary reactions slower than oxygen grafting ones, but this hypothesis fails to explain the whole behaviour. Another hypothesis corresponds better to the reality: since oxidation results from a “closed loop” radical chain process, its kinetic chain length  $\Lambda = \text{propagation rate} / \text{initiation rate}$ , characterized by a high initial value, decreases during the early time of exposure, to reach a value of unity in steady state. This means that during initial period propagation products, i.e. hydro peroxides and peroxides predominate and the mass increases. But initiation rate increases and tends to become equal to the propagation rate in steady state. Initiation results from POOH decomposition, this latter leads to alkoxy radicals of which a well known way of reaction is to rearrange by beta scission giving two fragments of relatively low molar mass and thus of relatively high volatility. The existence of a delayed predominant mass loss process is thus explained.

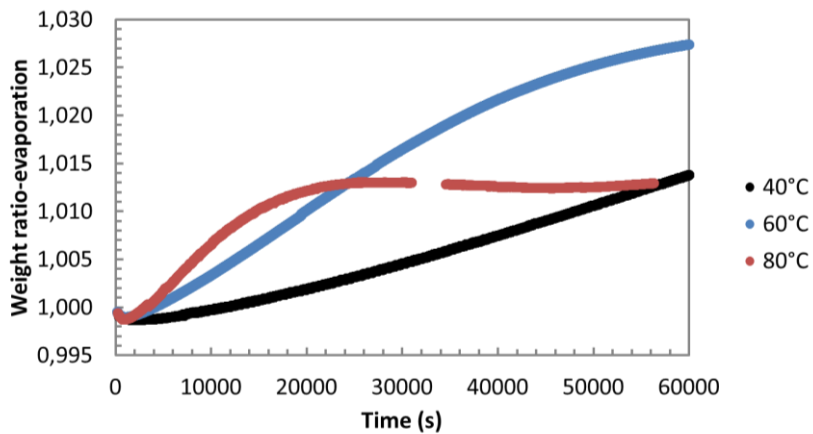
#### 4.3.3 Calculating oxygen scavenging capacity based on TGA

In order to see weight increase because just by thermo-oxidation, weight gained ( $W_o$ ) was calculated with equation 4.7.

$$W_{ot} = W_t - \frac{dm}{dt} t \quad 4.7)$$

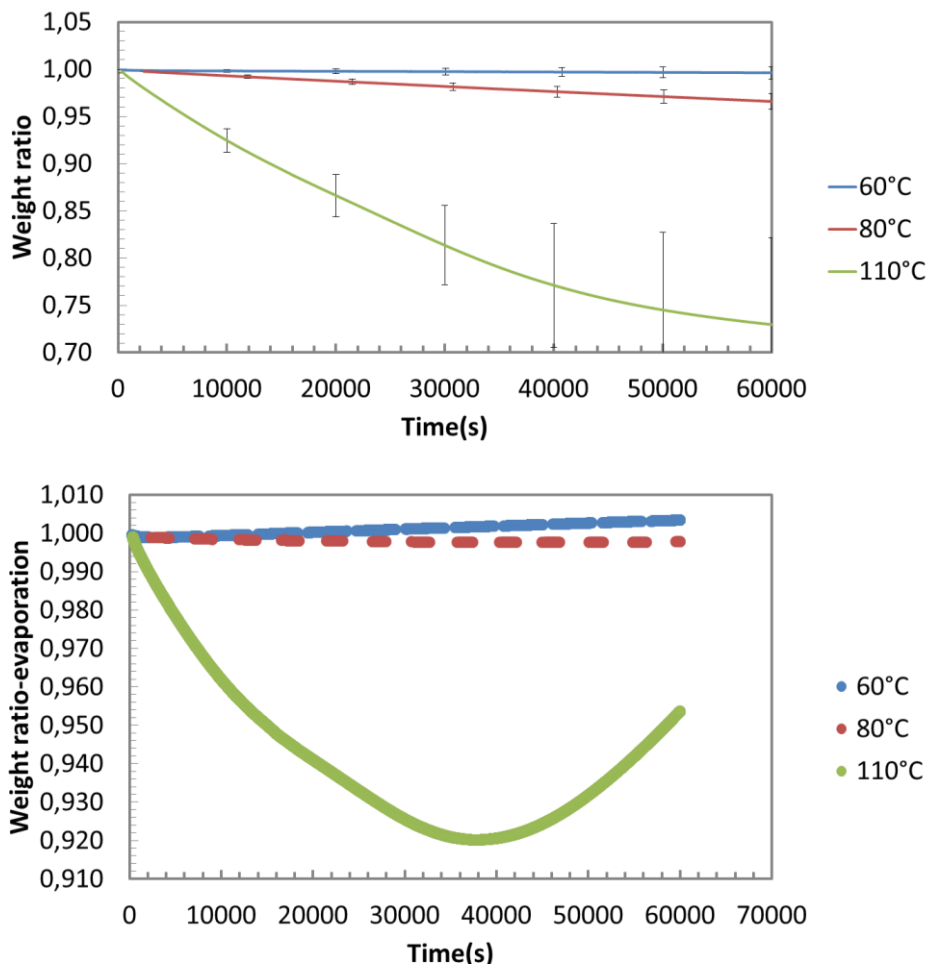
Where  $W_{ot}$  is the weight ratio gained solely by thermo-oxidation and  $W$  is the weight ratio obtained in TGA in oxidative atmosphere at different times  $t$ .

Figure 4.14 shows corrected TGA data of methyl linolenate in air atmosphere according equation 4.7; in isothermal tests done at 40°C, 60°C and 80°C is clear weight increase with time and also is possible to see how oxidation rate increases with temperature.



**Figure 4.14: Oxidation weight ratio calculated for Methyl Linolenate in atmosphere of Air.**

In the case of methyl oleate in oxygen the correction proposed compensates weight loss at 60°C and 80°C, still weight decrease is observed at 110°C during the first 40.000 seconds followed by an increase of 3% which does not reach the unity at least after 60.000 s.



**Figure 4.15: Oxidation weight ratio calculated Methyl Oleate in atmosphere of 99% Oxygen.**

For the case of methyl linoleate in oxygen atmosphere is interesting to see the increase with the temperature of the rate of oxygen grafting (Figure 4.16 Bottom); evaporation of oxidation products begins after 6.000 seconds for 80°C and at 2.000 seconds for 110°C.

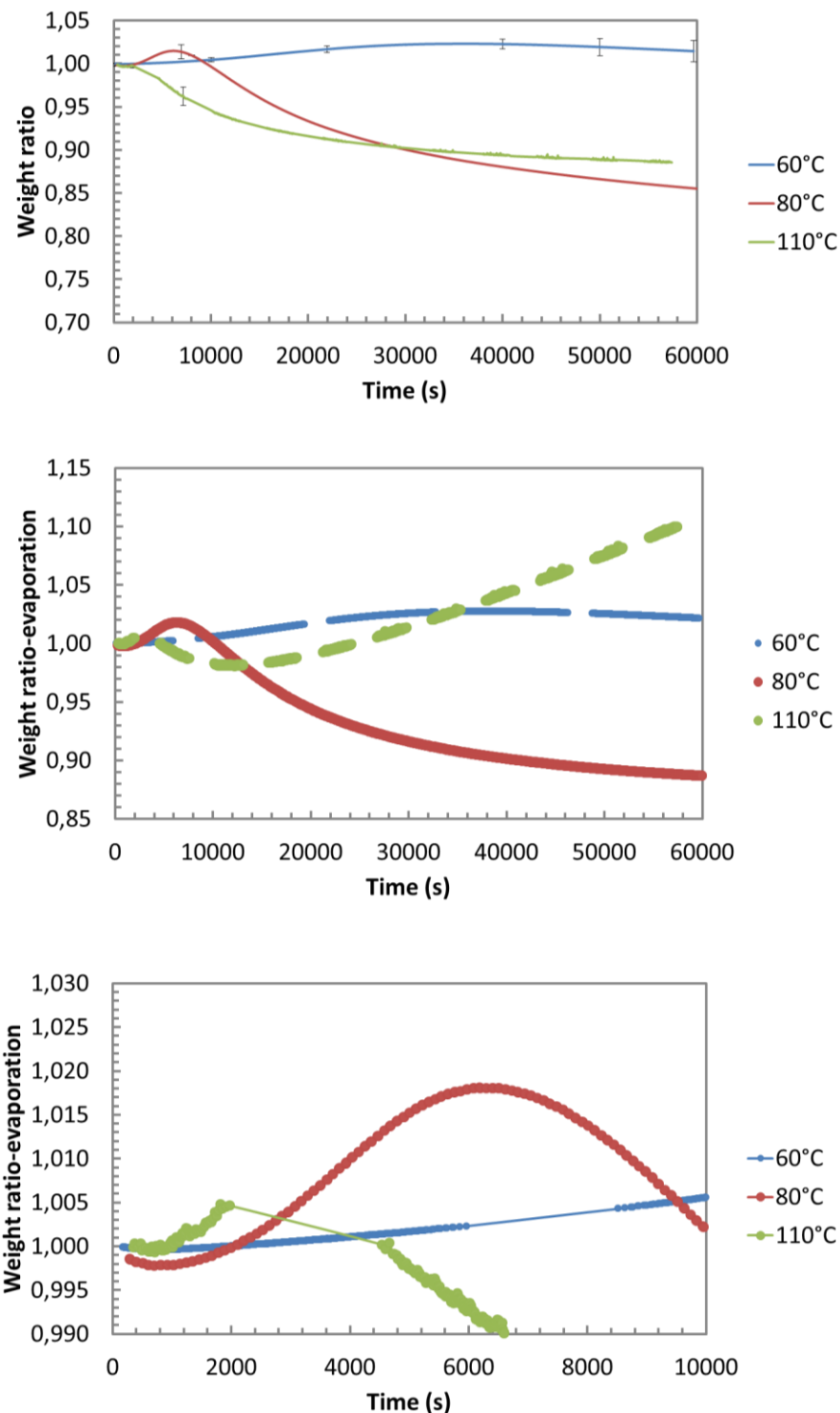
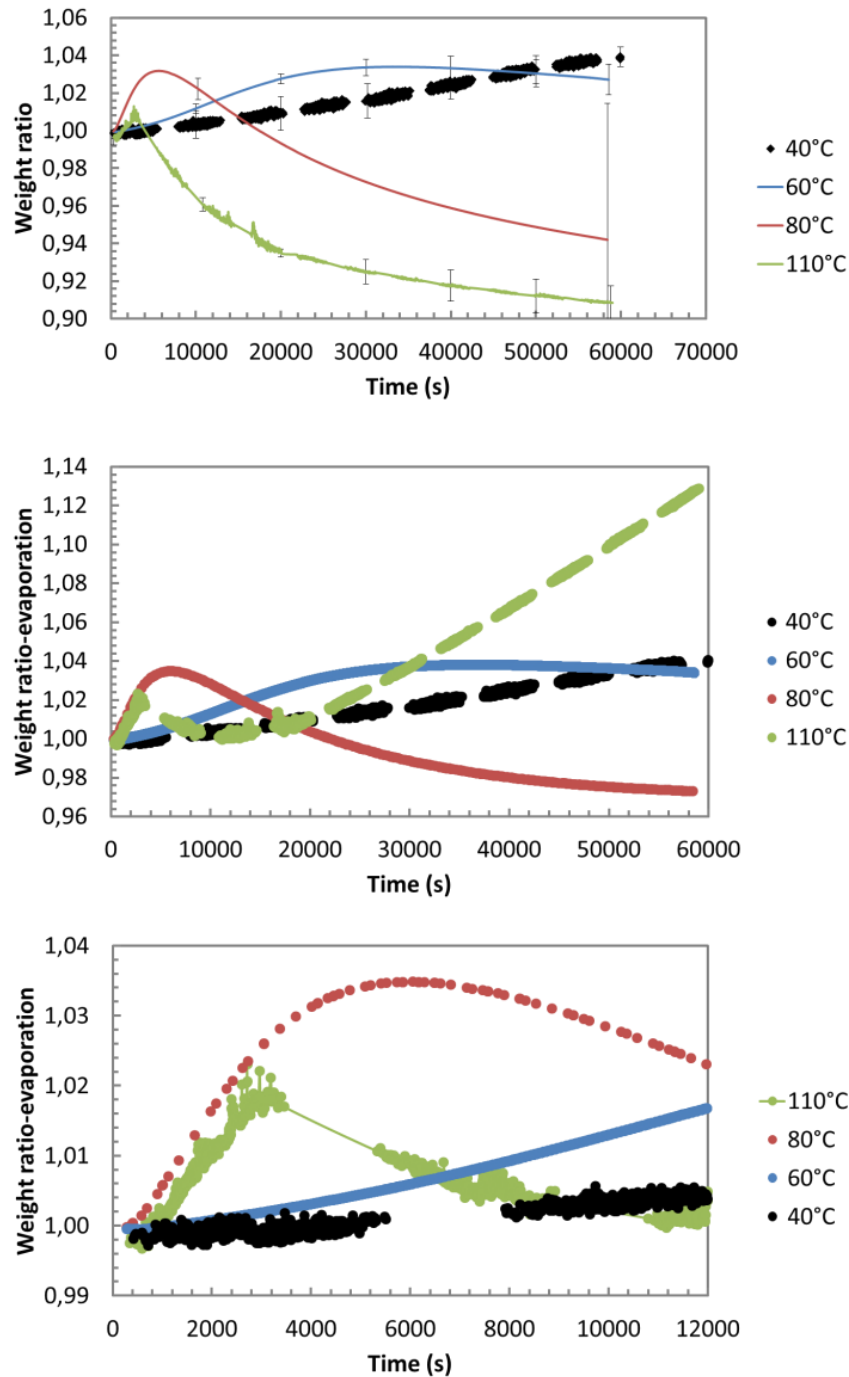


Figure 4.16: Oxidation weight ratio calculated for Methyl Linoleate in atmosphere of 99% Oxygen.

In the case of methyl linolenate (Figure 4.17) rate of oxygen grafting at 80°C and 110°C seem to be very similar.



**Figure 4.17: Oxidation weight ratio calculated for Methyl Linolenate in atmosphere of 99% Oxygen.**

Comparing Methyl Linoleate and Methyl Linolenate weight increase because oxygen grafting is higher for linolenate because it has one double bond more than linoleate (Figure 4.18).

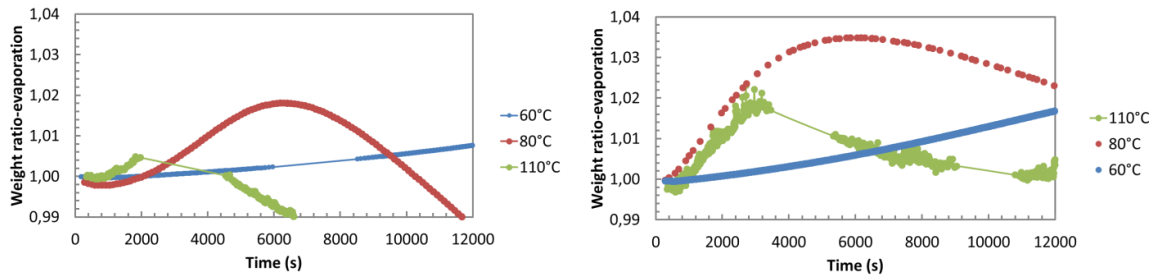


**Figure 4.18:**Comparison between oxidation weight ratio calculated for Methyl Linoleate in atmosphere of 99% Oxygen (left) and Methyl Linolenate in atmosphere of 99% Oxygen (right).

Effect of oxygen concentration can be observed comparing methyl linolenate in atmosphere of air and oxygen (Figure 4.19). In air, the oxygen available is lower, then the substance does not reach a maximum weight ratio as happens in oxygen atmosphere, also is observable than in air atmosphere the substance has a asymptotic behaviour while in oxygen atmosphere is observable a maximum weight ratio and after a rapid weight decrease because evaporation of products, at least at 80°C.

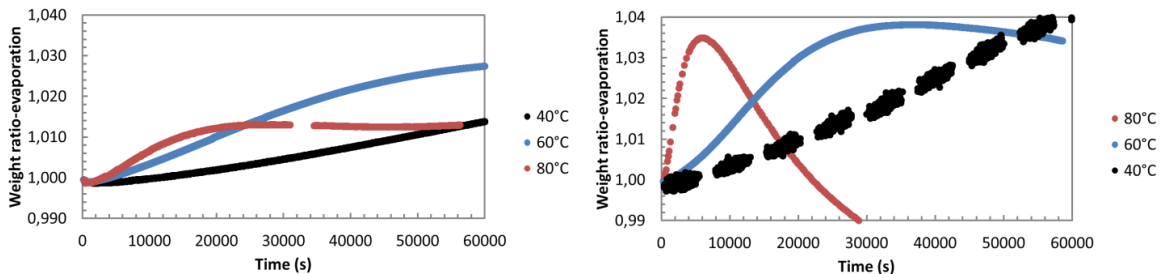


**Figure 4.19:** Comparison between oxidation weight ratio calculated for Methyl Linolenate in air atmosphere (left) and Methyl Linolenate in atmosphere of 99% Oxygen (right).

## References

Richaud, E., Audouin, L., Fayolle, B., Verdu, J., Matisová-Rychlá, L., & Rychlý, J. (2012). Rate constants of oxidation of unsaturated fatty esters studied by chemiluminescence. *Chemistry and Physics of Lipids*, 165(7), 753-759.  
doi:<http://dx.doi.org/10.1016/j.chemphyslip.2012.09.002>



# V

## Simulation approach

### CONTENT

---

INDEX OF FIGURES 103

INDEX OF TABLES 104

RESUME DU CHAPITRE V 105

---

INTRODUCTION	106
5.1 KINETIC MODELING	106
5.2 MODEL PARAMETERS ASSESSMENT	108
5.2.1 <i>Parameters known</i>	108
5.2.2 <i>Strategy to assess kinetic constants <math>k_{1b}</math>, <math>k_6</math>, <math>k_4</math> and <math>k_5</math></i>	109
5.3 INITIAL CONCENTRATIONS OF GROUPS $[\text{PH}]_0$ AND $[\text{POOH}]_0$	110
5.4 PSEUDOCODE	111
5.5 OXIDATION SIMULATIONS OF PURE OILS	113
5.5.1 <i>Simulation of linolenate mass changes in oxygen excess</i>	113
5.5.2 <i>Simulation of linolenate mass changes in air</i>	113
5.5.3 <i>Simulation of linseed oil mass changes in air</i>	114
5.5.4 <i>Values of <math>k_b</math>, <math>k_4</math>, <math>k_5</math> and <math>k_6</math></i>	115
5.5.5 <i>Simulations of oxygen absorbed for linseed oil at 40°C</i>	116
5.6 OXIDATION SIMULATIONS OF ACTIVE PACKAGING	117
5.6.1 <i>Modeling approach</i>	117
5.6.2 <i>Oxygen diffusion parameter</i>	118
5.6.3 <i>Simulations</i>	118
REFERENCES	125

## INDEX OF FIGURES

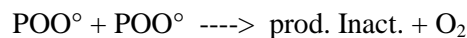
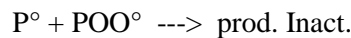
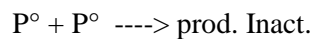
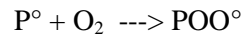
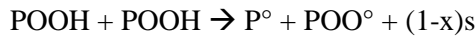
FIGURE 5. 1: WEIGHT RATIO SIMULATIONS FOR LINOLENATE MASS CHANGES IN OXYGEN EXCESS (SOLID LINE) AND EXPERIMENTAL DATA.....	113
FIGURE 5.2: WEIGHT RATIO SIMULATIONS OF LINOLENATE MASS CHANGES IN AIR (SOLID LINE) AND EXPERIMENTAL DATA.....	114
FIGURE 5.3: WEIGHT RATIO SIMULATIONS OF LINSEED OIL MASS CHANGES IN AIR (SOLID LINE) AND EXPERIMENTAL DATA.....	115
FIGURE 5.4: OXYGEN ABSORBED SIMULATIONS OF LINSEED OIL IN AIR (SOLID LINE) AND EXPERIMENTAL MASS CHANGES DATA AT 60°C.....	116
FIGURE 5.5: OXYGEN ABSORBED SIMULATIONS OF LINSEED OIL IN AIR (SOLID LINE) AND EXPERIMENTAL MASS CHANGES DATA AT 60°C.....	117
FIGURE 5.6: OXYGEN ABSORBED SIMULATIONS OF LINSEED OIL IN AIR FOR 50 µM THICK FILM.....	119
FIGURE 5.7: OXYGEN ABSORBED SIMULATIONS OF LINSEED OIL IN AIR FOR 100 µM THICK FILM.....	120
FIGURE 5.8: OXYGEN ABSORBED SIMULATIONS OF LINSEED OIL IN AIR FOR 150 µM THICK FILM.....	120
FIGURE 5.9: OXYGEN ABSORBED SIMULATIONS OF LINSEED OIL IN AIR FOR 150 µM THICK FILM.....	121
FIGURE 5.10: AVERAGE OXYGEN ABSORBED SIMULATIONS OF LINSEED OIL/PP IN AIR FOR DIFFERENT THICKNESSES.....	121
FIGURE 5.11: OXYGEN ABSORBED SIMULATIONS OF LINSEED OIL/PP IN 5% OXYGEN FOR 50 µM THICK FILM.....	122
FIGURE 5.12: OXYGEN ABSORBED SIMULATIONS OF LINSEED OIL/PP IN 5% OXYGEN FOR 100 µM THICK FILM.....	123
FIGURE 5.13: OXYGEN ABSORBED SIMULATIONS OF LINSEED OIL/PP IN 5% OXYGEN FOR 150 µM THICK FILM.....	123
FIGURE 5.14: AVERAGE OXYGEN ABSORBED SIMULATIONS OF 1% LINSEED OIL/PP IN 5% OXYGEN FOR DIFFERENT THICKNESSES.....	124

## INDEX OF TABLES

TABLE 5.1: VALUES OF $K_{03}$ , $E_3$ , $K_{3(40^\circ C)}$ , $K_{3(60^\circ C)}$ , $K_{3(80^\circ C)}$ AND $K_{3(110^\circ C)}$ FOR ACTIVE INGREDIENTS.....	109
TABLE 5. 2: VALUES OF $M_1$ , $M_2$ AND $[PH]_0$ FOR NEAT ESTERS.....	110
TABLE 5. 3: LINSEED OIL CHARACTERIZATION FROM GLC (METHOD A.O.C.S CE 1-62) AND VALUES CALCULATED OF $[PH]_{i0}$ .....	110
TABLE 5. 4: $[POOH]_0$ VALUE USED FOR SIMULATIONS.....	111
TABLE 5. 5: VALUES OF THE ARRHENIUS PARAMETERS OF ACTIVE INGREDIENTS .....	115
TABLE 5.6: VALUES OF $K_6$ AT DIFFERENT TEMPERATURES FOR ACTIVE INGREDIENTS.....	116
TABLE 5.7: VALUES OF $K_4$ , $K_5$ FOR ACTIVE INGREDIENTS.....	116
TABLE 5.8: VALUES OF OXYGEN DIFFUSION PARAMETERS $D_{O_2}$ IN POLYPROPYLENE FROM LITERATURE.....	118

## Résumé du chapitre V

Le modèle cinétique est dérivé d'un schéma mécanistique classique dans lequel l'amorçage résulte de la décomposition bimoléculaire des hydro peroxydes :



Où s'est une scission de chaîne et  $x < 1$ .

On écrit le système d'équations différentielles exprimant les vitesses de variation des différentes espèces réactives :  $\text{P}^\circ$ ,  $\text{POO}^\circ$ ,  $\text{POOH}$ ,  $\text{PH}$  et  $\text{O}_2$ . La vitesse de consommation d'oxygène, en absence de contrôle par la diffusion, serait :

$$d[\text{O}_2]/dt = -k_2[\text{P}^\circ][\text{O}_2] + k_6[\text{POO}^\circ]^2$$

Les paramètres du modèle sont déterminés comme suit : Une première simulation est réalisée en supposant que les paramètres cinétiques sont les mêmes que ceux, déjà connus, du linoléate de méthyle (composant majeur de l'HL). On procède ensuite à un ajustement des valeurs de ces paramètres pour parfaire la simulation. Un pseudocode est enfin proposé pour une utilisation en routine du modèle.

## Introduction

To model thermo-oxidation of unsaturated fatty acids, C-H bonds adjacent to double bonds were considered as unique active sites, at moderate temperature (<150°C). Section 5.1 presents the kinetic model used to simulate thermo-oxidation of UFE and linseed oil by considering mass changes driven by oxidation; in section 5.2, the method to determine kinetic parameters is presented, the third section presents the pseudocode used in Matlab to solve equations, and in the last two section are presented examples for pure linseed oil and for a practical case where the linseed oil is dispersed in a polypropylene matrix, for samples having different thicknesses.

### 5.1 Kinetic Modelling

A model for a hydrocarbon substrate with a single reactive site has been proposed by other authors (Audouin, Gueguen, Tcharkhtchi, & Verdu, 1995; Richaud et al., 2012; Tobolsky, Metz, & Mesrobian, 1950). The main feature of the model is that the initiation of radical chain oxidation is associated to hydro peroxide decomposition, whereas other mechanisms have been proposed in literature such as thermal decomposition of the substrate PH giving an alkyl radical ( $\text{PH} \rightarrow \text{P}^\circ$ ) or the decomposition of unknown impurities. As a result, considering the classical mechanisms for propagation and termination, hydro peroxide is a reactive specie and a product in the same time. That's why the model is often called the close-loop model.

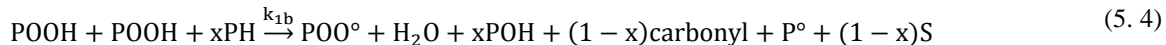
First, considering the initiation mechanisms, two ways are possible: the unimolecular decomposition ( $\text{POOH} \rightarrow \text{PO}^\circ + \text{OH}^\circ$ ) and the bimolecular decomposition ( $\text{POOH} + \text{POOH} \rightarrow \text{POO}^\circ + \text{PO}^\circ + \text{H}_2\text{O}$ ). In the case of unsaturated fatty acids oxidation studied by chemiluminescence Richaud et al., 2012 proposed that the bimolecular decomposition is the predominant mechanism over the unimolecular one since the activation energy for experimental induction period is close to 110 kJ/mol. Indeed, unimolecular decomposition activation energy is higher than 140 kJ/mol according to Denisov (Denisov & Afanas' ev, 2005).

As a result, we will consider only the bimolecular decomposition in our case:

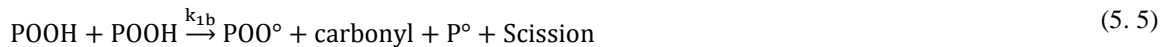


Where S is a chain scission

Summing up the three sub-reactions is obtained the balance reaction below



If  $x$ , which is the fraction of  $\text{PO}^\circ$  which forms  $\text{POH}$  is neglected in a first approach then the expression reduced for the initiation is obtained.

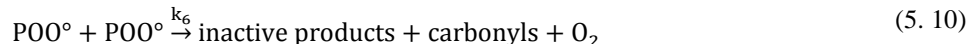
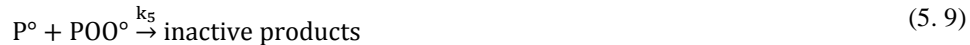


For propagation and termination the following classical scheme was proposed:

Propagation:



Termination



In order to express the concentration changes of every specie involved, a set of ordinary differential equations was derived. Equations (5. 11) to (5. 14) correspond to the alkyl radical ( $\text{P}^\circ$ ), peroxy radical ( $\text{POO}^\circ$ ), hydro peroxide ( $\text{POOH}$ ) and substrate ( $\text{PH}$ ) concentrations respectively; Equation (5. 15) expresses the rate at which oxygen is consumed by thermo-oxidation and  $k_{1b}$ ,  $k_2$ ,  $k_3$ ,  $k_4$ ,  $k_5$ , and  $k_6$  are the rate constants for reactions (5.5) to (5.10).

$$\frac{d[\text{P}^\circ]}{dt} = k_{1b}[\text{POOH}]^2 - k_2[\text{P}^\circ][\text{O}_2] + k_3[\text{POO}^\circ][\text{PH}] - 2k_4[\text{P}^\circ]^2 - k_5[\text{P}^\circ][\text{POO}^\circ] \quad (5.11)$$

$$\frac{d[\text{POO}^\circ]}{dt} = k_{1b}[\text{POOH}]^2 + k_2[\text{P}^\circ][\text{O}_2] - k_3[\text{POO}^\circ][\text{PH}] - k_5[\text{P}^\circ][\text{POO}^\circ] - 2k_6[\text{POO}^\circ]^2 \quad (5.12)$$

$$\frac{d[\text{POOH}]}{dt} = -2k_{1b}[\text{POOH}]^2 + k_3[\text{POO}^\circ][\text{PH}] \quad (5.13)$$

$$\frac{d[\text{PH}]}{dt} = -k_{1b}[\text{POOH}]^2 - k_3[\text{POO}^\circ][\text{PH}] \quad (5.14)$$

$$\frac{d[\text{O}_2]}{dt} = k_2[\text{P}^\circ][\text{O}_2] - k_6[\text{POO}^\circ]^2 \quad (5.15)$$

The main feature of this approach is that no assumption is done about possible stationary state and substrate (PH) consumption.

Oxygen consumed/absorbed in the thermo-oxidation can be calculated after solving the differential equation system by equation (5. 15).

It must be highlighted the competitiveness between  $k_2$  and  $k_4$  (Reactions (5. 6) and (5. 8)), for radical species  $P^\circ$ . The influence of oxygen will be studied changing the oxygen concentration by means of oxygen pressure at a given temperature. Influence of temperature will be studied changing the isotherm in thermogravimetric analyses.

To simulate thermogravimetric analyses, we will consider that mass changes are only associated to the oxygen consumed by oxidation since evaporation mechanism is taken into account in the data treatments (see previous chapter). As a result, mass changes can be calculated by equation (5. 16):

$$\frac{d[m]}{dt} = \frac{32}{\rho} (k_2[P^\circ][O_2] - k_6[POO^\circ]^2) \quad (5. 16)$$

Where  $\rho$  is the polymer density in g/L

## 5.2 Model parameters assessment

The kinetic values and other model parameters for each substance are explained below. In the case of kinetic parameters for linseed oil, which are unknown, the model was solved initially with the same values as methyl linolenate<sup>1</sup>.

### 5.2.1 Parameters known

Kinetic parameters for  $k_2$ ,  $k_3$  and their corresponding activations energies will be considered as already known from literature or other criteria, as follows:

- The step 2 being very fast because it involves only “radicals”  $P^\circ$  and  $O_2$ ,  $k_2$  has been chosen equal to  $10^7 \text{ L mol}^{-1} \text{ s}^{-1}$ . As a consequence, activation energy  $E_2$  is equal to 0.
- With the values presented of  $k_{3(30^\circ\text{C})}$  in Richaud et al, 2012 (Table 2, pg. 755),  $k_{03}$ ,  $E_3$ ,  $k_{3(T)}$  were calculated according equations (5. 17) and (5. 18) and after  $k_3$  was calculated at  $40^\circ\text{C}$ ,  $60^\circ\text{C}$ ,  $80^\circ\text{C}$ , and  $110^\circ\text{C}$ , values are presented in Table 5.1.

---

<sup>1</sup> For linseed oil same values of methyl linolenate were used because according to Gas-Liquid chromatography (GLC) it contains 52.6% of linolenic acid.

$$k_3(T) = k_{d3} \exp\left(\frac{-Ea}{RT}\right) \quad (5.17)$$

$$k_{03} = \frac{k_3(T)}{\exp\left(\frac{-Ea}{RT}\right)} \quad (5.18)$$

**Table 5.1: Values of  $k_{03}$ ,  $E_3$ ,  $k_{3(40^\circ\text{C})}$ ,  $k_{3(60^\circ\text{C})}$ ,  $k_{3(80^\circ\text{C})}$  and  $k_{3(110^\circ\text{C})}$  for active ingredients.**

Substance	$E_3$ [KJ mol <sup>-1</sup> ]	$k_{03}$ [L mol <sup>-1</sup> s <sup>-1</sup> ]	$k_3$ [L mol <sup>-1</sup> s <sup>-1</sup> ]			
			40°C	60°C	80°C	110°C
Methyl oleate	47	$8.28 \times 10^7$	1.20	3.54	9.26	32.46
Methyl linoleate	31	$3.50 \times 10^6$	23.63	48.31	91.08	208.27
Methyl linolenate	31	$3.50 \times 10^6$	23.63	48.31	91.08	208.27
Linseed oil	31	$3.50 \times 10^6$	23.63	48.31	91.08	208.27

## 5.2.2 Strategy to assess kinetic constants $k_{1b}$ , $k_6$ , $k_4$ and $k_5$

The strategy to assess model parameters unknown is the following:

1. Simulation of methyl linolenate mass changes under pure oxygen (1 bar). In these conditions, the termination steps ( $k_4$  and  $k_5$ ) involving alkyl radicals ( $P^\circ$ ) will be considered as negligible compared to the propagation step ( $P^\circ + O_2$ ), this exposure condition is called “oxygen excess”. In the regime of oxygen excess values of  $k_4$  and  $k_5$  for all substances were taken equal to zero.  $k_b$  and  $k_6$  will be assessed by comparing experimental curves and experimental data obtained at 60, 80 and 110°C.
2. Simulation of methyl linolenate mass changes under air to assess  $k_4$  and  $k_5$  corresponding to the “oxygen default” regime. Knowing that these termination steps involve alkyl radicals, their activation energy  $E_4$  and  $E_5$  will be considered equal to 0.

5.2.3 Simulation of linseed oil mass changes under air at 60, 80 and 110°C to adjust  $k_6$  and  $E_6$  compare to methyl linolenate mass changes.

### 5.3 Initial concentrations of groups $[PH]_0$ and $[POOH]_0$

Values of  $[PH]_0$  for UFE were calculated by taking into account the number of sites  $m_1$  and  $m_2$  of every molecular structure.

**Table 5. 2: Values of  $m_1$ ,  $m_2$  and  $[PH]_0$  for neat esters.**

Name	Number of double bonds	Number of sites $m_1$	Number of sites $m_2$	$[PH]_0^a$ [mol/ L]
Methyl oleate	1	2 <sup>a</sup>	0	6.0
Methyl linoleate	2	2	1 <sup>a</sup>	3.0
Methyl linolenate	3	2	2 <sup>a</sup>	6.0

$m_1$ , sites in  $\alpha$  position of one double bond;  $m_2$ , sites in  $\alpha$  position of two double bonds.

<sup>a</sup> Corresponds to the most reactive hydrogens in concentration  $[PH] = \rho \times (m_1 \text{ or } m_2)/M$ .

For the case of linseed oil,  $[PH]_0$  was calculated according equations (5. 19) and (5. 20)

$$[PH]_0 = \sum_{i=1}^n [PH]_{i0} \quad (5. 19)$$

$$[PH]_{i0} = X_i \times (m_1 \text{ or } m_2) \quad (5. 20)$$

Where  $n$  is the total number of components  $i$  identified by GLC and  $X_i$  is the molar concentration of every component  $i$ . Table 5. 3 shows values of  $[PH]_{i0}$  for linseed oil.

**Table 5. 3: Linseed oil characterization from GLC (Method A.O.C.S Ce 1-62) and values calculated of  $[PH]_{i0}$**

Component	Concentration obtained from GLC (% w/w)	Concentration calculated [mol/g]	Number of double bonds	Number of sites $m_1$	Number of sites $m_2$	$[PH]_{i0}$ [mol/g] <sup>a</sup>
Palmitic acid	5.9	$2.30 \times 10^{-4}$	0	0	0	0

Stearic acid	3.4	$1.20 \times 10^{-4}$	0	0	0	0
Oleic acid	19.2	$6.81 \times 10^{-4}$	1	2	0	$1.36 \times 10^{-3}$
Linoleic acid	16.2	$5.79 \times 10^{-4}$	2	2	1	$5.79 \times 10^{-4}$
Linolenic acid	52.6	$1.89 \times 10^{-3}$	3	2	2	$3.78 \times 10^{-3}$
Unknown	2.7					
$[PH]_0 \text{ Linseed oil} = 1.36 \times 10^{-3} + 5.79 \times 10^{-4} + 3.78 \times 10^{-3} = 5.72 \times 10^{-3}$						

<sup>a</sup>Corresponds to the most reactive hydrogens in concentration

Before exposure, radicals concentration ( $P^\circ$  and  $\text{POO}^\circ$ ) will be considered as equal to 0 since all the species are highly reactive and transformed into hydro peroxide. As a result, initial conditions are only linked to hydro peroxide concentration  $[\text{POOH}]_0$ .  $[\text{POOH}]_0$  value is necessarily lower than  $10^{-1} \text{ mol.L}^{-1}$  in our case, since it was not detectable by FTIR. Table 5. 4 shows the values proposed in the literature and used for our simulations.

**Table 5. 4:  $[\text{POOH}]_0$  value used for simulations.**

Substance	$[\text{POOH}]_0$ [mol.L <sup>-1</sup> ]
Methyl oleate	$5 \times 10^{-2}$
Methyl linoleate	$2 \times 10^{-2}$
Methyl linolenate	$5 \times 10^{-1}$
Linseed oil	$5 \times 10^{-1}$

#### 5.4 Pseudocode

Equations (5. 11) to (5. 15) were resolved using MatLab. Pseudocode with their corresponding explanation is presented below.

Explanation		Pseudo code
Variable declaration	Kinetic parameters	<code>kb k2 k3 k4 k5 k6</code>
	Initial concentration of species	<code>ph0 pooh0</code>

	Density of the ester	$\rho_{HO}$
	Solubility of oxygen in the ester	$s$
	Initial concentration of oxygen in the ester	$C_s = s * \text{Partial pressure of oxygen}$
	Interval de time studied	$t_0$ $t_{final}$
Vector which contains initial radicals concentration of the form [P° RO2° POOH PH]		$y_0 = [y_{01} \ y_{02} \ y_{03} \ y_{04}]$
Options for ordinary differential equation solver	MaxStep: Upper bound on solver step size  AbsTol: Absolute Tolerance  RelTol: Relative error tolerance that applies to all components of the solution vector $y$	<pre>options=odeset('MaxStep',3600,'Abstol',1e-8,'RelTol',1e-6);</pre>
Assignment of each row to corresponding radical concentration		<pre>n=length(t); t=t(1:1:n); np=length(t); p=y(1:1:n,1); po2=y(1:1:n,2); pooh=y(1:1:n,3); ph=y(1:1:n,4);</pre>
Solver of differential equations (3.13 to 3.16 in this document)		<pre>[t,y]=ode23s('YDERIVEformphvar',[t0 tfinal],y0);</pre>
Numerical solution to find $[O_2]$ at each time step and conversion of oxygen concentration to mass (dmass)		<pre>dO2=k2*p*Cs-k6*po2.*po2; %mass dmass=32*k2*p*Cs-32*k6*po2.*po2;</pre>

	<pre> mass (1)=0;  O2 (1)=0; FFO2 (2:np)=DEMISUM(t,dO2,np-1); FFmass (2:np)=DEMISUM(t,dmass,np-1); for i=2:np     mass (i)=mass (i-1)+FFmass (i);     O2 (i)=O2 (i-1)+FFO2 (i); end </pre>
Save solution of final concentrations	<pre> t=t; MatMO=[t p po2 pooh ph CO O2]; </pre>

## 5.5 Oxidation simulations of pure oils

### 5.5.1 Simulation of linolenate mass changes in oxygen excess

First, we propose the simulations at different temperatures in oxygen excess on one model compound: methyl linolenate. In this temperature range, no clear induction period appears but a slight auto acceleration at the first stage of exposure is observed, especially at 40°C. After the auto acceleration period, weight ratio reaches an asymptotic value due to the total substrate consumption PH. We observe that the model simulates experimental data up to the maximum value (weight ratio close to 1.04), the observed decrease for the experimental data can be attributed to a supplementary evaporation process not taken into account here. However, we will consider that the time to reach the maximum weight ratio could correspond to the “lifetime” in term of capability to absorb oxygen.

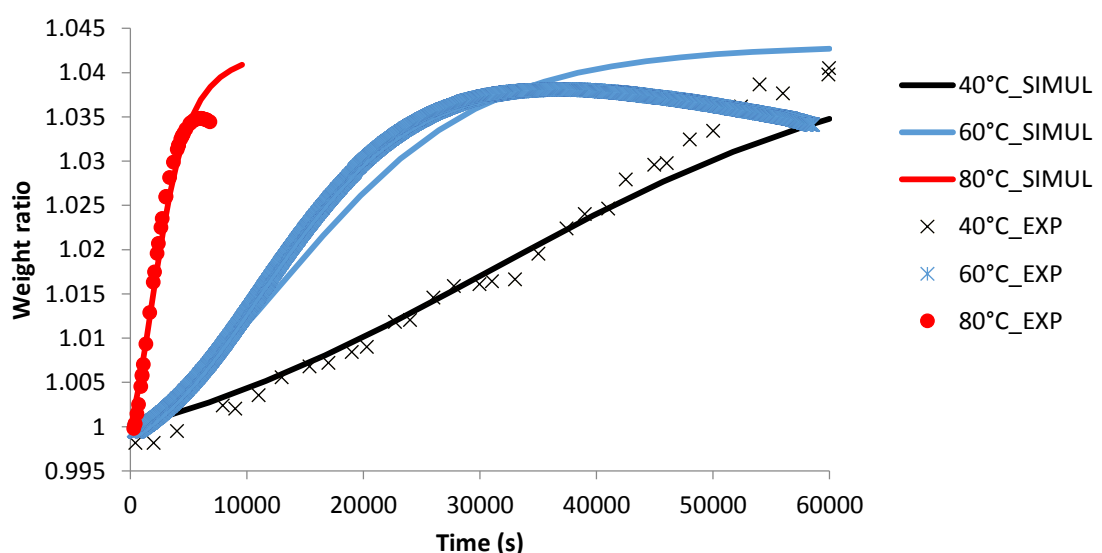


**Figure 5.1: Weight ratio simulations for linolenate mass changes in oxygen excess (solid line) and experimental data.**

### 5.5.2 Simulation of linolenate mass changes in air

Since  $k_b$  and  $k_6$  have been assessed successfully in oxygen excess, simulations are now performed by adding the terminations  $k_4$  and  $k_5$  keeping all the other parameters set. The main consequence to add these termination reactions is to decrease oxidation rate. Obviously, initial oxygen concentration is 5 times lower than in the previous case. Since  $k_4$  and  $k_5$  have been assessed to simulate weight ratio in air, the modelling with  $k_4$  and  $k_5$  have to simulate experimental data obtained in oxygen excess. Acceptable agreement is observed whatever the exposure temperature (Figure 5.2).

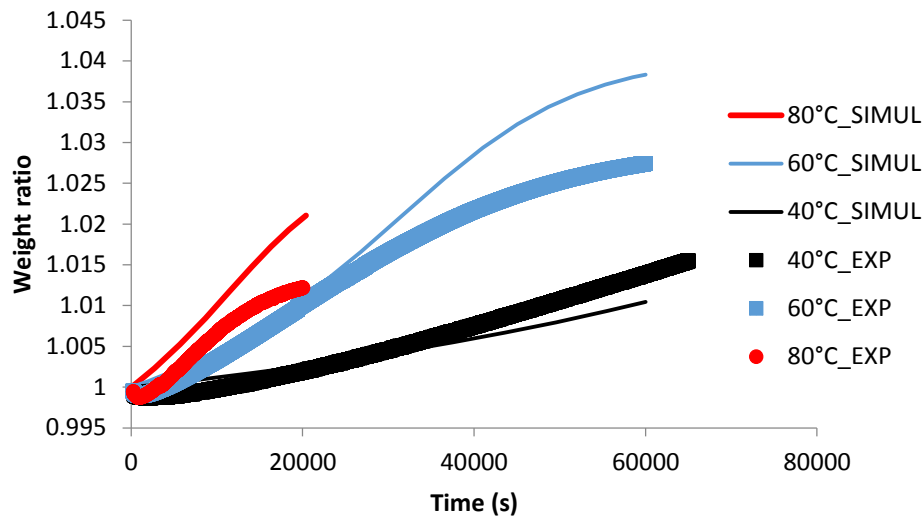


**Figure 5.2: Weight ratio simulations of linolenate mass changes in air (solid line) and experimental data.**

### 5.5.3 Simulation of linseed oil mass changes in air

Since  $k_4$  and  $k_5$  have been assessed on the model compound, simulations are compared to experimental data obtained on the linseed oil. The main difference between linolenate and linseed oil is the initial substrate concentration  $[PH]_0$ . Similar trends are observed but linseed oil shows an oxidation rate slightly higher than linolenate. In order to have a good description of the weight ratio curves,  $k_6$  values has been reasonably modified.

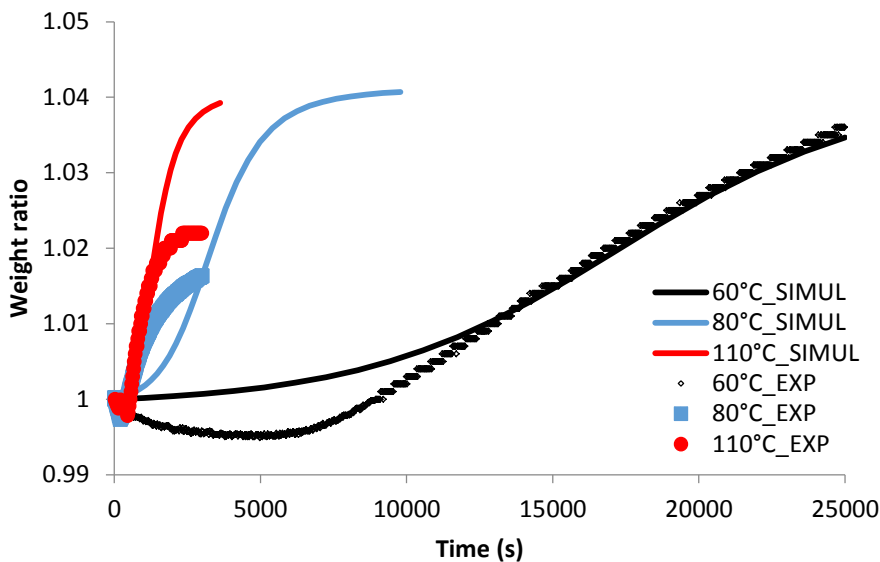


**Figure 5.3: Weight ratio simulations of linseed oil mass changes in air (solid line) and experimental data.**

#### 5.5.4 Values of $k_b$ , $k_4$ , $k_5$ and $k_6$

Values of  $k_b$  for neat esters are those reported by (Richaud et al., 2012)<sup>2</sup> and are presented in

Table 5. 5.

**Table 5. 5: Values of the Arrhenius parameters of active ingredients**

Substance	$K_{1b0}$	$E_{1b}$	$k_{1b}(150^\circ\text{C})$
Methyl oleate	$3.37 \times 10^{10}$	107.4	$1.86 \times 10^{-3}$
Methyl linoleate	$3.66 \times 10^8$	80.8	$3.88 \times 10^{-2}$
Methyl linolenate	$4.09 \times 10^{10}$	105.5	$1.21 \times 10^{-2}$
Linseed oil	$4.09 \times 10^{10}$	105.5	$1.21 \times 10^{-2}$

$k_6$  values used were the same as those reported by Richaud et al. 2012 and are presented in Table 5.6

<sup>2</sup> Richaud 2012, assumes values of  $E_6=0$ ,  $k_6=10^8 \text{ L mol}^{-1} \text{ s}^{-1}$ .

**Table 5.6: Values of  $k_6$  at different temperatures for active ingredients.**

Substance	$k_6$ [L mol <sup>-1</sup> s <sup>-1</sup> ]			
	40°C	60°C	80°C	110°C
Methyl oleate	3.01x10 <sup>6</sup>	9.52x10 <sup>6</sup>	2.64x10 <sup>7</sup>	1.00x10 <sup>8</sup>
Methyl linoleate	4.30x10 <sup>7</sup>	1.07x10 <sup>8</sup>	2.41x10 <sup>8</sup>	6.95x10 <sup>8</sup>
Methyl linolenate	2.57x10 <sup>7</sup>	7.95x10 <sup>7</sup>	2.17x10 <sup>8</sup>	8.00x10 <sup>8</sup>
Linseed oil	8.572x10 <sup>6</sup>	3.42x10 <sup>6</sup>	7.67x10 <sup>7</sup>	12.00x10 <sup>7</sup>

$k_4$  and  $k_5$  values are presented in Table 5.7. These values have to be taken into account to describe the influence of the oxygen concentration on the oxidation rate. Since the rate constant values are very high because they involve only radicals, as a result their activation energy is equal to 0.

**Table 5.7: Values of  $k_4$ ,  $k_5$  for active ingredients.**

Substance	$k_4$	$k_5$
	[L mol <sup>-1</sup> s <sup>-1</sup> ]	[L mol <sup>-1</sup> s <sup>-1</sup> ]
Methyl linolenate	3 x10 <sup>11</sup>	1 x10 <sup>10</sup>
Linseed oil	3 x10 <sup>11</sup>	1 x10 <sup>10</sup>

### 5.5.5 Simulations of oxygen absorbed for linseed oil at 40°C

Since weight ratio changes are correctly described, we propose here to use the modelling to discuss the oxygen absorption capability for the linseed oil at 40°C. For this purpose, the Figure 5.4 shows in a same plot the experimental weight ratio and the oxygen absorbed concentration by the oxidation process from the modelling. As expected, it appears a strong correlation between weight ratio changes and oxygen absorbed. As a result, this confirms that TGA experiment is a good tool to monitor oxygen scavenger property for a given oil.

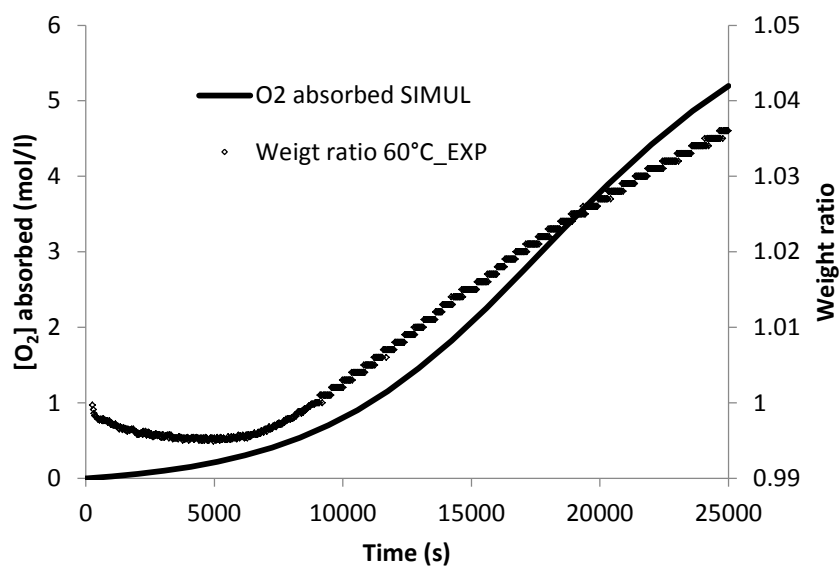


**Figure 5.4: Oxygen absorbed simulations of linseed oil in air (solid line) and experimental mass changes data at 60°C.**

To confirm the fact that the maximum weight ratio is linked to substrate consumption, we have plotted in a same graph the substrate concentration [PH] and the weight ratio changes. In Figure 5.5, it appears clearly that the maximum weight ratio is reached when [PH] tends towards 0.

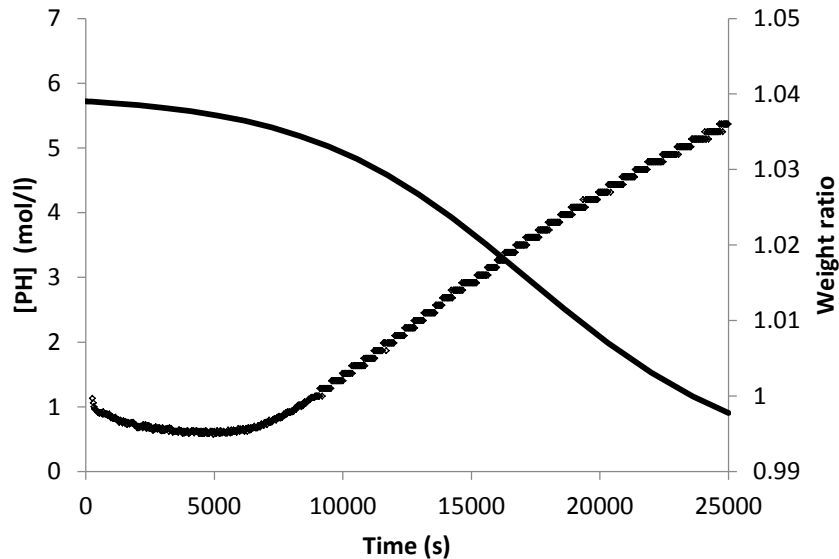


**Figure 5.5: Oxygen absorbed simulations of linseed oil in air (solid line) and experimental mass changes data at 60°C.**

## 5.6 Oxidation simulations of active packaging

### 5.6.1 Modelling approach

To model oxygen absorption of the active packaging, we will consider here that packaging consists on a polypropylene (PP) film where linseed oil is well dispersed into the PP matrix. In a first approach, the percentage of linseed oil into the matrix modified the substrate concentration at the initial state  $[PH]_0$ ,<sup>3</sup> the polypropylene will be considered as non oxidizable compare to linseed oil. We will assume that linseed oil is not oxidized during the film processing.

In this case of polymer film, it is well known that oxidation process can be controlled by oxygen diffusion, this phenomenon is often called diffusion limited oxidation in the literature. In our case, if oxidation rate is driven by the linseed oil oxidation, oxygen molecules have to diffuse through the PP from the surface to the core of the film. To take into account of this process, we propose to include the Fick's law for oxygen diffusion into the previous oxidation modelling. As a result, the differential equation system is the following:

$$\frac{d[P^{\circ}]}{dt} = k_{1b}[POOH]^2 - k_2[P^{\circ}][O_2] + k_3[POO^{\circ}][PH] - 2k_4[P^{\circ}]^2 - k_5[P^{\circ}][POO^{\circ}] \quad (5.21)$$

<sup>3</sup> 6/100mol/L of PH

$$\frac{d[POO^\circ]}{dt} = k_{1b}[POOH]^2 + k_2[P^\circ][O_2] - k_3[POO^\circ][PH] - k_5[P^\circ][POO^\circ] - 2k_6[POO^\circ]^2 \quad (5. 22)$$

$$\frac{d[POOH]}{dt} = -2k_{1b}[POOH]^2 + k_3[POO^\circ][PH] \quad (5. 23)$$

$$\frac{d[PH]}{dt} = -k_{1b}[POOH]^2 - k_3[POO^\circ][PH] \quad (5. 24)$$

And an equation describing the oxygen balance including oxygen consumption by oxidation and oxygen input by diffusion.

$$\frac{d[O_2]}{dt} = D_{O2} \frac{d^2[O_2]}{dx^2} - k_2[P^\circ][O_2] + k_6[POO^\circ]^2 \quad (5. 25)$$

Where  $D_{O2}$  is the diffusion coefficient for oxygen through the polypropylene,  $x$  the axis linked to the film thickness.

To monitor oxygen scavenger property, the oxygen absorbed is calculated in a post treatment as function of  $x$  by using the eq. (5. 15)

### 5.6.2 Oxygen diffusion parameter

Before to perform simulations coupling oxidation and oxygen diffusion, oxygen diffusion parameters must be determined. In our case, oxygen molecules diffuse through the PP matrix. For this purpose, we propose in the following table a literature compilation of oxygen diffusion values. According to these values, we will perform simulation with a  $D_{O2}$  value equal to  $1 \times 10^{-11} \text{ m}^2 \text{ s}^{-1}$  at  $60^\circ\text{C}$ .

**Table 5.8: Values of oxygen diffusion parameters  $D_{O2}$  in polypropylene from literature.**

T (°C)	$D_{O2} (\text{m}^2 \cdot \text{s}^{-1})$	Reference
25	4.7E <sup>-11</sup>	Kiryushkin S.G., Gromov B.A., <i>Vys. Soed.</i> , <b>14A</b> , 1715 (1972).
25	6.6E <sup>-11</sup>	R.M. FELDER, R.D. SPENCE & J.K. FERRELL, <i>J. Chem. Eng. Data</i> , <b>20</b> (1975) 235.
25	4.7E <sup>-11</sup>	S.G. Kiryushkin, B.A. Gromov, <i>Vysokmol. Soed.</i> , <b>A14</b> , 1715 (1972).
25	6.6E <sup>-11</sup>	S.G. Kiryushkin, B.A. Gromov, <i>Vysokmol. Soed.</i> , <b>A14</b> , 1715 (1972).
30	1.4E <sup>-12</sup>	Stannet V., in "Diffusion in polymers", edited by J. CRANK & G.S. PARK, Academic Press, NY, 41, 1968.
93	7.0E <sup>-11</sup>	E.T. Denisov, Y.B. Shilov, <i>Vysokmol. Soed.</i> , <b>A15</b> , 1196 (1983).
110	2.0E <sup>-11</sup>	G.A. George, in <i>Developments in Polymer Degradation-3</i> , 198 (1981).
130	6.0E <sup>-10</sup>	S.G. Kiryushkin, V.P. Filipenko, V.T. Gontkovskaya, <i>Karbonchain Polymers</i> , Moscow: Nauka, 182 (1971).

### 5.6.3 Simulations

**Influence of thickness on oxygen absorbed in air (20% oxygen)**

First, we consider a 1% linseed oil PP film during an exposure of 60h in air on both sides at 60°C. Oxygen absorbed is plotted as function of time and thickness for several thicknesses: 50 µm, 100 µm and 150 µm.

Oxygen absorbed for a 50 µm thick film is shown in Figure 5.6. The linseed oil oxidation is homogenous across the thickness, in other terms oxidation is not limited by diffusion. Since the film contains only 1% linseed oil, the global oxidation rate is strongly slowed down compare to pure linseed oil oxidation and the maximum oxidation rate correspond to the initial rate (see Figure 5.6).

Oxygen absorbed for 100 and 150 µm thick films are shown in Figure 5.7 and Figure 5.8. For both thicknesses, diffusion limited oxidation (DLO) appears. As expected, DLO effect increases with the film thickness. To observe clearly the oxidized layers during exposure, we propose in Figure 5.8 to show the oxygen absorption concentration in the time-thickness graph for the 150 µm film. Here, the increase of the oxidized layer thickness from 20 µm for a duration of 20h to 50 µm at 60 h can be observed.

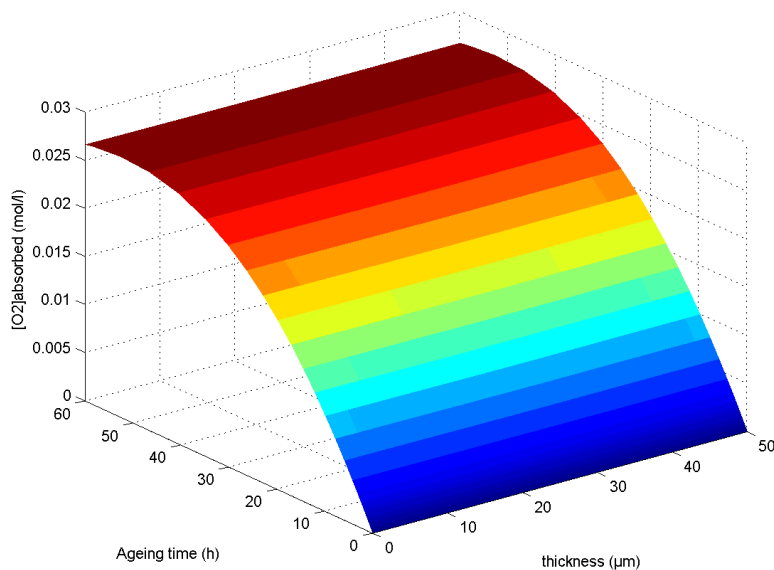


**Figure 5.6: Oxygen absorbed simulations of linseed oil in air for 50 µm thick film**

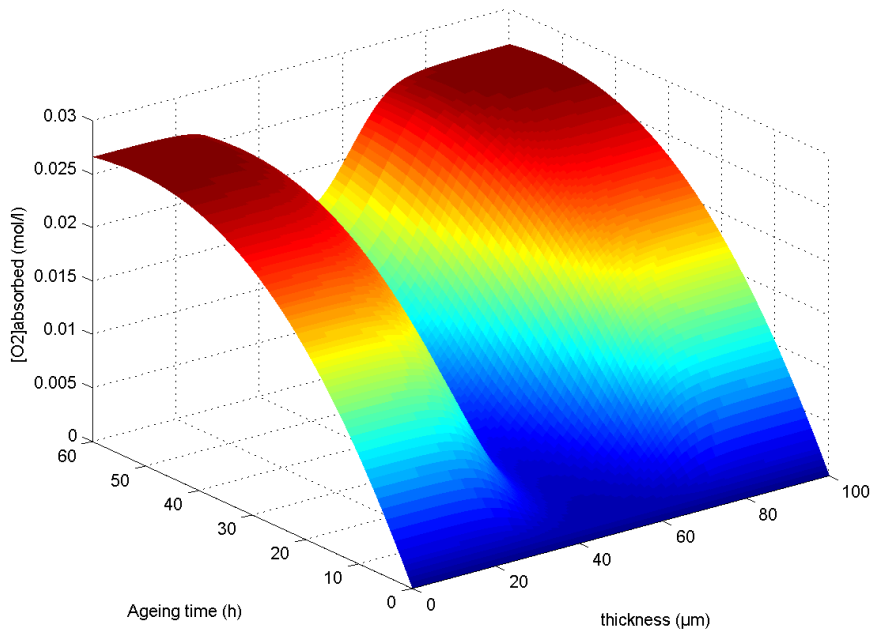


**Figure 5.7:** Oxygen absorbed simulations of linseed oil in air for 100  $\mu\text{m}$  thick film

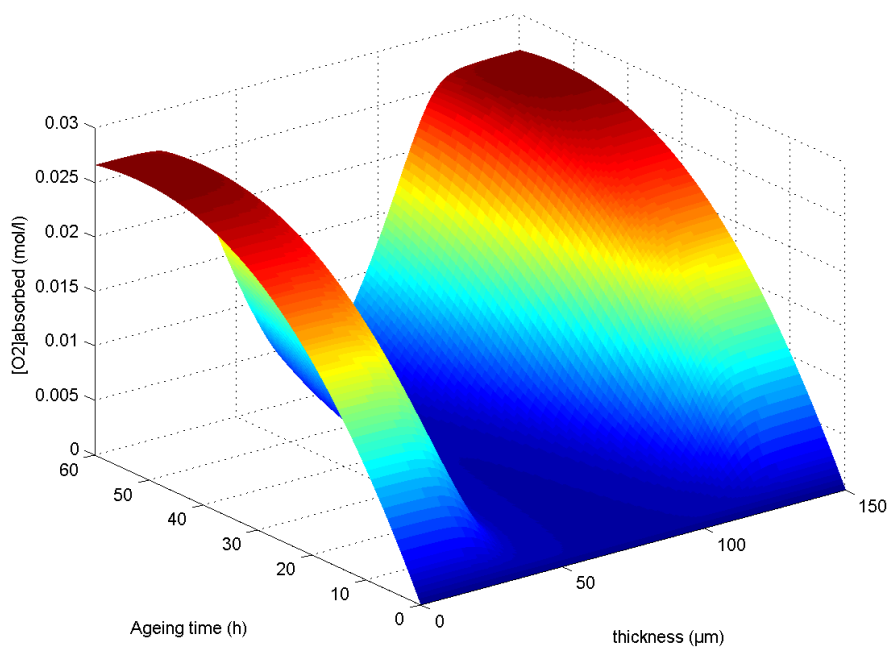


**Figure 5.8:** Oxygen absorbed simulations of linseed oil in air for 150  $\mu\text{m}$  thick film

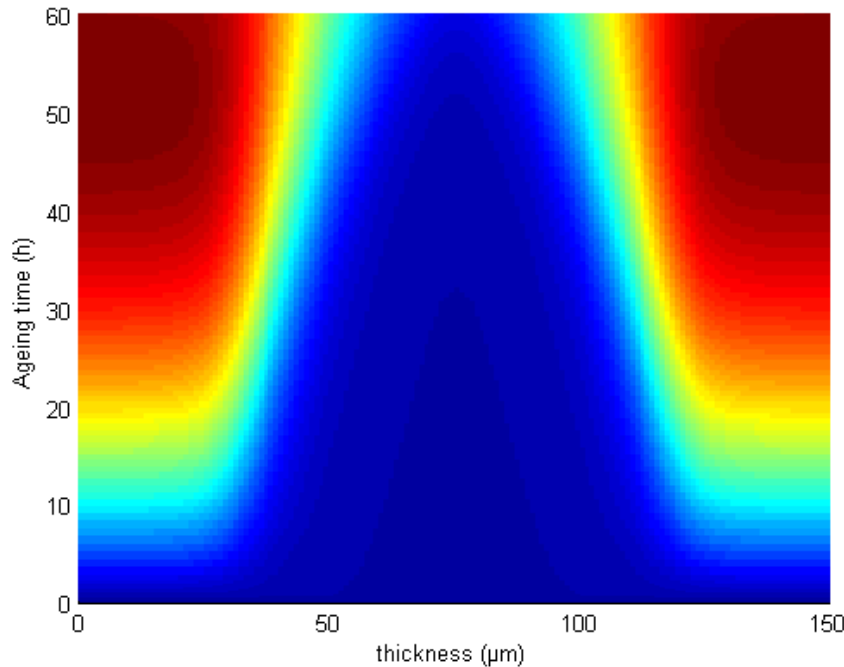


**Figure 5.9: Oxygen absorbed simulations of linseed oil in air for 150  $\mu\text{m}$  thick film**

In order to illustrate the influence of thickness on the average oxygen absorption rate of the film, we have plotted the average oxygen absorbed as a function of time for all the thicknesses simulated. It appears clearly that an increase of thickness leads to decrease the global oxidation rate. Furthermore, an increase of thickness leads also to increase the “lifetime” of the packaging.

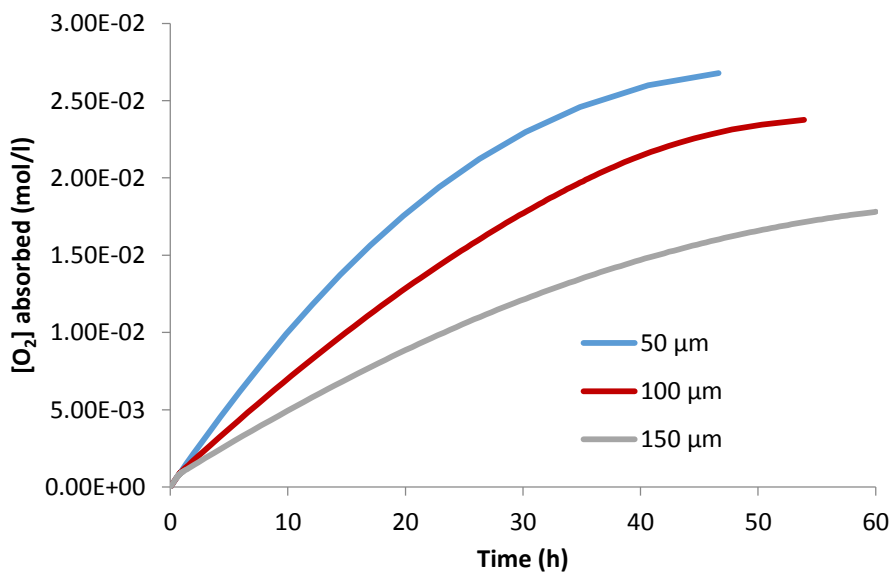


**Figure 5.10: Average oxygen absorbed simulations of linseed oil/PP in air for different thicknesses.**

### *Influence of thickness on oxygen absorbed in 5 % oxygen*

Practically, active films for packaging can be used in air containing only 5% oxygen (modified atmosphere packaging for instance). That's the reason why we propose here to simulate the oxygen absorption in this atmosphere for all three thicknesses explored previously (Figures 5.11, 5.12, 5.13).

First, by comparing Figure 5.6 and Figure 5.11, it appears that oxidation rate decreases with the initial oxygen concentration (20 to 5%). The effect has been expected since same trend has been observed experimentally between pure oxygen (100% O<sub>2</sub>) and air (20% O<sub>2</sub>).

On this other hand, if DLO effect is promoted by increasing the thickness as we have already seen, the shapes of the oxygen absorbed concentration across the thickness (Figure 5.11, 5.12, 5.13) are slightly different from ones obtained for 20% of oxygen (Figure 5.6, 5.7, 5.8). Indeed, the fact that the oxygen absorbed gradient for 5% is lower than the one for 20% can be explained by the decrease of oxidation rate. Since DLO effect results from the competition between oxidation rate and oxygen diffusion, an oxidation rate decrease promote an oxidation more "homogeneous". As a result, the average oxygen absorbed concentration curves simulated for the three thicknesses (Figure 5.14) are closer than the three curves shown in Figure 5.10.

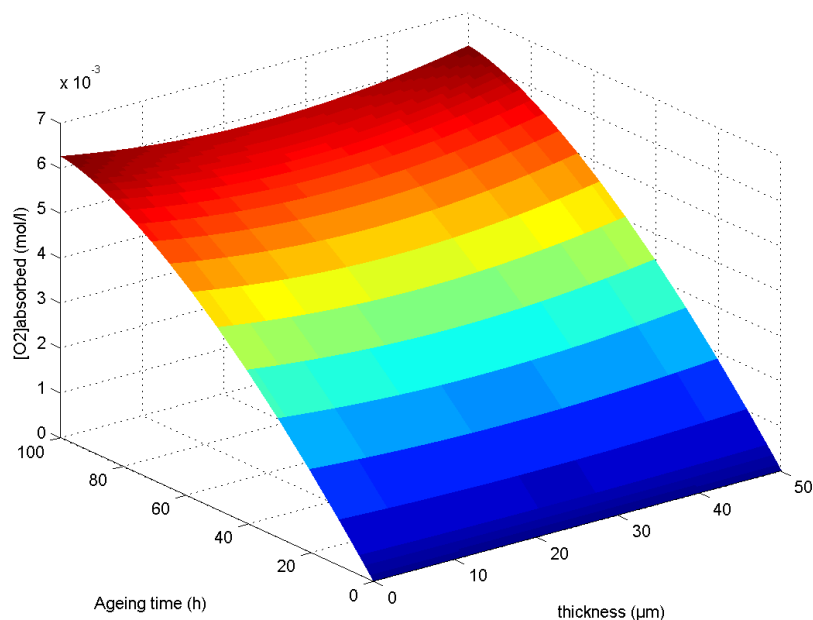


**Figure 5.11: Oxygen absorbed simulations of linseed oil/PP in 5% oxygen for 50  $\mu\text{m}$  thick film.**

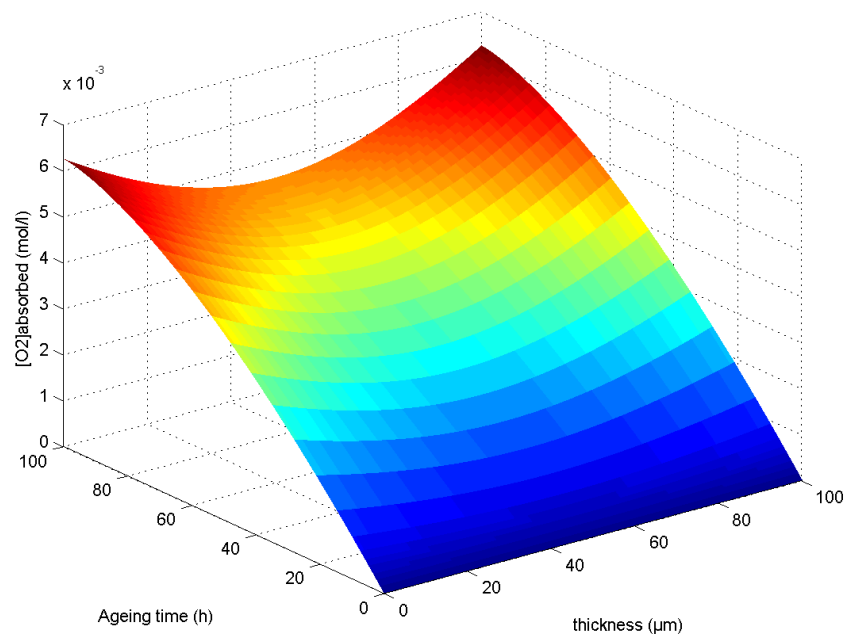


**Figure 5.12:** Oxygen absorbed simulations of linseed oil/PP in 5% oxygen for 100  $\mu\text{m}$  thick film

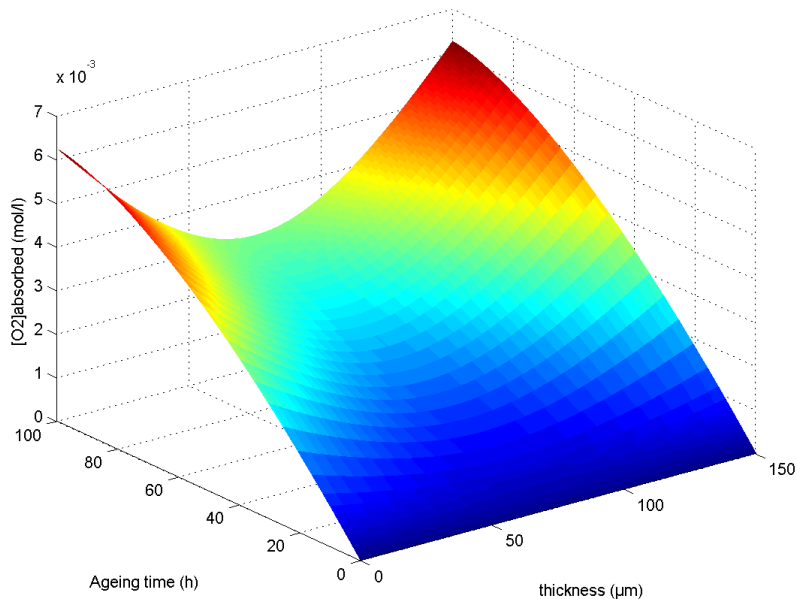


**Figure 5.13:** Oxygen absorbed simulations of linseed oil/PP in 5% oxygen for 150  $\mu\text{m}$  thick film

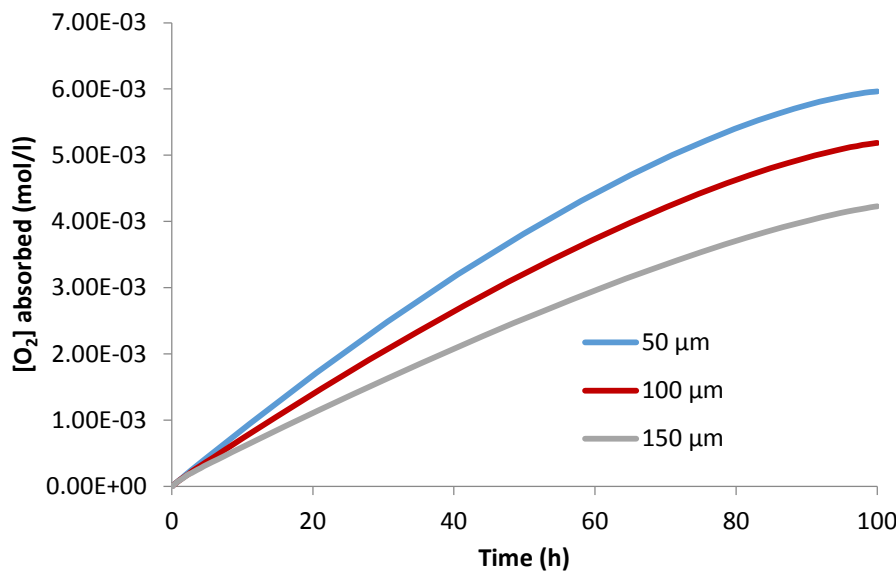


**Figure 5.14: Average oxygen absorbed simulations of 1% linseed oil/PP in 5% oxygen for different thicknesses.**

To conclude this simulation part, we have developed a kinetic modelling for the linseed oil oxidation. To assess the parameters of the kinetic modelling, we have used experimental data from TGA measurements performed on a model compound (linolenate oil) in pure oxygen and in air. This modelling has been adapted for pure linseed oil and validated on TGA measurements in air.

By coupling the linseed oil modelling and oxygen diffusion, we have simulated the oxygen absorptions of polypropylene films containing 1% of linseed oil. The main hypotheses to simulate the active packaging film are that the linseed oil is well dispersed in the PP matrix and that oxygen diffusion is governed by the PP matrix. Simulations of absorbed oxygen concentration have been performed for films having different thicknesses when they are exposed in air (20% of oxygen) and in an atmosphere of 5% of oxygen. It appears oxidation is controlled by diffusion for films having a thickness higher than 50 μm. As a result, we have shown that active packaging films properties are strongly dependent on the film thickness.

## References

- Audouin, L., Gueguen, V., Tcharkhtchi, A., & Verdu, J. (1995). "Close loop" mechanistic schemes for hydrocarbon polymer oxidation. *Journal of Polymer Science Part A: Polymer Chemistry*, 33(6), 921-927.
- Denisov, E. T., & Afanas'ev, I. B. (2005). *Oxidation and antioxidants in organic chemistry and biology*: CRC press.
- Holman, R. T., & Elmer, O. C. (1947). The rates of oxidation of unsaturated fatty acids and esters. *Journal of the American Oil Chemists' Society*, 24(4), 127-129.
- Richaud, E., Audouin, L., Fayolle, B., Verdu, J., Matisová-Rychlá, L., & Rychlý, J. (2012). Rate constants of oxidation of unsaturated fatty esters studied by chemiluminescence. *Chemistry and Physics of Lipids*, 165(7), 753-759.  
doi:<http://dx.doi.org/10.1016/j.chemphyslip.2012.09.002>
- Tobolsky, A. V., Metz, D. J., & Mesrobian, R. B. (1950). Low Temperature Autoxidation of Hydrocarbons: the Phenomenon of Maximum Rates1, 2. *Journal of the American Chemical Society*, 72(5), 1942-1952.



## **Conclusions and future work**

## CONCLUSIONS

Active packaging has been proposed as a technology able to improve quality and shelf life of products by means of components that might interact with the packaged food by releasing to, or absorbing from the surrounding, environment substances directly related to the degradation process.

Being oxygen scavengers one of the most important technology of active packaging, the *Grupo de Materiales y Manufactura* (CIPP-CIPEM) of *Universidad de los Andes* began five years ago its research about oxygen scavengers (OS) formulations and applications in plastic packaging.

In the first objective of this thesis, processing variables involved in the active film manufacturing, with active ingredients encapsulated, were studied; demonstrating that processes demanding high residence times or temperature changes will have a negative effect in the oxygen scavenger property and must be taking into account for future applications. Encapsulation can be effective against early thermo-oxidation to OS, until 250°C but causes delay in the oxygen uptake capacity of OS because diffusion effect.

The second objective is concentrated in the linseed oil's thermo-oxidation, followed by experimental tests and simulated with a classical kinetic model of auto-oxidation initiated by hydro peroxides.

In the experimental work, measurements of the oxygen in headspace were done, obtaining faster oxygen uptake with increase of temperature, the maximum oxygen consumed was 1.20mmol of oxygen per gram of linseed oil at 110°C after ~30 minutes in a headspace of 20ml of air.

TGA was proposed as a new alternative to follow oxygen scavenging capability, less demanding in time and number of tests than headspace measurements, obtaining comparable oxygen uptake capabilities (0.70mmol O<sub>2</sub>/g linseed oil). In order to study deeply TGA application to obtain OS efficiency, model substances of Unsaturated Fatty Esters (UFE) were analysed by TGA in oxidative and non-oxidative atmospheres and a simple method to calculate oxygen uptake, avoiding evaporation effects, is proposed. Through TGA was observed the effect in the number of unsaturations in oxygen grafting capability of each UFE, verifying the hypothesis of oxidation initiated by allylic hydrogens; this was also verified experimentally with peroxide value measurements by iodine titration were can be observed the higher peroxide value at higher oxidation rates (Figures 3.24 and 3.25).

In simulation part, a kinetic modelling for the methyl linolenate oxidation was developed, validated by TGA experiments in pure oxygen and air. This model was adapted for pure linseed oil obtaining corresponding kinetic constants for this substance in oxygen excess and limiting oxygen atmospheres.

By coupling the linseed oil modelling and oxygen diffusion, oxygen absorptions of polypropylene films containing 1% of linseed oil were simulated, with hypotheses of well dispersion of linseed oil in PP matrix, and oxygen diffusion governed by the PP matrix.

Simulations of absorbed oxygen concentration were performed for films having different thicknesses when they are exposed in air (20% of oxygen) and in an atmosphere of low oxygen (5%). It appears oxidation is controlled by diffusion for films having a thickness higher than 50 µm and therefore active packaging films properties are strongly dependent on the film thickness.

## CONTRIBUTION

This thesis provides the following contributions

- 1 Study of the effect of milling time, size and screw rate in the oxygen scavenger property of active films manufactured with linseed oil encapsulated and polypropylene.
- 2 Chemical characterization of double boiled linseed oil obtaining by FTIR and GLC, identifying each of the unsaturated acids attendant of oxidation.
- 3 A new application of TGA to follow oxygen scavengers efficiency, which allows analyse the effect of temperature and oxygen concentrations.
- 4 Values of oxygen uptake capacity of three UFE and linseed oil at moderate temperatures and two oxidative atmospheres: Oxygen and air.
- 5 Kinetic model, including kinetic constants, activation energies and all the parameters to simulate thermo-oxidation of UFE and linseed oil at different oxygen concentrations.
- 6 Tool of simulation of films containing UFE and linseed oil as oxygen scavengers or as additive of polymeric matrices of different thicknesses and frontier conditions.

## FUTURE WORK

This thesis is proposed as a new step in the research of oxygen scavengers and the path may be addressed in the next directions.

1. Sol-gel encapsulation must be incorporated in the simulation tool taking into account the corresponding effects of oxygen diffusion through silica matrix.

2. Comparison of commercial formulations of oxygen scavengers against linseed oil in terms of oxygen uptake efficiency.
3. Now that the kinetic model of thermo-oxidation is proposed and all the parameters defined, may be studied a mixed oxidation which begins with temperature activation (short time exposure) followed by exposure to ambient or cold chain conditions, with the aim to simulate the real situation of an active packaging activated by temperature.
4. Although here was proposed thermo-oxidation of linseed oil, may be studied also oxidation initiated by other ways, like UV radiation in order to propose new activation methods.

## ANNEX 1

# Publications and presentations done during the Thesis

## CONTENT

---

LINSEED OIL AS ACTIVE INGREDIENT IN ACTIVE PACKAGING	132
DESARROLLO, CARACTERIZACIÓN Y COMPARACIÓN DE NUEVOS INGREDIENTES ACTIVOS PARA SU USO EN EMPAQUES CON PROPIEDADES DE ABSORCIÓN DE OXÍGENO	136
MODELAMIENTO DE LA VIDA DE ANAQUEL EN PELÍCULAS DE POLÍMEROS REACTIVOS	141
METHODOLOGY TO EVALUATE PERFORMANCE OF ACTIVE INGREDIENTS AS OXYGEN SCAVENGERS	149

---

## LINSEED OIL AS ACTIVE INGREDIENT IN ACTIVE PACKAGING

**García Mora Angela María, Salas Muñoz Juan Camilo, Medina Perilla Jorge Alberto**

*Grupo de Materiales y Manufactura CIPP-CIPEM, Universidad de los Andes*

*Departamento de Ingeniería Mecánica, Universidad de los Andes, Bogotá, Colombia,  
Carrera 1 No. 18 A 12*

### **Abstract**

Ingredients that are intended to make active packaging, must be efficient, controllable, and, in the case of plastic packages, compatible with polymer technologies. In the field of oxygen scavengers, substances like linseed oil are attractive because of the high content of unsaturated lipids susceptible to oxidation.

### **Introduction**

The Food and Agriculture Organization of the United Nations (FAO) estimates that post-harvest losses in developed countries are between 5% and 25% of the produced volume, while in developing countries this value reaches of between 20 and 50% (O. d. l. N. U. p. l. A. y. l. A. FAO & I. I. d. C. p. l. A.-P. d. A. d. l. A. R. p. A. L. y. e. C. IICA/PRODAR, 2005).

In active packaging, components that would release or absorb substances into or from the packaged food or the environment surrounding the food, are incorporated in order to increase the shelf life of food products ("REGLAMENTO (CE) N o 450/2009," 2009). The current patents in the field of oxygen scavenger compositions could be classified mainly in iron-based, organic compound-based and polymer-based scavengers (de Fátima et al., 2009). The principal method for activate, or initiate the reaction between oxygen and scavengers, is moisture, and consequently in the scavenger composition is necessary to include moisture absorbers, materials with water permeation, that could mean less efficiency in all the packaging system because as well the oxygen causes depletion of food products, the excess of moisture is the major cause of food spoilage.

### **Problem Statement**

Unsaturated lipids are easily susceptible to auto-oxidation process; this chain reaction could be initiated by the presence of oxygen amount, presence of catalyst, UV radiation, temperature, free radicals among others. While in the area of oils conservation, the purpose is avoid oxidation, having linseed oil as a possible oxygen scavenger is of interest study a faster and controlled method to initiate its oxidation.

In addition to the activation by moisture, temperature, UV radiation and catalyst were studied as alternative activators

### **Experimental**

Double boiled Linseed oil from Vandeputte (Belgium), containing 80% of unsaturated lipids, was studied as future active ingredient of oxygen scavengers.

Linseed oil was triggered with different techniques, alone or mixed. The techniques used were moisture, UV radiation, blends with iron sulphate as catalyst, and temperature. Activation by moisture was performed exposing the samples to 90%RH, in a humidity chamber during 1 hour; in the case of UV radiation, the samples were exposed to 313 nm or 356 nm, from 1 to 60 minutes; in the blends were used mass ratios (catalyst/linseed oil) of 0, 0.50 and 2.00, and the activation by temperature was done at 80, 100, and 190°C.

The joint effect of the activation techniques on the oxygen uptake was studied with a factorial design, and the response variable were the percentages of oxygen after 4 and 6 days, data from gravimetric, and infrared spectra obtained in a Nicolet 380 in a range of wavenumber from 600 to 4000 cm<sup>-1</sup>.

In order to follow the reaction, the samples were packaged in cardboard boxes wrapped with aluminum foil, and the oxygen in the headspace was measured during different days with an oxygen analyzer (Quantek Instruments, Model 901); every sample had four replicates in order to consider the error of measurement.

### **Activation**

According to the statistical analysis, the catalyst had the major effect in the activation process, because in sulphate, the iron is in its ferrous state, which increases the presence of free radicals of lipids via Fenton type reactions (Mei, Decker, & McClements, 1998). About the effect of its quantity, changing the mass ratio (catalyst:linseed oil) from 0.5:1 to 2:1 increased the kinetic constant 2.5 times.

Although blends catalyst/linseed oil, without any additional process, had high efficiency removing oxygen on their own (88 mol of oxygen/g of blend), UV radiation improved oxygen-uptake efficiency (100 mol of oxygen/ g of blend).

With the purpose of compare oxygen-uptake efficiency of every activation treatment, data were fitted to the kinetic model shown in Eq. (1), or a first order kinetic model; the adjusting error was in average of 2.1%. The values of the kinetic constants (*k*) are between 0.00145 and 0.00548 h<sup>-1</sup>, being the higher value the corresponding to a blend linseed oil/iron sulphate (67% catalyst) activated with UV radiation, wavelength 356 nm, power 6000W during 1 minute. Currently, kinetic constants of commercial scavengers, in a first order, are between 0.03 and 0.615 h<sup>-1</sup>(Berenzon & Saguy, 1998; Charles et al., 2006).

$$\frac{d[O_2]}{dt} = -k[O_2] \quad (1)$$

## Infrared Analysis

Figure 1 shows the principal differences between infrared spectra (FTIR) found in a oxidized and a non-oxidized oil. There are three important zones of analysis, first between 3000 and 3600 cm<sup>-1</sup>, the second one around 1600 cm<sup>-1</sup>, and the last one from 600 to 1300 cm<sup>-1</sup>.

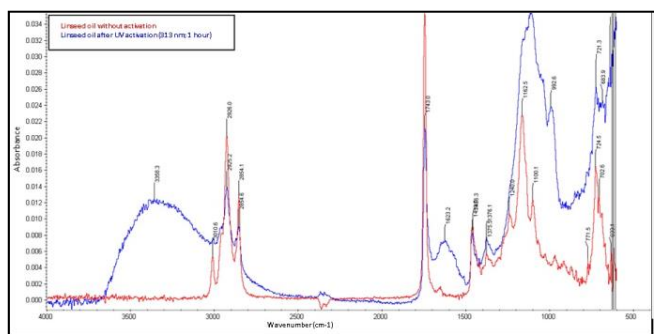
Zone with the higher wavenumbers is characteristic of stretching vibrations of the bond O-H, while the apparition of one peak at 1623 cm<sup>-1</sup>, indicates the presence of carbonyl groups because oxidation, and the changes in the zone between 600 and 1300 cm<sup>-1</sup> are the signal of the transformation of C-C bonds to C-O bonds (B. C. Smith, 2009).

## Summary and Conclusions

Experimental results and computer simulation are in good agreement with regards to the lifespan time of the preferred fine-celled bubbles in rotational foam moulding. They show that this time is significantly shorter than the inherently lengthy heating portion of the rotational moulding process, so that fine-celled bubbles seldom reach the solidification stage of the cycle, thereby leaving only the coarser-celled bubbles to participate in the final cellular structure.

## References

1. FAO, and IICA/PRODAR, *en América Latina, Poscosecha y servicios de apoyo a la comercialización* (2005).
2. REGULATION No. 450/2009, EUROPEAN COMISSION.
3. de Fátima, F.S.N., et al., *Recent patents on active packaging for food application. Recent patents on food, nutrition & agriculture*, 2009. 1(2): p. 171.
4. Mei, L., E.A. Decker, and D.J. McClements, *Evidence of Iron Association with Emulsion Droplets and Its Impact on Lipid Oxidation*. Journal of Agricultural and Food Chemistry, 1998. 46(12): p. 5072-5077.
5. Berenzon, S. and I.S. Saguy, *Oxygen Absorbers for Extension of Crackers Shelf-life*. Lebensmittel-Wissenschaft und-Technologie, 1998. 31(1): p. 1-5.
6. Charles, F., J. Sanchez, and N. Gontard, *Absorption kinetics of oxygen and carbon dioxide scavengers as part of active modified atmosphere packaging*. Journal of Food Engineering, 2006. 72(1): p. 1-7.
7. Smith, B.C., *Fundamentals of Fourier transform infrared spectroscopy*. 2009: CRC.



# Desarrollo, caracterización y comparación de nuevos ingredientes activos para su uso en empaques con propiedades de absorción de oxígeno

*Jorge Medina<sup>1\*</sup>, Jacques Verdu<sup>2</sup>, Bruno Fayolle<sup>2</sup>, Angela García<sup>1</sup>, Juan Salas<sup>1</sup>*  
**1:** Grupo de Materiales y Manufactura CIPP-CIPEM, Universidad de los andes. Bogotá, Colombia  
**2:** Procédés et Ingénierie en Mécanique et Matériaux. PIMM  
*\* jmedina@uniandes.edu.co*

## 1. INTRODUCCIÓN

La organización de las Naciones Unidas para la alimentación y la agricultura (FAO por sus siglas en inglés) ha estimado las pérdidas postcosecha en países en vías de desarrollo alcanza entre el 20 y el 50% del volumen producido total (Organización de las Naciones Unidas para la Agricultura y la Alimentación FAO & Instituto Interamericano de Cooperación para la Agricultura-Programa de Apoyo de la Agroindustria Rural para América Latina y el Caribe IICA/PRODAR, 2005); las causas son múltiples y abarcan desde factores genéticos y climáticos hasta prácticas culturales y procedimientos de manejo post cosecha (Kader & Rolle, 2004), dentro de los cuales se destaca la operación de empaque y embalaje.

Una de las principales funciones de un empaque de alimentos es mantener la calidad y seguridad del producto, inclusive proporcionando un ambiente propicio para una mayor vida de estante en comparación con un alimento sin empacar. Es así como actualmente se cuenta con propuestas tecnológicas, dirigidas al aumento de la vida útil de productos perecederos, como lo son los empaques activos.

### 1.1 Empaques activos

En los empaques activos, se incorporan componentes que liberan o atrapan sustancias que se encuentran en el ambiente circundante al alimento, y tienen un efecto sobre su calidad (Comisión Europea, 2009). En el tipo que liberan sustancias se encuentran por ejemplo, liberadores de dióxido de carbono (CO<sub>2</sub>), de humedad y aromas; mientras que, los absorbentes pueden ser secuestradores de radicales libres, de oxígeno o de etileno, siendo éstos últimos los más utilizados y patentados en el campo de empaques activos (Day., 2008).

### 1.2 Secuestradores de oxígeno y activación

Además de la función y composiciones de cada tecnología activa, es importante conocer su método de activación, es decir, el modo por el cual los componentes incorporados en el empaque activo, iniciarán el proceso de absorción o liberación de las sustancias deseadas.

En el caso de secuestradores de oxígeno las composiciones más relevantes son a base de hierro, moléculas orgánicas y polímeros oxidables, y el principal método de activación ha sido la humedad (F. Soares et al.,

2009), lo cual significa incorporar en la estructura del empaque capas absorbentes o permeables al agua, que pueden tener efectos negativos sobre la propia estructura del empaque, o bien, sobre el alimento, ya no a causa del oxígeno sino por la actividad de agua.

### 1.3 Objetivos

El grupo de materiales y manufactura de la Universidad de los Andes (CIPP-CIPEM) ha venido investigando, junto con el Instituto de capacitación e investigación del plástico y del caucho (ICIPC), nuevas composiciones y métodos de activación de secuestradores de oxígeno con el fin de ampliar a futuro la oferta local de este tipo de tecnologías, y ofrecer a la industria de empaques y alimentos respaldo técnico en la evaluación e incorporación de este tipo de propuestas.

En este trabajo se presenta la comparación entre ingredientes activos propuestos por el grupo de investigación y otros que ya han sido patentados por otros investigadores; así como técnicas de activación por temperatura y radiación UV, utilizando datos experimentales de consumo de oxígeno en el tiempo, gravimetrías, calorimetrias y espectroscopias de infrarrojo.

Con el propósito de analizar a profundidad los procesos químicos que ocurren en los ingredientes activos propuestos, quisimos comparar su comportamiento experimental frente a las cinéticas de oxidación propuestas en otras investigaciones, de aceites insaturados para el caso del aceite de

linaza, y de fosfolípidos para el caso de la lecitina de soya (Holman & Elmer, 1947; Litwinienko, Daniluk, & Kasprzycka-Guttman, 1999; Reblova, Pokorny, & Panek, 1991; Ulkowski, Musialik, & Litwinienko, 2005).

## 2. MATERIALES Y MÉTODOS

### 2.1 Materiales

Los ingredientes activos propuestos como secuestradores de oxígeno son Eritorbato de sodio, aceite de linaza y lecitina de soya, todos estos de calidad grado alimenticio. También se trabajó con composiciones formadas por los ingredientes activos en mezcla con sulfato de hierro (II), grado industrial, por su capacidad de catálisis en las reacciones de oxidación. La relación molar ingrediente activo/sulfato de hierro fue de 2/1 en masa.

### 2.2 Procedimiento

#### 2.2.1 Activación

Se estudiaron mediante un diseño experimental factorial cuatro métodos de activación: humedad, temperatura y radiación UV. Cada uno con los niveles presentados en xxx. La variable de respuesta fue el consumo neto de oxígeno en porcentaje, normalizado por la masa de la composición y el volumen empacado, después de 4 días.

#### 2.2.2 Desempeño de ingredientes activos

El consumo de oxígeno de cada ingrediente activo se determinó experimentalmente por medición de porcentaje

de oxígeno en el espacio de cabeza de un volumen conocido.

Tabla 1. Factores y niveles de activación estudiados.

Factor	Niveles	
<b>Humedad</b>	-1	1 90%
	Sin tratamiento de humedad	Humedad relativa, durante 1 hora
<b>Temperatura</b>	Sin tratamiento por temperatura	100°C 1 hora
	UV	UV 313nm
<b>Radiación 313 nm.</b>	UV	1 hora

Se utilizaron recipientes plásticos para depositar el ingrediente activo y posteriormente se activan según el tratamiento correspondiente al diseño de experimentos. Despues de activar el ingrediente o la composición, las muestras se empacan en bolsas de foil de aluminio las cuales se sellan al calor, para evitar el ingreso o salida de oxígeno en el espacio de cabeza.

El porcentaje de oxígeno en cada muestra se mide con un analizador de oxígeno Quantek 901 (Quantek Instruments), el cual mediante una aguja que se inserta en la bolsa de foil de aluminio, toma una muestra de aire e indica el porcentaje molar de oxígeno en la misma. Esta medición solo se puede realizar una vez a cada muestra ya que al tomar la

muestra de aire, se prescinde de la hermeticidad del empaque.

Además de medir la concentración de oxígeno, se realiza seguimiento gravimétrico.

Muestras con un mismo ingrediente activo se miden en diferentes días para obtener la curva de consumo de oxígeno en el tiempo, para cada tratamiento. En cada día se miden al menos dos muestras para tener en cuenta el error propio de la medición.

### 2.3 Análisis de datos

Con los datos de porcentaje de oxígeno y gravimetrías se elaboran curvas de consumo de oxígeno en función del tiempo. Se realiza una aproximación cinética sobre las curvas de concentración de oxígeno para evaluar la tasa de consumo en función de la concentración del gas.

El modelo matemático que se utiliza para el análisis cinético se presenta en la ecuación 1.

$$\frac{dC}{dt} = kC^n$$

Ecuación 1

Donde  $\frac{dC}{dt}$  es la tasa de consumo de oxígeno, k la constante cinética, C la concentración de oxígeno y n el orden de reacción. Estos modelos fueron comparados por lo presentado por la literatura según el ingrediente activo estudiado.

## 3. RESULTADOS Y DISCUSIÓN

### 3.1 Eficiencia y métodos de activación

En todos los casos la adición de sulfato de hierro a los ingredientes activos permitió activarlos para su oxidación y por lo tanto para que iniciara el consumo de oxígeno. En la figura 1 se presentan las curvas de

consumo de oxígeno para los ingredientes activos puros, y para mezclas de estos compuestos. Se puede apreciar el significativo incremento en la tasa de consumo de oxígeno, reflejado en la pendiente de la curva. La presencia de hierro en su estado ferroso conlleva el incremento de radicales libres por medio de reacciones Fenton (Mei et al., 1998) y por ello favorece la oxidación de los lípidos insaturados presentes en la lecitina; por otro lado, en el caso del Eritorbato se trata de una reacción electroquímica que de nuevo se ve favorecida por la presencia del hierro.

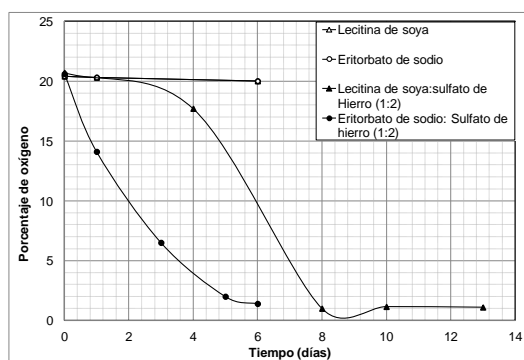


**Figura 1. Efecto del sulfato de hierro en mezclas con lecitina de soya ( $\blacktriangle$ ) y con Eritorbato de sodio ( $\bullet$ ), en comparación con los compuestos puros: lecitina de soya ( $\Delta$ ) y Eritorbato de sodio ( $\circ$ ). Activación: Humedad, 90%HR, 1 hora.**

El efecto del sulfato no resulta proporcional a su relación mísica dentro de la mezcla. En la figura 2 se muestra como, teniendo en cuenta el error experimental, las curvas de consumo de oxígeno parecen seguir el mismo modelo empírico con tres relaciones mísicas diferentes Lecitina de soya:sulfato de hierro.

La radiación UV mostró ser un medio eficiente de activación, sobre todo en el caso de las mezclas de aceite de linaza/sulfato

de hierro. La figura 3 presenta las curvas de consumo de oxígeno para estas mezclas con diferentes métodos de activación, junto con sus respectivos modelos empíricos. La pendiente es más pronunciada para el caso de activación UV a mayor longitud de onda y mayor potencia (6000 Watts), de ahí que los tiempos se reduzcan considerablemente frente a la activación a 313nm, con potencia de solo 1.22W/m<sup>2</sup>.

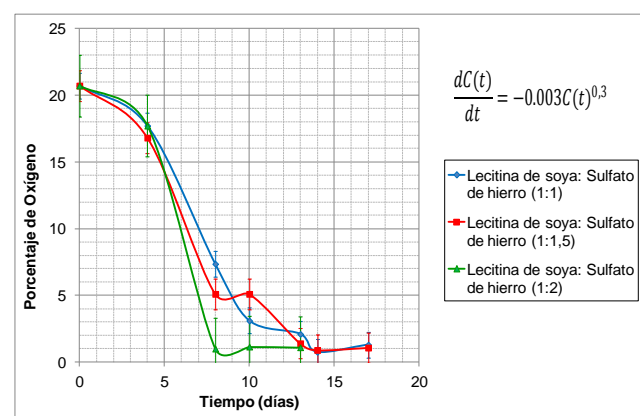
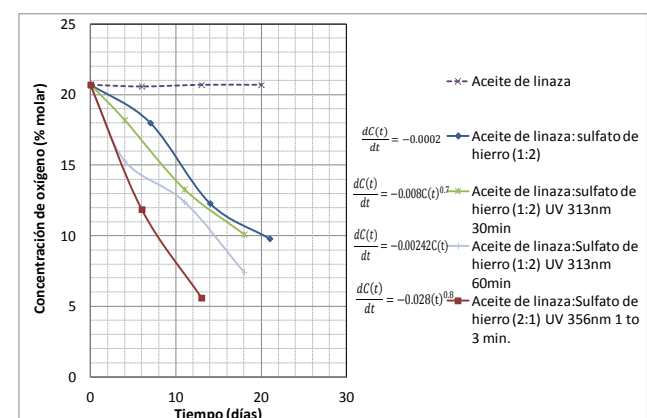


**Figura 2. Modelo empírico para el consumo de oxígeno en mezclas lecitina de soya/sulfato de hierro a diferentes relaciones mísicas.**



### 3.2 Comparación de modelos cinéticos

Los modelos cinéticos obtenidos a partir de los datos experimentales son diferentes a los modelos usualmente

presentados en la literatura para este tipo de ingredientes activos (Charles et al., 2006) comenzando por el orden de reacción, en general todos los absorbentes de oxígeno (*oxygen scavengers*) se presentan con modelos de primer orden, mientras que los materiales aquí estudiados tienen órdenes inferiores a uno en todos los casos. Inclusive, en el caso del aceite de linaza, el modelo de ajuste fue independiente de la concentración de oxígeno, es decir de orden cero.

## REFERENCIAS

Charles, F., Sanchez, J., & Gontard, N. (2006). Absorption kinetics of oxygen and carbon dioxide scavengers as part of active modified atmosphere packaging. *Journal of Food Engineering*, 72(1), 1-7. doi: 10.1016/j.jfoodeng.2004.11.006

REGLAMENTO (CE) No 450/2009 (2009).

Day., B. P. F. (2008). *Active Packaging of Food. Smart Packaging Technologies for Fast Moving Consumer Goods*: John Wiley & Sons, Ltd.

F. Soares, N. d. F., S. Pires, A. C., Camilloto, G. P., Santiago-Silva, P., P. Espitia, P. J., & A. Silva, W. (2009). Recent patents on active packaging for food application. *Recent patents on food, nutrition & agriculture*, 1(2), 171.

Holman, R. T., & Elmer, O. C. (1947). The rates of oxidation of unsaturated fatty acids and esters. *Journal of the American Oil Chemists' Society*, 24(4), 127-129.

Kader, A. A., & Rolle, R. S. (2004). *The role of post-harvest management in assuring the quality and safety of horticultural produce* (Vol. 152): Food and Agriculture Organization of the United Nations.

Litwinienko, G., Daniluk, A., & Kasprzycka-Guttman, T. (1999). Study on Autoxidation Kinetics of Fats by Differential Scanning Calorimetry. 1. Saturated C12-C18 Fatty Acids and Their Esters. *Industrial & Engineering Chemistry Research*, 39(1), 7-12. doi: 10.1021/ie9905512

Mei, L., Decker, E. A., & McClements, D. J. (1998). Evidence of Iron Association with Emulsion Droplets and Its Impact on Lipid Oxidation. *Journal of Agricultural and Food Chemistry*, 46(12), 5072-5077. doi: 10.1021/jf9806661

Organización de las Naciones Unidas para la Agricultura y la Alimentación FAO, & Instituto Interamericano de Cooperación para la Agricultura-Programa de Apoyo de la Agroindustria Rural para América Latina y el Caribe IICA/PRODAR. (2005). Curso de Gestión de Agronegocios en empresas asociativas rurales en América Latina *Poscosecha y servicios de apoyo a la comercialización* (Hernando Riveros, Especialista en Desarrollo de Agronegocios para la Región Andina- Director Ejecutivo PRODAR-IICA

Pilar Santacoloma, Oficial de Economía Agrícola –AGS- FAO

Florence Tartanac, Oficial de Agroindustria Rural –AGS-FAO

Division de Sistemas de Apoyo a la Agricultura (AGS-FAO) ed., Vol. Módulo 4).

Reblova, Z., Pokorny, J., & Panek, J. (1991). Autoxidation of stored soybean lecithin. *Food/Nahrung*, 35(6), 665-666.

Ulkowski, M., Musialik, M., & Litwinienko, G. (2005). Use of Differential Scanning Calorimetry To Study Lipid Oxidation. 1. Oxidative Stability of Lecithin and Linolenic Acid. *Journal of Agricultural and Food Chemistry*, 53(23), 9073-9077. doi: 10.1021/jf051289c

# **Modelamiento de la vida de anaquel en películas de polímeros reactivos**

*Angela García<sup>1</sup>, Jorge Medina<sup>1\*</sup>, Rodrigo Aguilar<sup>1</sup>, Bruno Fayolle<sup>2</sup>, Jacques Verdu<sup>2</sup>*

1: Grupo de Materiales y Manufactura CIPP-CIPEM, Departamento de Ingeniería Mecánica, Universidad de los Andes, Bogotá, Colombia

2: PIMM Paristech, Ecole Nationale d'Arts et Métiers, Paris, Francia

## **Abstract**

Se estudia el uso del aceite de linaza como ingrediente activo para estructuras de empaque con propiedades de absorción de oxígeno. El estudio se desarrolló desde el ingrediente en estado natural hasta una formulación que pudo utilizarse en composición con materiales poliméricos para la formación de capas activas. En el caso presentado se estableció una metodología de protección térmica del componente activo, se verificó el efecto de su tamaño de grano sobre la cinética de absorción y se validó su efectividad sobre un substrato de PP de 58 µm de espesor, alcanzando una reducción de oxígeno en un espacio de cabeza de volumen fijo desde 21% hasta menos del 1% en un término de 6 días. En paralelo al desarrollo experimental se propone un modelo de oxidación del ingrediente activo con capacidad de evaluar su desempeño bajo diferentes condiciones iniciales de concentración de oxígeno y temperatura.

**Palabras Clave:** secuestradores de oxígeno, empaques activos, modelado, oxidación, materiales compuestos.

## **1. INTRODUCCIÓN**

La organización de las Naciones Unidas para la alimentación y la agricultura (FAO) estima que las pérdidas post-cosecha en países desarrollados están entre el 5 y el 25% del volumen total producido, mientras que en países en desarrollo esta cifra alcanza entre el 20 y el 50% (FAO & IICA/PRODAR, 2005). El desarrollo de soluciones de empaque para aumentar la vida en estante de productos perecederos se convierte en una posible vía para la reducción de estas alarmantes cifras.

Los empaques activos se han propuesto como tecnologías con capacidad de ampliar la calidad y la vida útil de materiales perecederos. En estos empaques, se incorporan intencionalmente sustancias que pueden absorber o liberar componentes los cuales tienen un efecto directo en la calidad y vida de los productos empacados(Comisión Europea, 2009).

Actualmente, las composiciones secuestradoras de oxígeno son, junto a los reguladores de humedad, las tecnologías en empaques activos más utilizadas y patentadas debido al amplio espectro de productos perecederos que se ven afectados por procesos de oxidación o humidificación/deshumidificación.

Las composiciones de secuestradores de oxígeno se puede clasificar en aquellas basadas en hierro, compuestos orgánicos oxidables o bien en polímeros oxidables (F. Soares et al., 2009), y los

métodos para activar, o para iniciar el consumo de oxígeno por parte de los secuestradores, son en la mayoría de los casos operaciones de humidificación.

Los ejercicios de Prospectiva del Sector de Empaques Flexibles y Semirrígidos realizados bajo el auspicio de Acoplásticos y representantes de la cadena productiva de empaques para el 2004 y el 2011, han evidenciado la necesidad de incursionar en este tipo de nuevas tecnologías. El ICIPC y el CIPP de la Universidad de los Andes desarrollaron una primera fase investigativa en esta línea con el proyecto "Desarrollo de un compuesto termoplástico con base en Poliolefinas y con propiedades de absorción de oxígeno" en el 2009. Para el 2011 la Universidad de los Andes ha iniciado un proceso de patentamiento nacional y PCT con la invención COMPUESTO ABSORBEDOR DE OXÍGENO ENCAPSULADO EN UNA MATRIZ DE SILICA Y MÉTODO PARA PRODUCIRLO. El trabajo presentado representa una continuación de este trabajo inicial.

Se han evaluado diferentes ingredientes activos con capacidad de absorción de oxígeno (Á. García, Salas, & Medina, 2011) (Medina, Verdu, Fayolle, García, & Salas, 2012), dentro de los cuales se ha destacado el aceite de linaza (*García Mora, Salas Muñoz, & Medina Perilla*, 2012a) debido a que su composición, esencialmente formada por ácidos grasos insaturados, lo hace muy susceptible a procesos de auto oxidación; en el presente trabajo se toma este ingrediente activo y se estudian las trasformaciones a las que debe someterse el ingrediente activo para poder formar una composición que pueda incorporarse en capas poliméricas que lleguen a formar nuevas estructuras de empaques.

## 2. MATERIALES Y MÉTODOS

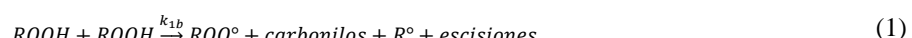
Se utilizó aceite de linaza doble cocido con 88% (p/p) de ácidos grasos insaturados. El mayor contenido (52,6% p/p) corresponde al ácido triinsaturado linolénico, 16,2% en ácido linoléico y 19,2% de ácido oleico.

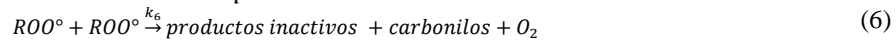
En las pruebas de seguimiento de la oxidación también se utilizaron Oleato, linoleato y linolenato de metilo grado Análisis (Sigma Aldrich). Para formar la capa activa se utiliza polipropileno homo polímero 03H96.

### a. Mecanismo de oxidación

Para modelar la oxidación del aceite de linaza se proponen las reacciones en cada etapa del proceso de auto oxidación.

#### Iniciación





A partir de las ecuaciones químicas (1) a (6) se derivan las expresiones cinéticas para

$$\frac{d[ROOH]}{dt}, \frac{d[R^\circ]}{dt}, \frac{d[ROO^\circ]}{dt}, \frac{d[RH]}{dt} \text{ y } \frac{d[O_2]}{dt}$$

El sistema de ecuaciones se resuelve numéricamente con ayuda del software Matlab™, donde además es posible cambiar los escenarios de las condiciones iniciales para evaluar el efecto que tendría la temperatura y la concentración de oxígeno inicial en el desempeño del ingrediente activo.

### b. Metodología de fabricación propuesta

En la figura 1 se presentan las operaciones que se llevaron a cabo para la fabricación de la capa activa.

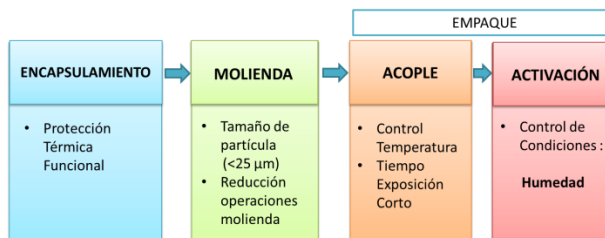


**Figura 1. Diagrama de bloques de fabricación de película activa.**

La figura 2, muestra el esquema utilizado para la protección del aceite de linaza en una matriz de sílicagel. Se utilizan como reactivos ácido clorhídrico y silicato de sodio, ambos de grado industrial.

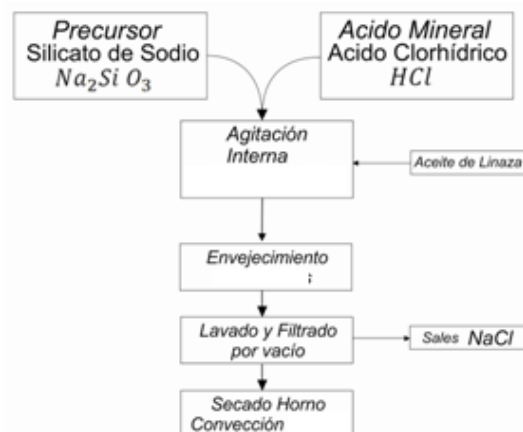


**Figura 3. Proceso de encapsulamiento en gel de sílice empleado.**

Debido a la importancia del proceso de encapsulamiento, dentro de la investigación, se evalúa el efecto del pH en el cual se introduce el aceite de linaza al sistema sol-gel. Se realizaron inserciones de aceite de linaza de acuerdo a un diseño experimental factorial y se estudió la eficacia de las operaciones de lavado y filtrado del gel mediante microscopía electrónica de barrido (SEM). Para la reducción de tamaño de partículas se utilizó molino de bolas US Stoneware. La etapa de extrusión se llevó a cabo en un equipo doble tornillo Brabender PlastiCorder TSE 30.

Para iniciar el proceso de oxidación del ingrediente activo se prueba con activación por humedad en Cámara Blue M humedad a 90% de humedad relativa durante 1 hora, y activación UV 1.40 W/m<sup>2</sup> a una longitud de onda de 340 nm., durante 1.5 horas.

#### c. Cinética y seguimiento del consumo de oxígeno

Como variable de respuesta de la eficacia de la película activa, o de los productos intermedios, se sigue el consumo de oxígeno en un espacio confinado durante diez días. El material absorbente de oxígeno se introduce en un envase de foil de aluminio de volumen fijo y sellado térmicamente. El seguimiento de oxígeno se realiza con el analizador Quantek 901 (Quantek Instruments) por método electroquímico. Se trata de una medición invasiva, por lo tanto diferentes embalajes con las misma condiciones se miden en diferente días para obtener una curva de oxígeno (%molar) vs. Tiempo.

### 3. RESULTADOS Y DISCUSIÓN

#### a. Modelado de auto oxidación

En la figura 4 se observa el potencial de consumo de oxígeno del aceite de linaza, calculado a partir de las ecuaciones químicas (1) a (6). Se observa un consumo acelerado alrededor de los primeros 90 minutos para luego llegar a un comportamiento asintótico de consumo de 0,5 mol/l de O<sub>2</sub>. Además de los valores de absorción de oxígeno, es importante conocer la forma cinética que tiene el ingrediente activo, porque de ello también dependerán las aplicaciones a futuro.

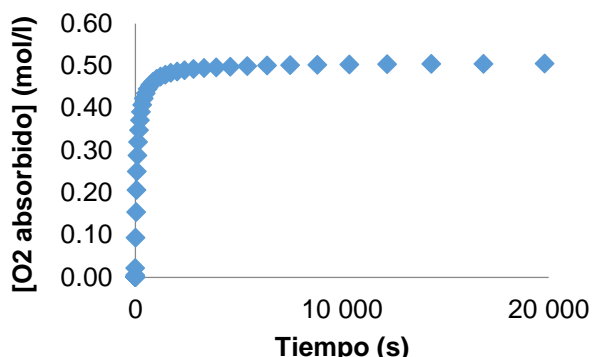


**Figura 4. Resultados de modelado de la auto oxidación del aceite de linaza.**

#### b. Etapa de encapsulamiento

Los factores más relevantes en esta etapa son pH de inserción y temperatura de secado. El diseño experimental sugiere mayor eficacia en el consumo de oxígeno con pH de inserción debajo de 3.0 y temperatura de secado de 60°C para evitar termo oxidación.

El encapsulamiento con presencia de catalizador (T2 en figura 5) prueba ser de alta calidad y se desempeña positivamente luego de la activación con 90% de humedad, absorbiendo un 19,32% de O<sub>2</sub> equivalente al 95.63% del elemento en la atmósfera de empaque en un total de 10 días.

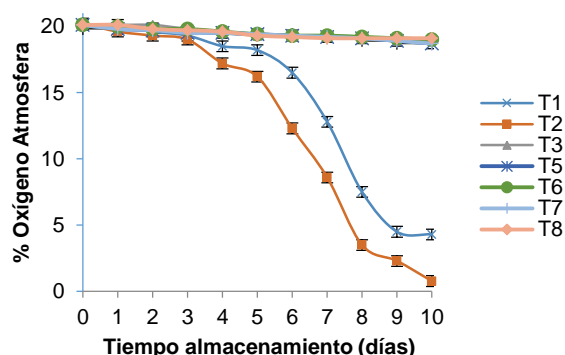


**Figura 5. Estudio experimental de encapsulamiento**

El encapsulamiento se verifica mediante espectroscopia infrarroja. La figura 6 muestra los espectros correspondientes a aceite de linaza puro, el blanco de sílicagel y aceite de linaza encapsulado en sílicagel. En el espectro correspondiente al ingrediente activo (aceite de linaza encapsulada) se puede observar una banda ancha entre 3700 -3100 cm<sup>-1</sup> y una banda más pequeña a 1651cm<sup>-1</sup> correspondientes a las vibraciones del grupo Silanol Si-OH características de la sílica. Se puede observar adicionalmente la presencia de picos en 2929 y 2856 cm<sup>-1</sup> correspondientes a las extensiones del enlace C-H del aceite de linaza y una banda fuerte para la extensión C=O del grupo éster a

$1747\text{cm}^{-1}$  del aceite lo cual significa que el aceite de linaza se encuentra en el nuevo compuesto elaborado.

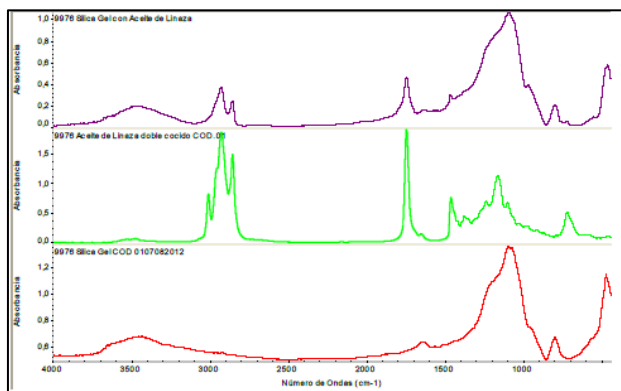


**Figura 6. Espectros de FTIR para aceite de linaza encapsulado en sílica gel (—), aceite de linaza (—) y blanco de sílica gel (—)**

#### c. Etapa de molienda

Se estudió el efecto del tiempo de molienda del ingrediente activo en el tamaño final obtenido y en la eficacia de consumo de oxígeno. Tiempo de molienda mayor a 180 minutos disminuyen la eficacia de absorción de oxígeno en un 80% (Figura 7), sugiriendo una prematura activación del ingrediente por fenómenos térmicos a causa de la fricción. La medición de la temperatura al interior del tambor de molienda muestra un aumento de cerca de  $12^\circ\text{C}$  respecto a la temperatura inicial.

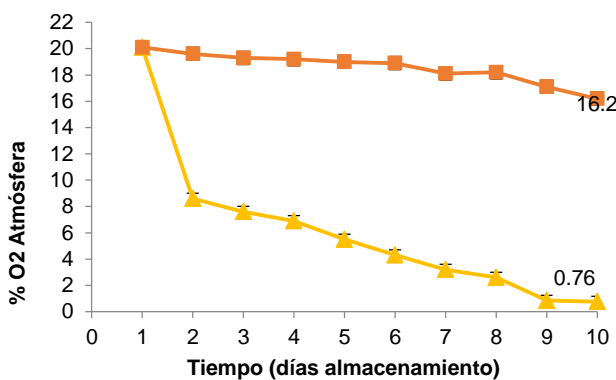


**Figura 7 Resultados de consumo de oxígeno de ingrediente activo a tamaño de  $45-25\mu\text{m}$  obtenido luego de 90min (▲) y 180 min (■) de molienda y activado en Cámara Blue M humedad 90% por 1 hora.**

#### d. Inclusión de composición activa en polipropileno

La mejor mezcla con el mejor desempeño de consumo de oxígeno (Figura 8) se mezcló con el PP por extrusión doble tornillo a temperatura constante de  $190^\circ\text{C}$  en todas las zonas y posterior activación de la película por humedad. La figura 8 muestra el efecto en la absorción de oxígeno de la película activa PP/Aceite de linaza encapsulado de diferentes tamaños de partícula.

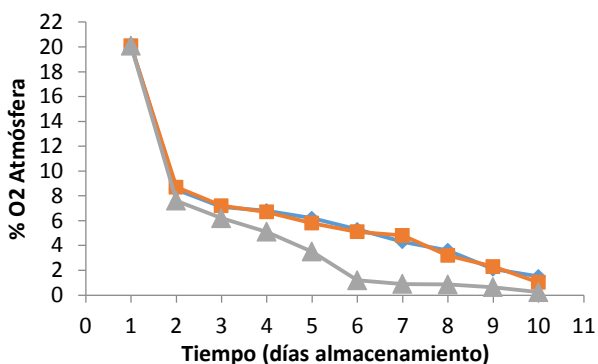


**Figura 8. Desempeño de consumo de oxígeno de película activa Polipropileno/Aceite de linaza encapsulado con tamaño de partícula inferior a 25  $\mu\text{m}$  ( $\blacktriangle$ ), entre 45 y 25  $\mu\text{m}$  ( $\blacksquare$ ) y entre 105 y 45  $\mu\text{m}$  ( $\blacklozenge$ ), activación 90% humedad 1 h, espesor 58  $\mu\text{m}$ .**

## CONCLUSIONES

Se logró la obtención de una composición con base en aceite de linaza y capacidad de absorción de oxígeno, que además puede integrarse en materiales compuestas de matriz polimérica.

La reducción del tamaño de partícula de la composición final (Aceite encapsulado en sílicagel) afecta positivamente la cinética de absorción de oxígeno del mismo. Se encontró que las partículas de 45 a 25  $\mu\text{m}$  activadas con el mecanismo de alta humedad 90% pueden ser incluidas en una capa de empaque en PP, con resultados muy favorables, llegando a niveles de hasta 0.64% de oxígeno después de 10 días de interacción.

El tiempo de molienda en molino de bolas es relevante para evitar la activación del aditivo en el proceso. Se encontró que una molienda superior a 120 minutos lleva a la activación y por ende a la total ausencia de actividad secuestradora de oxígeno en el espacio de cabeza del empaque.

Se encontraron relaciones entre la concentración necesaria de aditivo con propiedades de absorción y la cinética de oxidación encontrando que se debe garantizar al menos un 0.75% en peso de aditivo para alcanzar resultados significativos.

## REFERENCIAS

REGLAMENTO (CE) No 450/2009 (2009).

F. SOARES, N. D. F., S. PIRES, A. C., CAMILLOTO, G. P., SANTIAGO-SILVA, P., P. ESPITIA, P. J., & A. SILVA, W. Recent patents on active packaging for food application. *Recent patents on food, nutrition & agriculture*, 1(2), 171. (2009).

*GARCÍA MORA, A. M., SALAS MUÑOZ, J. C., & MEDINA PERILLA, J. A.* Linseed oil as active ingredient in active packaging. *Paper presented at the Polymer Processing Society Americas Conference 2012*, Niagara, Ontario. (2012).

*GARCÍA, Á., SALAS, J., & MEDINA, J.* Comparación de la cinética de absorbentes de oxígeno destinados a estructuras de empaques de alimentos. *Artículo presentado en el VI Congreso Internacional de Materiales (CIM 2011)*, Bogotá, Colombia. (2011).

*MEDINA, J., VERDU, J., FAYOLLE, B., GARCÍA, A., & SALAS, J.* Desarrollo, caracterización y comparación de nuevos ingredientes activos para su uso en empaques con propiedades de absorción de oxígeno. *Artículo presentado en el XIII Simposio Latinoamericano de Polímeros*, Bogotá, Colombia. (2012).

# Methodology to Evaluate Performance of Active Ingredients as Oxygen Scavengers

Angela M. García<sup>1\*</sup>, Jorge A. Medina<sup>1</sup>, Jacques Verdu<sup>2</sup> and Bruno Fayolle<sup>2</sup>

<sup>1</sup> Grupo de Materiales y Manufactura CIPP-CIPEM, Departamento de Ingeniería Mecánica,  
Universidad de los Andes, Bogotá, Colombia

<sup>2</sup> Ecole Nationale Supérieure d'Arts et Métiers, PIMM Paristech, Paris, France

\*Corresponding author. Email: am.García228@uniandes.edu.co

**Abstract:** The development of oxygen scavengers for active packaging covers various sources of active components, e.g. inorganic elements, unsaturated compounds, acids, enzymes, clays, and polymers ("Active packaging film prevents lipid oxidation in oil-in-water emulsion systems," 2013; Cahill et al., 2004; Carranza et al., 2012; Charles et al., 2006; Garcia Mora, Salas Muñoz, & Medina Perilla, 2012b; Vermeiren, Devlieghere, Van Beest, De Kruijf, & Debevere, 1999). Despite the advances in active formulations, there is a lack of detailed information concerning the performance of oxygen scavengers. Data provided by manufactures may be limited and generalized (Merchán Sandoval, 2006; Solis & Rodgers, 2001). In addition, considerable differences between commercial data sheets and experimental studies have been reported (Miltz & Perry, 2005). Thus, there is an increasing need for tools to evaluate performance of polymeric and organic formulations.

Active ingredients used in this study were unsaturated esters and linseed oil. In this research, a new methodology is proposed with the aim to evaluate the performance of unsaturated-lipid compounds as oxygen scavengers. This methodology has an experimental section and other one of modelling. Experimentally, measurements of oxygen in headspace and thermogravimetric analyses (TGA) were performed at different temperatures and atmospheres (nitrogen, air, and oxygen) and served to determine the actual oxygen scavenging capacity of the active ingredients; and the model, is a series of chain reactions based on the thermo-oxidation of unsaturated hydrocarbons.

Industries that already use active packaging, and those interested in this developing technology, can use the proposed methodology as a useful and simple tool to evaluate the oxygen scavenging performance in their specific applications and environments.

Keywords: oxygen scavengers, performance, temperature, modelling, unsaturated lipids, active packaging.

## Introduction

Active packaging technologies are able to improve quality and shelf life of products, by means of components that would release or absorb substances into or from the packaged food, or the environment surrounding the food (Comisión Europea, 2009). In 2011, gas scavengers accounted nearly 36% of the total market of active, intelligent and smart packaging, within these, oxygen scavengers are the most used because degradation of many products is related with oxidation (Visiongain, 2010).

In the present research, unsaturated fatty acids and esters are proposed as possible active ingredients for oxygen scavengers because they are susceptible to auto-oxidation initiated or activated by metals, UV radiations or temperature. Oxidation activated by temperature was evaluated by thermogravimetric tests and headspace measurements. In parallel thermo-oxidation has been modelled based on the oxidation of C-H bonds adjacent to double bonds as active sites.

## 1. Materials and methods

Analytical grade neat unsaturated esters: methyl oleate, methyl linoleate and methyl linolenate were used. Linseed oil used was grade double boiled and its composition was obtained by Gas-Liquid Chromatography (GLC) and is presented in table 1.

**Table 1:** Composition of Linseed oil double boiled

Co mponent	Weight concentration from GLC (% w/w)
Pal mitic acid	5,9
Stea ric acid	3,4
Olei c acid	19,2
Lin oleic acid	16,2
Lin olenic acid	52,6
Unk nown	2,7
Total	100

### 1.1 Thermal gravimetric analysis (TGA)

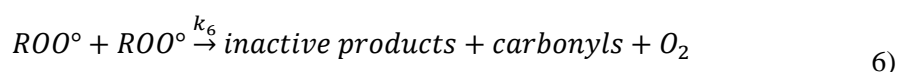
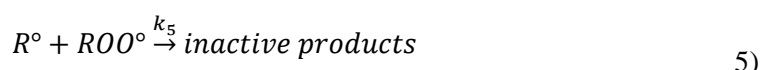
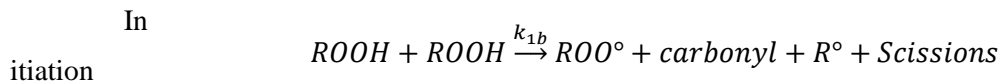
In the presence of oxygen, an increase in the mass of the oils caused by oxidative reactions is expected. Samples of the neat esters and linseed oil were analysed using TGA 500 (TA Instruments) with isotherms of 60°C, 80°C and 110°C reached at a heating rate of 20°C/min. Themograms were obtained under nitrogen, air and pure oxygen atmospheres. In order to improve repeatability and reproducibility, and to avoid the effect of heat transmission by diffusion in TGA analysis, the mass in all the experiments was, in average, 4mg and duplicates were done in all cases.

### 1.2 Headspace measurements

Several samples of 1 ml. of active ingredient were placed into glass containers of 20 ml and after heated at 60°C, 80°C or 110°C to study thermo-oxidation; the oxygen in the headspace of the containers was measured at different times, using a portable spot check oxygen analyser Model 901 (Quantek). Each sample was punctured once. Three replicates and two empty containers were measured each time to separate the effect of change of gas volume because increase of temperature.

## 2. Thermo- oxidation model

The following oxidation mechanism, of a hydrocarbon substrate with a single reactive site under oxygen excess at moderate temperature (<150°C), was proposed based on previous research (Richaud et al., 2012).



### 3. Results

#### 3.1 Thermogravimetric tests

Thermogravimetric tests in nitrogen atmosphere showed evaporation phenomena caused by increase of temperature; a thermogram for methyl linolenate is given in Figure 1.

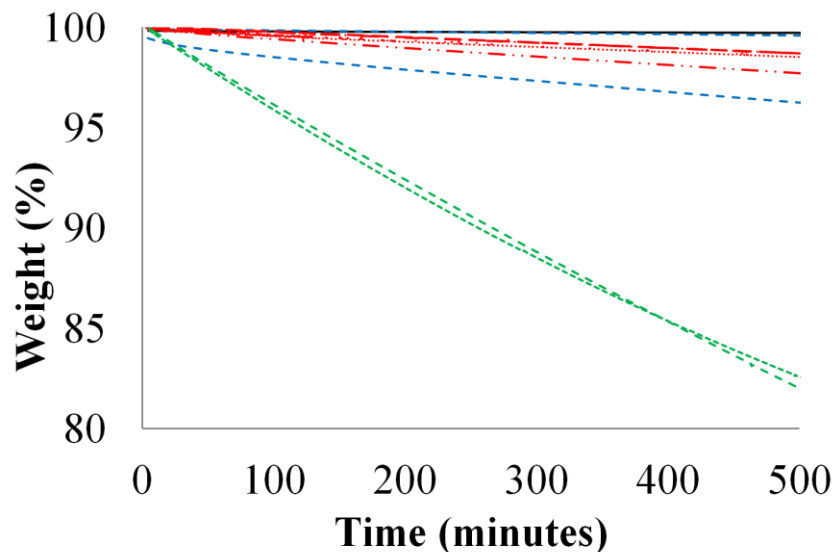


**Figure 1:** TGA of methyl linolenate at 40 °C (—), 60°C (—), 80°C (—) and 110°C (—),, nitrogen atmosphere

Slopes of the plot in the thermogram under nitrogen atmosphere were calculated to include the effect of evaporation in subsequent analyses. Slope values for all active ingredients are plotted in Figure 2 below.

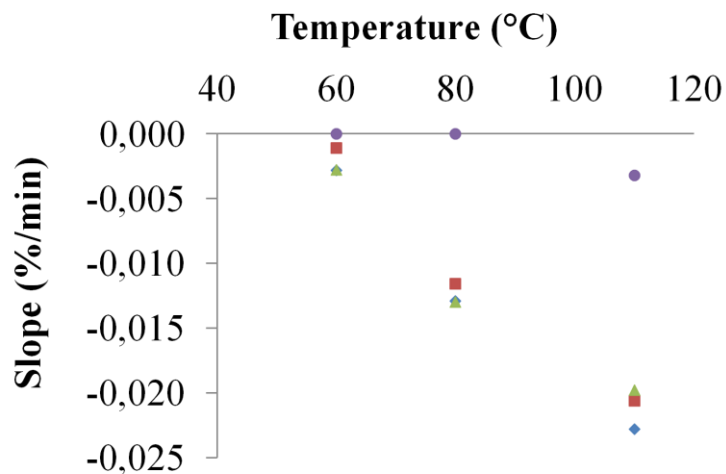


**Figure 2:** Values of slopes calculated from TGA under nitrogen atmosphere form methyl oleate (♦), methyl linoleate (■), methyl linolenate (▲) and linseed oil (●) at 60°C, 80°C and 110°C.

As expected, evaporation rate decreases at higher temperatures and the values for the slopes of neat esters are very close because they have similar molecular weights. Linseed oil slopes are less negative than slopes of neat esters in all the temperatures, which can be related with cross linking phenomena (Lazzari & Chiantore, 1999).

Although reactions of thermo–oxidation occur on air and pure oxygen atmospheres, slope values of thermograms obtained were negative at the highest temperatures because oxidation is combined with evaporation; at low temperatures the weight gained because oxidation can be better appreciated. Figure 3 shows results for methyl linolenate in air atmosphere.

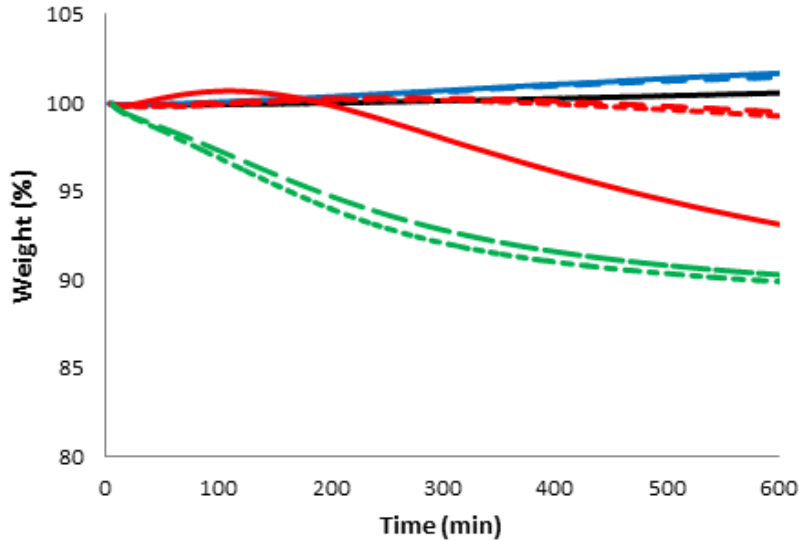


**Figure 3:** TGA of methyl linolenate on air atmosphere at 40°C (—), 60°C (—), 80°C (—) and 110°C (—).

In order to see oxidation phenomena solely, oxidation weight ( $W_o$ ) was obtained as is shown in (7) and (8).

$$W_o(\%) = W_{air}(\%) - W_N(\%) \quad 7)$$

$$W_o(\%) = W_{Oxygen}(\%) - W_N(\%) \quad 8)$$

Where  $W_o$  is the weight gained just by oxidation,  $W_{air}$  is the weight obtained in TGA in air atmosphere,  $W_N$  the weight obtained in TGA under nitrogen atmosphere and  $W_{Oxygen}$  the weight obtained in experiments under 100% oxygen atmosphere. Eliminating the effect of evaporation, the increase in oxidation rate with temperature can be appreciated (Figure 4)

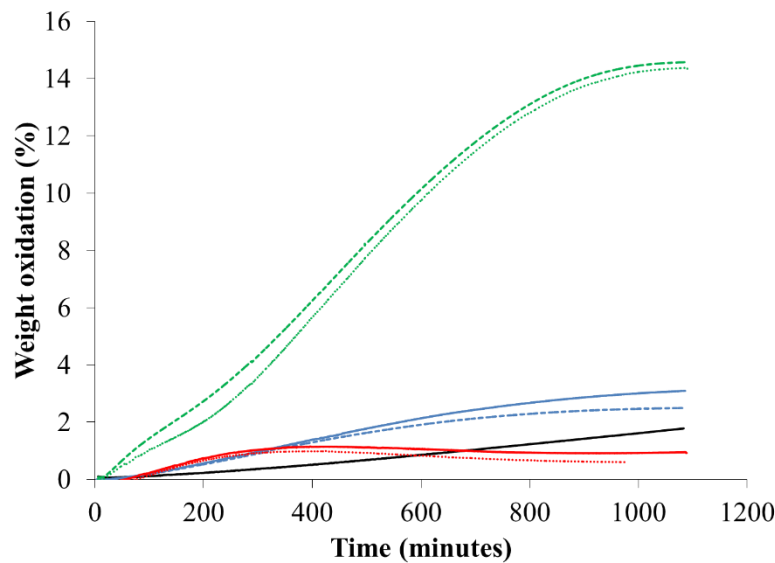


**Figure 4:** Results from TGA of methyl linolenate on air atmosphere at 40°C (—), 60°C (—), 80°C (—) and 110°C (—), expressed as  $W_o$  (equation 7)

Mass gained expressed as mmol O<sub>2</sub>/g ester was calculated with the data of TGA in atmosphere of air and pure oxygen. Figure 5 and Figure 6 show the results for methyl linolenate and linseed oil.

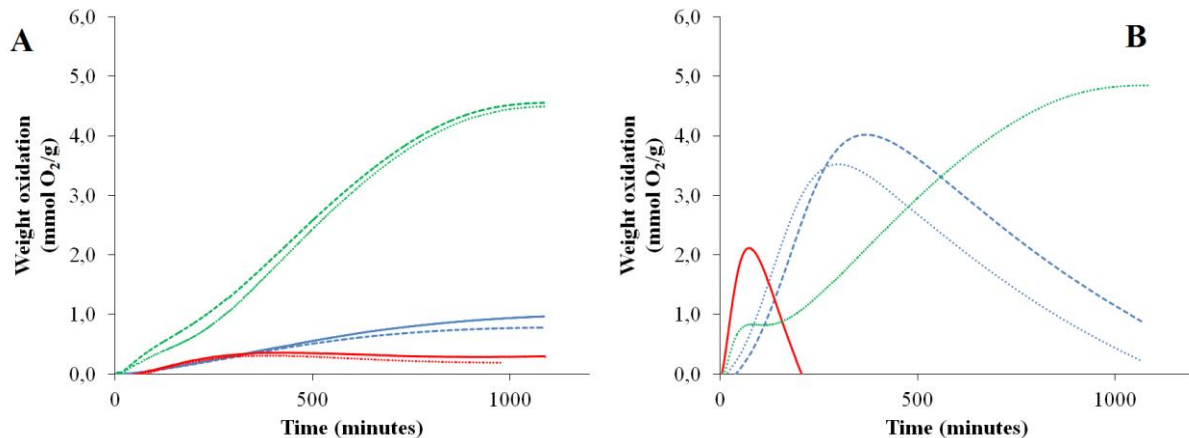


**Figure 5:** Weight gained vs. time for methyl linolenate at 60°C(—), 80°C(—) and 110°C (—) in atmosphere of **A.** air and **B.** oxygen.

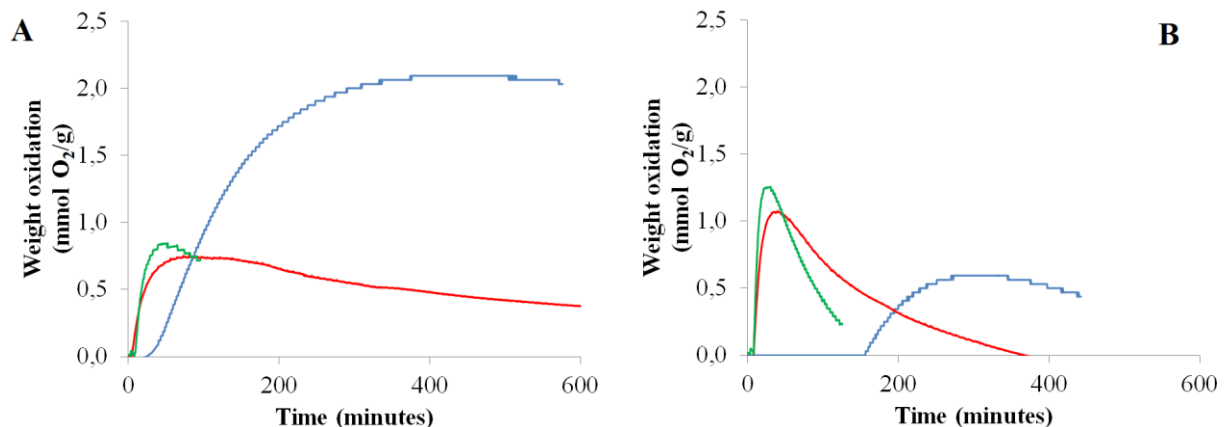


**Figure 6:** Weight gained vs. time for linseed oil at 60°C(—), 80°C(—) and 110°C (—) in atmosphere of **A.** air and **B.** oxygen

Higher values of oxygen uptake were obtained for methyl linolenate, which have the highest number of unsaturations. The maximum conversion for methyl linolenate was 4 mmol O<sub>2</sub>/g ester equivalents to 1.2 mmol O<sub>2</sub>/mmol of methyl linolenate obtained at 110°C.

### 3.2 Headspace measurements

Similar calculations of oxygen consumed can be obtained by headspace measurements. Data collected can be plotted as the change of oxygen concentration in the headspace vs. time as shown in Figure 7 for linseed oil. In a confined headspace of 19 ml, 1 ml of linseed oil is capable to diminish the oxygen concentration of the headspace more rapidly at 110°C.

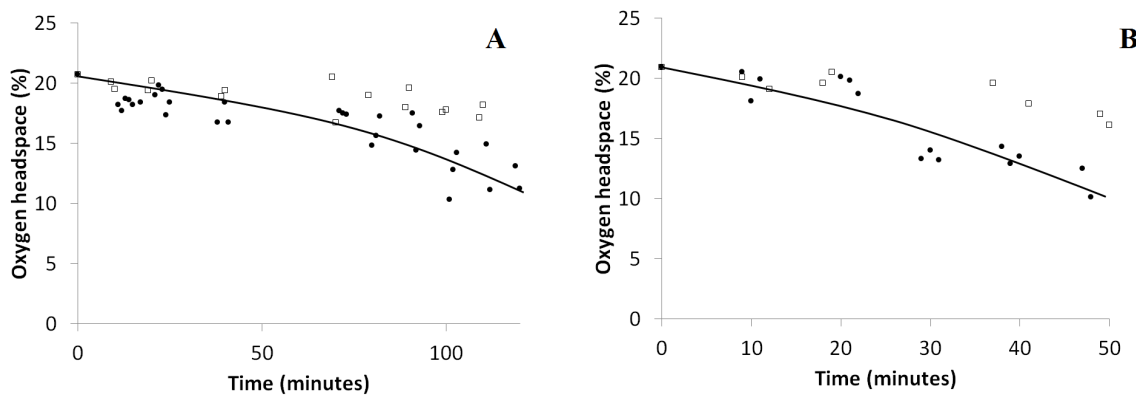


**Figure 7:** Oxygen concentration in the headspace vs. time for flasks with 1 ml of linseed oil at (A) 80°C (●) and (B) 110°C (●) in comparison with the change of oxygen concentration for empty flasks (□) at the same temperature conditions.

Based on data from headspace measurement, oxygen consumed can be calculated, Figure 8 shows a comparison between data calculated from TGA and from headspace experiments for linseed oil at 110°C in air atmosphere. Both plots show the same behaviour but differences in the values of oxygen scavenging capacity are observable. From headspace measurements maximum conversion was 0.1 mmol O<sub>2</sub>/g of linseed oil, while from TGA was 2.1 mmol O<sub>2</sub>/g of linseed oil, this can be attributed to confined headspace volume in the case of headspace experiments. These results reveal the importance of a correct calculus and measurement of the oxygen scavenging capacity for active ingredients.

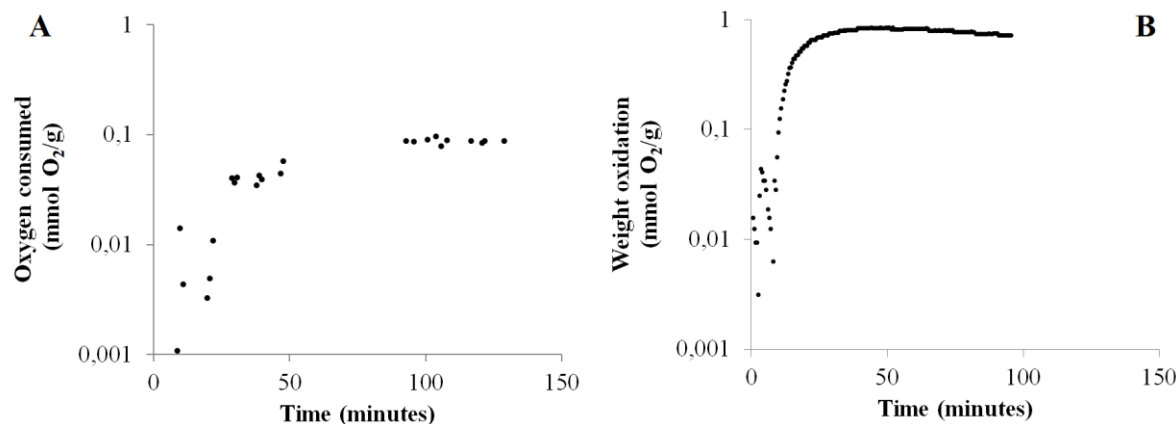


**Figure 8:** A. Change in headspace oxygen concentration expressed as mmol O<sub>2</sub>/g linseed oil, obtained from headspace measurements at 110°C. B. Weight change expressed as mmol O<sub>2</sub>/g linseed oil, obtained from TGA experiments 110°C in air atmosphere.

## Conclusions

Quantitative equivalence between headspace measurements and thermogravimetric experiments had been demonstrated, showing the later as a novel, simple and rapid method to evaluate oxygen scavenging capacity for ingredients activated by temperature.

In the case of active ingredients studied, more promising results were for methyl linolenate at 110°C.

## References

1. Charles, F., J. Sanchez, and N. Gontard, 2006, "Absorption kinetics of oxygen and carbon dioxide scavengers as part of active modified atmosphere packaging", *Journal of Food Engineering*. 72(1): pp. 1-7.
2. Garcia Mora, A.M., J.C. Salas Muñoz, and J.A. Medina Perilla, 2012, "Linseed oil as active ingredient in active packaging", in *Polymer Processing Society Americas Conference*. Niagara, Ontario.
3. 2013,"Active packaging film prevents lipid oxidation in oil-in-water emulsion systems". *Emerging Food R&D Report*, 23(10): pp. 5-5.
4. Vermeiren, L., et al., "Developments in the active packaging of foods", 1999, *Trends in Food Science & Technology*, 10(3): pp. 77-86.
5. Carranza, S., D.R. Paul, and R.T. Bonnecaze, 2012, "Multilayer reactive barrier materials", *Journal of Membrane Science*, 399–400(0): pp. 73-85.
6. Cahill, P.J., et al., 2004, "Active oxygen Scavenging property- Imparted Copolymer". Japan.
7. Solis, J.A. and B.D. Rodgers, 2001, "Factors affecting the performance of new oxygen scavenging polymer for packaging applications", *Journal of plastic film and sheeting*, 17(4): pp. 339-349.
8. Merchán Sandoval, J.P., 2006, Implementación de un absorbedor de oxígeno en película para empaque activo, in *Ingeniería Mecánica*. Universidad de los Andes. pp. 87.
9. Miltz, J. and M. Perry, 2005, "Evaluation of the performance of iron based oxygen scavengers, with comments on their optimal applications", *Packaging Technology and Science*. 18(1): pp. 21-27.
10. Comisión Europea, 2009, Reglamento (CE) No 450/2009.: *Diario Oficial de la Unión Europea*.
11. Visiongain, 2010, *The Active, Intelligent and Smart Food & Drink Packaging Market 2011-2021*.
12. Richaud, E., et al., 2012, "Rate constants of oxidation of unsaturated fatty esters studied by chemiluminescence", *Chemistry and Physics of Lipids*. 165(7): pp. 753-759.
13. Lazzari, M. and O. Chiantore, 1999, "Drying and oxidative degradation of linseed oil", *Polymer degradation and stability*. 65(2): pp. 303-313.



# KINETIC MODELING OF OXYGEN ABSORPTION BY UNSATURATED ESTERS AND LINSEED OIL TO BE USED AS OXYGEN SCAVENGERS

## RESUME :

Les capteurs d'oxygène sont le plus grand apport dans la technologie des emballages actifs parce qu'ils permettent de retarder la dégradation oxydante des aliments et ainsi éviter la perte de saveurs et le développement microbien au sein des aliments. Bien que le développement des emballages actifs existe depuis les années 70 dans des pays producteur agricole, la recherche sur ces emballages reste encore embryonnaire, en particulier sur les critères techniques portant sur l'absorption d'oxygène de films. Cette thèse constitue une contribution sur l'étude des cinétiques d'absorption d'oxygène de l'huile de lin comme capteur d'oxygène. L'oxydation de l'huile et d'esters insaturés (composé modèle de l'huile) est suivie sous différentes conditions d'exposition (températures comprises entre 40-110°C et pressions partielles d'oxygène entre 0 et 1 bar). Expérimentalement, on propose de caractériser l'absorption d'oxygène liée à l'oxydation de l'huile par thermogravimétrie (ATG), suivi de concentration d'oxygène et titrage de peroxyde. Un modèle cinétique basé des schémas classiques avec décomposition des hydro peroxydes, est proposé pour simuler l'oxydation de l'huile de lin et des esters insaturés modèles. Ce modèle est ensuite extrapolé à des films de différentes épaisseurs de polypropylène (PP) contenant 1% d'huile de lin en considérant que cette dernière est bien dispersé dans la matrice PP et que la diffusion d'oxygène est pilotée par la matrice PP.

**Mots clés:** Emballages actifs, capteur d'oxygène, huile de lin, thermo-oxydation, modélisation cinétique, prédition de l'absorption d'oxygène

# KINETIC MODELING OF OXYGEN ABSORPTION BY UNSATURATED ESTERS AND LINSEED OIL TO BE USED AS OXYGEN SCAVENGERS

## ABSTRACT:

Oxygen scavengers (OS) are one of the most important technology of active packaging, because prevents oxidative degradation related with off-flavours, off-odours and microbial growth in food. Although active packaging has been proposed since 1970s, in developing countries with a large agricultural base, active packaging still remains unexplored both in terms of application and research, there is a lack of technical criteria on O<sub>2</sub> scavenging films, labels, sheets, and trays. This PhD thesis is a contribution in the study of linseed oil as active ingredient for OS providing a kinetic characterization of its thermo-oxidation between 40°C and 110°C in atmospheres with different oxygen concentration. In the experimental approach, innovative application of TGA was proposed to study oxygen uptake capacity complemented by headspace and peroxide value measurements. The kinetic model, derived from a classic mechanistic scheme where initiation of thermo-oxidation results from decomposition of hydro peroxides, was capable to simulated linseed oil oxidation, and also oxygen absorptions of polypropylene films, of different thickness, containing 1% of linseed oil, with hypotheses of well dispersion of linseed oil in PP matrix, and oxygen diffusion governed by the PP matrix.

**Keywords :** active packaging, oxygen scavengers, linseed oil, thermal oxidation, kinetic model, hydroperoxides, oxygen uptake prediction.

